Improving circularity of inverted T-girders

Structural assessment of the prefabricated inverted T-girder system

N.H.V. (Noah) le Mair

TU Delft

Improving circularity of inverted T-girders

Structural assessment of the prefabricated inverted T-girder system

by

N.H.V. (Noah) le Mair

to obtain the degree of Master of Science
at the Delft University of Technology,
to be defended publicly on Thursday September 12, 2024 at 15:00 PM.

Faculty of Civil Engineering and Geosciences
Track "Structural Engineering"
Specialisation "Structural Mechanics"

In collaboration with:

Student number:	4561929		
Thesis committee:	Dr. ir. Y. (Yuguang) Yang,	TU Delft	Chairman
	Ir. I. (Ivor) Zonderwijk,	Dura Vermeer	Daily supervisor
	Ing. W.J. (Jasper) Schilder,	Dura Vermeer	Company supervisor
	Prof. dr. ir. M.A.N. (Max) Hendriks,	TU Delft	University supervisor
	Prof. dr. H.M. (Henk) Jonkers,	TU Delft	University supervisor

An electronic version of this thesis is available at http://repository.tudelft.nl/.

TU Delft

Preface

This thesis marks the culmination of my studies at the Delft University of Technology and the completion of my Master's degree in Structural Engineering at the Faculty of Civil Engineering and Geosciences. This research focuses on exploring the potential of adapting the inverted T-girder system to facilitate the reuse of girders, thereby maximising their reuse potential and enhancing overall sustainability. Exploring this topic has been both intriguing and challenging, leading to many rewarding experiences and valuable lessons. This project provided me with the opportunity to apply the knowledge I gained from my master's courses in a practical context. I would like to take this opportunity to extend my sincere gratitude to several individuals who have been particularly supportive throughout this journey.

First and foremost, I would like to express my gratitude to my daily supervisor, Ivor Zonderwijk, for providing me with the opportunity to complete my graduation at Dura Vermeer. His enthusiasm, extensive knowledge, and support were invaluable throughout this project. Moreover, his kindness and approachability made me feel comfortable seeking guidance whenever needed. I would also like to extend my gratitude to Jasper Schilder for his insightful perspectives and valuable contributions. My time at Dura Vermeer has been a transformative experience, stimulating both personal and professional growth.

My gratitude also goes to my chair supervisor at Delft University of Technology, Yuguang Yang, for his support, critical insights, and for motivating me by posing challenging questions and suggestions. I would like to thank the other committee members, Max Hendriks and Henk Jonkers, for their expertise, valuable suggestions, and constructive feedback during our progress meetings.

Finally, I would like to thank my family, friends, and girlfriend for their unconditional support and belief in me. It is with pride that I present this Master's thesis, and I hope you will enjoy reading it.

N.H.V. (Noah) le Mair
Rotterdam, September 2024

Abstract

Transitioning towards a more circular construction industry is crucial for achieving climate-neutral and fully circular operations by 2030. One significant contribution to this goal is fully utilising the reuse potential of prefabricated inverted T-girders. The primary challenge lies in adapting the inverted T-girder system to enhance the circularity of the girders. To address this, a comprehensive literature review is conducted to understand the structural response and disassembly challenges associated with the system, providing valuable insights into potential improvements. This study employs a numerical model based on the Finite Element Method using DIANA FEA to assess the impact of various design adjustments, specifically the removal of end transverse diaphragms and increasing deck slab thickness. The numerical model uses horizontal and vertical curved shell elements and is subjected to several critical load cases to determine the maximum stresses for different design parameters. The results indicate that eliminating the end transverse diaphragms has minimal impact on the distribution of longitudinal bending moments and shear forces. However, it causes a localised increase in support forces by 17%. Additionally, significant differences are observed in the deck slab, necessitating an additional capacity of 16% for transverse bending moments and 17% for twisting moments. The study also examines the effect of skew angles to evaluate the applicability of orthogonal system findings to skewed systems. As the skew angle decreases, a greater proportion of forces and moments is absorbed by the deck slab rather than the composite girders. However, the mutual differences between systems with and without end transverse diaphragms generally vary by up to 2.6%, indicating that the findings for the orthogonal system are broadly applicable to skewed systems as well.

Executive summary

In a world where natural resources are depleting and climate change is becoming increasingly evident, the importance of sustainability is more widely recognised than ever. Achieving this means fulfilling the needs of the present while ensuring that future generations have the resources to meet their own needs. A circular economy addresses this by efficiently using resources, minimising waste and closing loops of products. The gradations of circularity emphasise that refusing unnecessary elements is the highest level of circularity. This approach leads to optimised material use and smarter product designs, thereby enhancing overall sustainability.

The construction industry, known for its significant environmental impact, is evolving towards a more circular model where reuse and design optimisation play crucial roles. In the Netherlands, this transition is primarily driven by the Ministry of Infrastructure and Water Management of the Netherlands, which has set an ambitious goal to operate climate-neutral and fully circular by 2030. Previous studies have shown that prefabricated inverted T-girders, due to their high quality of concrete, are ideal for direct reuse. However, the traditional design of the inverted T-girder system does not incorporate the concept of reuse, leading to significant costs associated with disassembly. These costs can diminish the benefits of reuse, making it less competitive with the use of new girders. To fully leverage the reuse potential of prefabricated inverted T-girders, this study evaluates various design adjustments aimed at enhancing the reusability of these girders.

The objective of this study was to make optimal use of the reuse potential of inverted T-girders by modifying the design of the girder system. The focus is on making design adjustments to enhance the disassembly process of the girders without compromising their structural capacity. A structural analysis of the inverted T-girder system was conducted to better understand the force and stress distribution within the system, revealing the influence of each structural component. This analysis offers crucial insights into the feasibility of design adjustments that facilitate both disassembly and future use of the girders while ensuring structural integrity. To achieve this objective, the following main research question was formulated:

> ”How can the inverted T-girder system be adapted to improve the circularity during the disassembly and reassembly process in the future?”

To make adjustments to the inverted T-girder system, it is crucial to understand the contribution of different components to the overall structural integrity. A literature review was conducted to detail the arrangement of structural components and their added value to the system’s performance. This review also assessed the residual stress distribution of individual inverted T-girders, revealing concerns when reusing these girders. Evaluating current methodologies for disassembling the girders highlighted challenges primarily associated with the transverse elements, such as the deck slab and end transverse diaphragms. Due to the significantly greater dimensions of the end transverse diaphragms compared to the deck slab thickness, detaching the girders from the end transverse diaphragms is assumed to be the most challenging task.

To explore the potential of eliminating the end transverse diaphragms effectively, their impact has been studied through literature. Limited research has been found on this topic, but the available studies indicate that the absence of end transverse diaphragms has little to negligible impact on the force and moment distribution of other structural components. The findings suggest that removing the end transverse diaphragms could be feasible, thereby simplifying the disassembly process of the girders and enhancing their reusability.

Assessing the impact of various design adjustments on the system starts by developing a numerical model based on the Finite Element Analysis (FEM). To observe the effects of the various design adjustments, a base system was derived from a case study. The case study consisting of an inverted

T-girder system was reduced to an orthogonal configuration with symmetrical characteristics to balance the dead loads. The linear elastic model focuses only on the behaviour of prefabricated and cast in-situ concrete elements. Furthermore, the system is subjected to four critical scenarios, each designed to generate maximum internal stresses. Thereby, only vertical dead and live loads are considered, excluding self-weight and horizontal loads.

Given the connectivity of diverse structural components and their complex orthogonal arrangement, a modelling approach using horizontal and vertical curved shell elements is considered the most suitable. Integrating the results of a shell element model over the entire cross-section allows for the determination of internal forces and moments within the composite system. The numerical model in DIANA FEA employs composed line elements to determine the forces and bending moments of every inverted T-girder and in the transverse direction of the deck slab.

After elucidating the global operation of the system by analysing the deflection, force distribution, and moment distribution, various design adjustments were evaluated, specifically focusing on the effect of eliminating end transverse diaphragms. Recognising the potential reduction in transverse stiffness, the impact of increased deck slab thickness in a system without end transverse diaphragms was explored. Although the additional self-weight from increasing the full-width deck slab thickness leads to higher maximum values, self-weight is excluded from this analysis to focus on the impact of increased stiffness. The outcomes of these modified systems are compared to those of the base system, offering a thorough insight into their effects on overall structural performance.

The findings indicate that removing the end transverse diaphragms has a negligible impact on the maximum longitudinal bending moments and shear forces across the composite girders. However, this modification leads to a 17% increase in maximum support forces. Despite this localised increase, the substructure is considered capable of withstanding the additional load, as it is generally constructed with a higher capacity than is typically utilised. More significant changes are observed in the deck slab, where transverse bending moments increase by 16% and twisting moments by 17%. These additional demands can be met with relatively minor adjustments, primarily by increasing the amount of reinforcement within the deck slab. Additionally, increasing the deck slab thickness to compensate for the reduced transverse stiffness caused by the absence of end transverse diaphragms is not considered advantageous. This modification minimally contributes to a better distribution of maximum values across the girders and significantly increases bending and twisting moments in the deck slab.

To ensure broader applicability for the findings, an additional analysis was conducted to assess the effects of different skew angles. Keeping the system geometry and characteristics unchanged, all systems were tested and subjected to three different skew angles compared to the reference orthogonal system. This comparison focused only on the maximum values of various design parameters generated by their critical load cases, adjusted for the skew angle.

As the skew angle decreases, a larger share of forces and moments are absorbed by the deck slab rather than the composite girders. With two exceptions, the findings demonstrate a maximum mutual difference of 2.6% across the various skew angles between the systems with and without end transverse diaphragms. This indicates that the results for the orthogonal system are representative of other skewed systems. Conversely, the system with increased deck slab thickness shows more significant mutual differences from the base system as the skew angle decreases, especially in the deck slab. These substantial differences highlight the skew angle's impact, making this design adjustment less suitable.

This study suggests that the inverted T-girder system can be modified by eliminating the end transverse diaphragms without significantly impacting overall structural performance. This adjustment enhances the circularity of the girder during disassembly and reassembly. Additionally, these findings also apply to skewed systems with skew angles up to 45 degrees.

Contents

List of Figures

List of Tables

1 Introduction

1.1. Background and relevance

In a world where natural resources are rapidly depleted and climate change has become tangible, the importance of sustainability is acknowledged more than ever. Sustainability is defined as 'meeting the needs of the present without compromising the ability of future generations to meet their own needs' [6]. To achieve this, the economy has to change from a linear to a circular economy. A circular economy aims for efficient use of resources by minimising waste and closing loops of products [47]. The concept of circular economy can be important for sustainable development [39]. Various circular economy concepts can be found in scientific and research papers. Kirchherr et al. (2017) [38] published the 10R framework based on varying degrees of circularity [67]. Figure 1.1 shows the 10R model and what is needed to change and develop the economy into a circular economy. The highest level of circularity is not 'reuse', but can be defined by the term 'refuse'. This level can be reached by smarter product use and manufacture, which requires a change in the design process.

The construction industry is widely recognised for its substantial environmental impact [34]. Traditionally regarded as a conservative sector, it predominantly follows a linear life-cycle model, commonly referred to as a 'cradle-to-grave' approach. This model represents a process where materials are used to create a product, which then becomes waste at the end of its life cycle. Reducing the amount of generated waste and resource usage can help evaluate this linear model to a more sustainable 'cradle-to-cradle' model. This model promotes circularity by reducing the need for demolition and instead emphasising disassembly, which allows for greater reuse of materials and components [13]. Moreover, as highlighted in Figure 1.1, adopting the circularity strategies of 'Reduce', 'Rethink', and 'Refuse' can further improve circularity. These strategies are designed to optimise product use and manufacturing processes, thereby advancing more sustainable practices.

The transition from a linear to a circular construction process is a complex challenge, but the sector holds significant potential for improvement. According to estimates by 'Het Rijksbrede programma Circulaire Economie', the Dutch construction industry accounts for 50% of the raw material consumption, 40% of the total energy consumption, and 30% of the total water consumption in the Netherlands [52]. Additionally, the construction industry is responsible for approximately 35% of the total carbon dioxide emissions of the country [52]. Acknowledging the critical role of this sector, the Ministry of Infrastructure and Water Management of the Netherlands has set an ambitious goal to achieve climate neutrality and full circularity by 2030 [46]. To support this goal, Rijkswaterstaat[1] has initiated several consortia to promote the development of circular solutions in Dutch infrastructure, with a particular emphasis on bridges and viaducts.

[1] Rijkswaterstaat is part of the Dutch Ministry of Infrastructure and Water Management and is responsible for the design, construction, management, and maintenance of the Netherlands' primary infrastructure facilities. (https://www.rijkswaterstaat.nl/en/about-us)

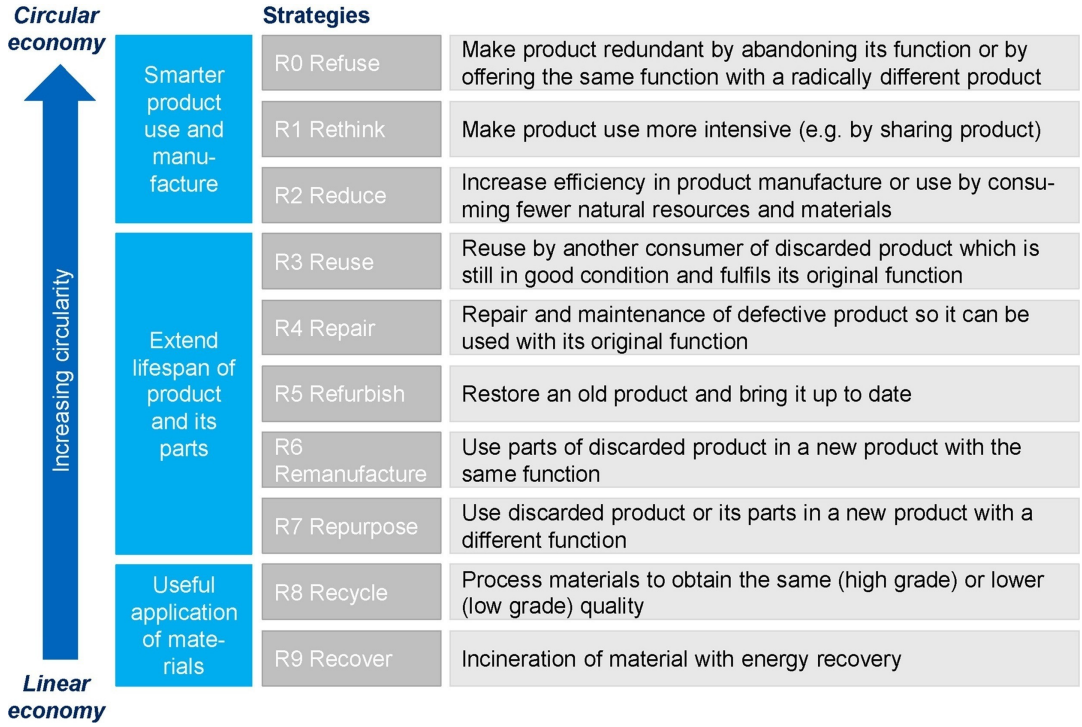

Figure 1.1: The 10R framework of circularity strategies [38]

The Dutch infrastructure consists of many concrete structures originating from the sixties of the last century. With increasing loads due to heavier and more frequent traffic, many of these structures are approaching their end of life or failing to meet current load capacity requirements. As a result, Rijkwaterstaat faces enormous challenges in terms of replacements and renovations in the coming years. The most significant challenges arise from major infrastructural projects within the Dutch road network, which includes approximately 1.700 bridges and viaducts constructed with prefabricated girders [63]. These girder bridges are composed of multiple concrete girders supporting the deck slab, allowing for the passage of traffic. Interestingly, 90% of the bridges and viaducts demolished over the past two decades did not reach their technical lifespan but were demolished for functional reasons [70]. These reasons often relate to changes in location and road design, causing the structures to no longer meet the requirements.

The girders from these types of bridges are prefabricated and prestressed, typically designed to last a hundred years. Due to early demolition for functional reasons, these girders often remain in good technical condition. The high quality of concrete used means that, in many cases, these prefabricated girders can last an additional hundred years. According to the feasibility study by SBIR Circulaire viaducten, prefabricated girders are suitable for direct reuse [63]. Not immediately reusing these girders for the same function is a missed opportunity to enhance circularity in this polluting industry. An adjustment in structural design could promote the reuse process and align with the ambitions of The Ministry of Infrastructure and Water Management.

1.2. Objectives

It has become clear that the potential of reusing prefabricated girders is enormous. However, the prefabricated girder systems do not take into account the idea of reusing these girders. This can lead to high costs due to dismantling, adjusting, and strengthening the girders. This research focuses only on the prefabricated inverted T-girders with a compression layer still in use in the Netherlands. The objective of this research is to make optimal use of the reuse potential of these prefabricated inverted T-girders. This is achieved by investigating several adjustments to the inverted T-girder system to facilitate future use of the girders. The focus is on design adjustments to enhance the disassembly

process of the girders without affecting the structural capacity. The outcome of this research will provide a better understanding of the force and stress distribution within the inverted T-girder system, revealing the influence of each structural component. Furthermore, the result offers a proposal for adjustments to the inverted T-girder system to facilitate both disassembly and future use of the girders while ensuring structural integrity.

1.3. Research questions

Following the objectives as stated in the previous section, the main research question is as follows:

> "How can the inverted T-girder system be adapted to improve the circularity during the disassembly and reassembly process in the future?"

In this context, improving the circularity refers to ensuring that the inverted T-girders can be relatively easily reused several times, including cost reduction, reduction of carbon dioxide emissions, and less energy consumption. This main research question is supported by several sub-research questions to clarify the intermediate steps that are necessary to answer the main research question:

- What are the main challenges in efficiently disassembling prefabricated inverted T-girders?
- How is the stress distributed within the current design of prefabricated inverted T-girder systems and what roles do different structural components play in maintaining overall stability and load-bearing capacity?
- How do different structural design adjustments aimed at improving the disassembly and reassembly efficiency of inverted T-girders affect the overall structural performance of the system?
- To what extent is the assessment of an orthogonal system representative of other systems with a certain skew angle?

1.4. Scope

The research conducted to address the research questions is confined to the following points, defining its scope:

- It is assumed that reusing girders contributes to a circular economy and provides environmental benefits, without determining the definitive environmental impacts.
- The systems covered are prefabricated, prestressed, concrete inverted T-girder systems with a cast-in-situ concrete compression layer part of the Dutch infrastructure.
- The case study used in this study is simplified to an orthogonal system with symmetrical characteristics.
- The system is modelled as simply supported on discrete bearing pads without incorporating reinforcement and prestressing steel
- The system is subjected to dead loads and live loads, excluding self-weight, impact, wind, seismic and thermal loads.
- The material properties and critical load configurations are based on the Eurocode and Dutch Annexes provision.
- A linear static analysis is conducted using shell elements.

1.5. Research methodology

This section outlines the research methodology employed to address the main research question through the development of structural design adjustments. A top-level view of the research methodology is presented by Figure 1.2.

First, a comprehensive literature review is conducted to provide relevant background information on the general design and structural performance of prefabricated inverted T-girder systems with a compression layer. This review includes a theoretical analysis of stress and force distribution within the inverted T-girder system. Additionally, current disassembly methods are examined to identify the challenges associated with the disassembly and reassembly processes of these girders.

Following the literature review, an extensive analysis is carried out using a numerical model based on the Finite Element Method (FEM). The model, developed with the DIANA FEA software, performs a linear analysis and serves multiple purposes. The numerical model helps to understand the structural behaviour of the base system by analysing the distribution of forces and stresses.

The model also provides a framework for evaluating various structural design adjustments to facilitate the disassembly of the girders. Various design modifications are modelled and assessed for their feasibility and impact on the system's structural performance.

To ensure broader applicability, the findings of the design adjustments are evaluated for their relevance to other systems with skew angles. This involves assessing the effect of skewed systems on all results to determine the validity of the findings obtained from the orthogonal system. Ultimately, the discussions and conclusions can be drawn upon the findings and their relevance across different system configurations.

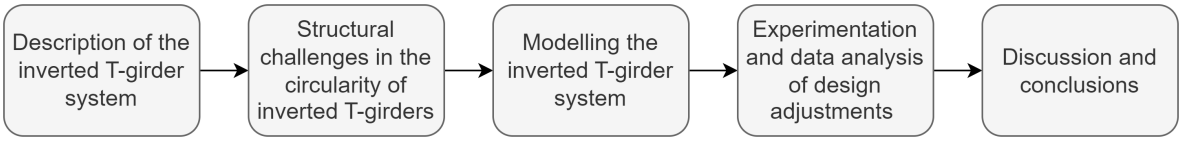

Figure 1.2: Top-level view of research methodology

1.6. Thesis outline

The report is structured into nine chapters: Introduction, Literature Review, Case Study, Finite Element Analysis, Structural Performance of the Inverted T-Girder System, Effect of Design Adjustments, Effect of Skewness on the Behaviour of Inverted T-Girder Systems, Discussion, and Conclusion and Recommendations. An overview of these chapters, along with the specific sub-questions addressed in each, is provided in Figure 1.3.

In chapter 2, a literature review provides essential background information on the operation of the inverted T-girder system, covering design principles and structural performance. Additionally, current methodologies for reusing girders are examined to identify the challenges associated with the reuse of inverted T-girders, addressing sub-question 1.

In chapter 3, a description of the case study used to construct the numerical model is presented. This includes details on structure geometry, supporting conditions, material properties, and loading conditions, including dead loads and critical live load configurations.

In chapter 4, the numerical considerations of the model are detailed. The modelling approach, boundary conditions, and loads are explained, along with the processing of the results.

In chapter 5, the structural performance of the inverted T-girder system is evaluated to answer sub-question 2. An analysis of the base system is conducted to explore the internal force and stress distribution, assessing the contribution of various structural components.

In chapter 6, the impact of various design adjustments on the inverted T-girder system is examined. The influence of these adjustments is evaluated under critical load conditions and compared to the base system, addressing sub-question 3.

In chapter 7, the effects of different skew angles on the modified systems are analysed to assess the applicability of the orthogonal system findings to skewed systems, answering sub-question 4.

In chapter 8, the results and model considerations are discussed comprehensively.

In chapter 9, the study's conclusions are presented through the answers to the research questions, followed by recommendations for future research.

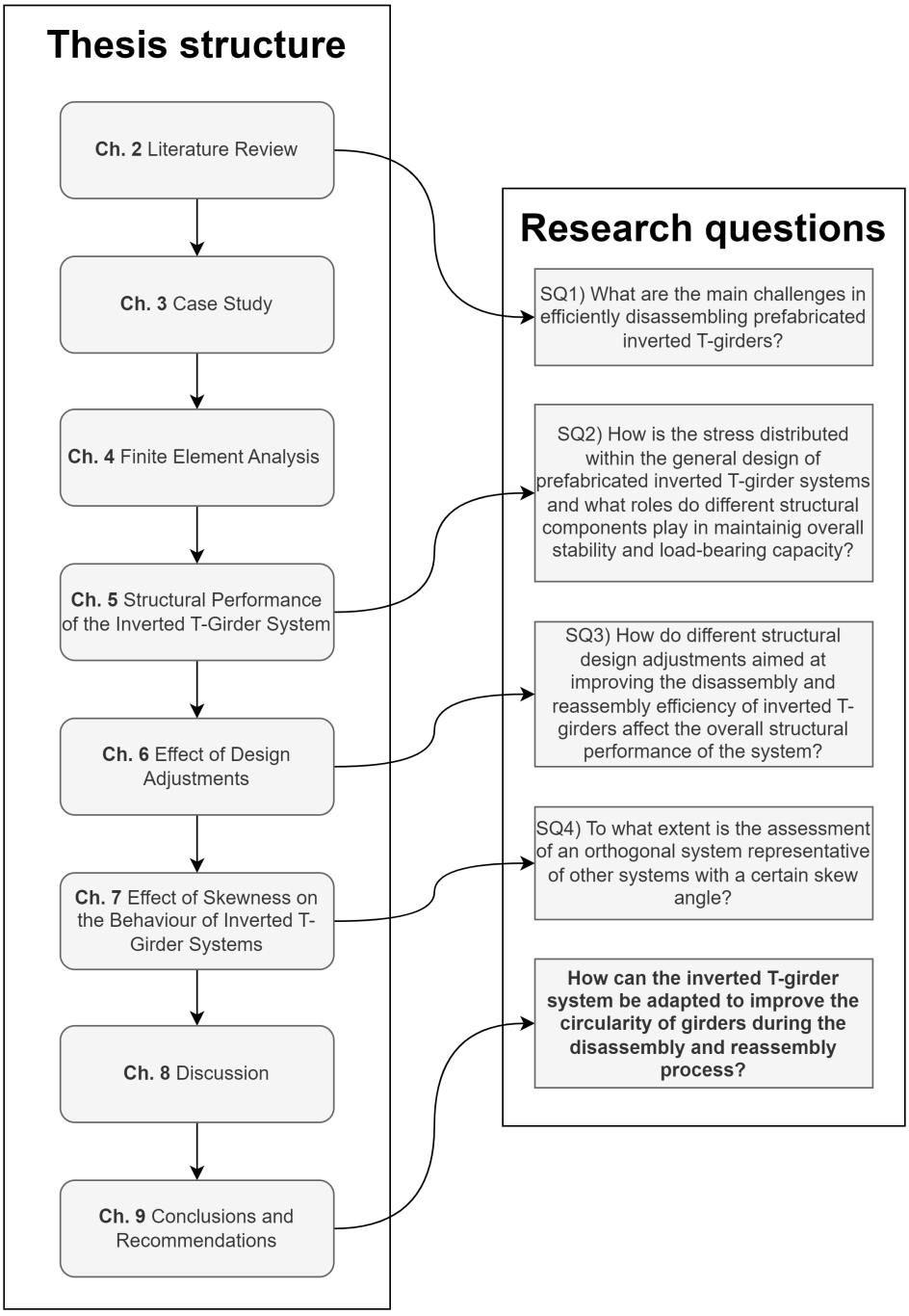

Figure 1.3: Thesis outline and overview of chapters addressing the research questions

2

Literature Review

This chapter offers relevant background information on the operation of an inverted T-girder system. It covers the design principles and contribution of structural components, providing a comprehensive understanding of its functionality and structural performance. Subsequently, current methodologies facilitating the reuse of girders are examined to explore the challenges in enabling the reuse of inverted T-girders.

2.1. General design of the prefabricated inverted T-girder system

As described in Section 1.4, this research focuses on prefabricated inverted T-girder systems, because this girder system is most commonly used in the Netherlands and has a beneficial ratio between prefabricated and cast-in-situ concrete for reusability. An overview of various types of prefabricated girder systems in the Netherlands is presented in Appendix A. In addition, the quantitative feasibility is high according to SBIR Circulaire Viaducten [63]. First, the layout of a general inverted T-girder system is described. Second, the commonly used types of inverted T-girders in the Netherlands are introduced and described.

2.1.1. Layout of prefabricated inverted T-girder system

A viaduct or bridge is a structure that spans horizontally between two supports to overcome various obstacles like roads and rivers. This civil engineering structure generally consists of a sub- and superstructure, as illustrated in Figure 2.1. The superstructure is the top part of the structure and mainly includes the girders and deck layers. The bottom part of the structure is referred to as the substructure and primarily includes the piers, abutment, and foundation. The main objective of a viaduct or bridge is to transfer the load coming from the superstructure to the soil. The different components of the superstructure and substructure are connected by bearings to ensure an even distribution of the loads.

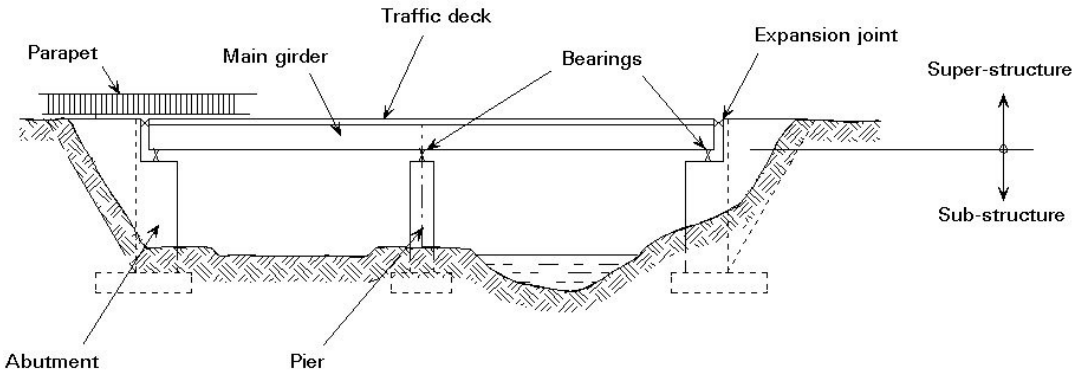

Figure 2.1: All major components of a concrete viaduct [4]

Superstructure

The superstructure of a prefabricated inverted T-girder viaduct consists of a series of prefabricated concrete inverted T-girders arranged side by side, topped with a cast-in-situ concrete deck. This deck serves as a platform to facilitate the passage of traffic and consists of a compression layer and a finishing layer. The compression layer forms a deck slab, which is connected to the girders through extended shear reinforcement from the web of the girders. The finishing layer, typically an asphalt layer, is applied over the compression layer to provide a smooth driving surface. The outer girders along the edges of the viaduct, known as edge girders, resemble the inverted T-girders but often have distinct shape characteristics. These edge girders are often accompanied by additional edge structures that serve an aesthetic function without contributing to the structural capacity of the superstructure. At each end of the span, cast-in-situ concrete beams, referred to as end transverse diaphragms, are constructed between the inverted T-girders to provide connectivity. These diaphragms are substantial, with their top matching the top of the compression layer and a typical width ranging from 500 to 1000 millimeters. Additionally, these diaphragms are provided with shear and bending reinforcement. While the top steel bars are placed above the girders, holes are created in the web of the girders to accommodate the bottom steel bars. The primary function of the superstructure components is to withstand vertical variable loads generated by traffic and transfer these loads through bearings to the substructure. The inverted T-girders are often prestressed with internal steel tendons, inducing compressive stress at the bottom of the girder. This prestressing stress helps counteract the tensile stresses that develop during service, enhancing the performance of the concrete girder [26].

Connecting different prefabricated concrete elements creates a complex structure where the development of stresses due to temperature variations and the shrinkage or swelling of concrete is a critical factor. Despite these challenges, a smooth transition between adjacent girders or between girders and the abutment is essential for traffic safety and comfort. To achieve this, expansion joints, as shown in Figure 2.2a, are employed. These joints allow for a smooth transition while enabling the individual elements to deform independently. Different expansion joints can be used to accommodate movements up to 900 millimeters [60]. The required deformation capacity depends on the total length of the span. The expansion joints are important in concrete structures because the complex functionality to withstand high loads while sealing the gap between two elements makes them vulnerable [60]. The leakage of water and deicing salts through the joints onto structural elements could impact the overall structural performance [18]. Besides, the generated disturbances by the joints in terms of noises and bumps should be mitigated as much as possible.

Moreover, the inverted T-girders in the superstructure might deform relative to each other, leading to internal stresses. To counteract these stresses, a unified structure with adequate transverse stiffness is created using cross beams. These cross beams are typically constructed on top of the supports at the ends of the span, known as end transverse diaphragms, as shown in Figure 2.2b.

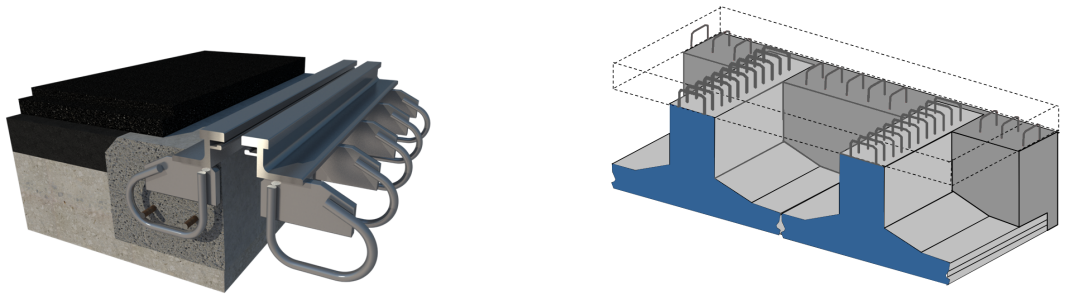

(a) Example of an expansion joint

(b) Example of an end transverse diaphragm

Figure 2.2: Examples of connection elements in the superstructure [79]

Bearings

The structural bearings form the connection between the super- and substructure and transfer forces. They stabilise the entire structure and permit translational and rotational movements while carrying

the loads. Translational movements include vertical and horizontal displacements, whereas rotational movements are induced by moments. The displacements and rotations at the supports can occur due to temperature changes, shrinkage of concrete, permanent and variable loads, and settlements of supports [33]. In theory, the pin bearing and roller-type bearing can be used in different combinations to create all possible degrees of freedom. However, in practice, these bearings are much more complex. They should permit longitudinal movements due to thermal expansion and contraction and allow rotations due to deflection caused by the dead and live loads [2]. Different bearing types are available to provide necessary restraints to the superstructure while avoiding unnecessary forces on both the super- and substructure by providing freedom to some displacements and rotations. Because of their complexity and vulnerability, bearings determine the durability and reliability of the complete structure [53]. It is therefore advisable to limit the number of bearings and make design provisions to make it possible to replace them [41].

The most common types of bearings at viaducts are the elastomeric bearing and pot bearing, which are shown in Figure 2.3. The elastomeric bearing consists of rubber layers separated by steel plates. The bearing accommodates movements by deformation and can take up small structural movements in longitudinal, transverse, and rotational directions [2]. In addition, the elastomeric bearing provides vibration isolation and is generally simple to install and perform maintenance [2]. The pot bearing comprises an elastomeric disk constrained by a metal cylinder and a close-fitting piston [33]. The dead load of the structure puts the elastomeric disk under high pressure and permits rotational movement in any direction. Translational movements can be accommodated by including a sliding surface. The pot bearing can accommodate greater movements and higher loads compared to the elastomeric bearing [33].

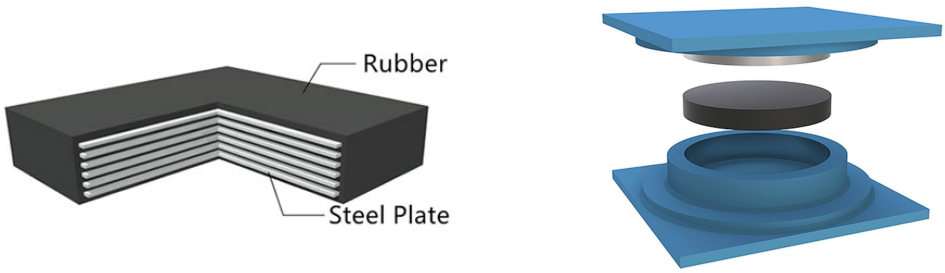

(a) Example of an elastomeric bearing **(b)** Example of a pot bearing

Figure 2.3: Most common types of bearings in viaducts

Substructure

The substructure of the prefabricated inverted T-girder viaduct includes all components located below the bearings. The primary components of the substructure include the piers, abutments, and foundation. The main function of these components is to transfer the load from the superstructure to the ground.

The piers are vertical structures that provide support to the superstructure, as illustrated in Figure 2.4. When the span required exceeds the maximum span capability of a single girder, intermediate piers are incorporated into the design. In the case of a prefabricated superstructure, a pier typically comprises one or more columns, a capping beam to support the girders, and a footing. Due to their substantial size and weight, piers are usually constructed with cast-in-situ concrete, as their large dimensions make transportation challenging.

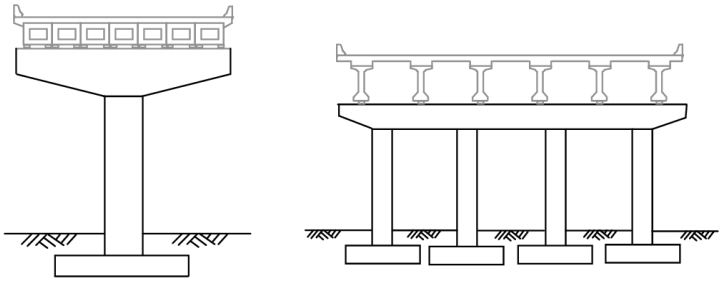

Figure 2.4: Different types of piers for prefabricated structures [37]

The abutments are located at the ends of the viaduct, as illustrated in Figure 2.5. They are designed to retain the soil behind the structure but also provide additional support to the structure in vertical and horizontal directions [76]. Many different types of abutments can be used in different configurations. The most common types of abutment support are piles, drilled shafts, and spread footings.

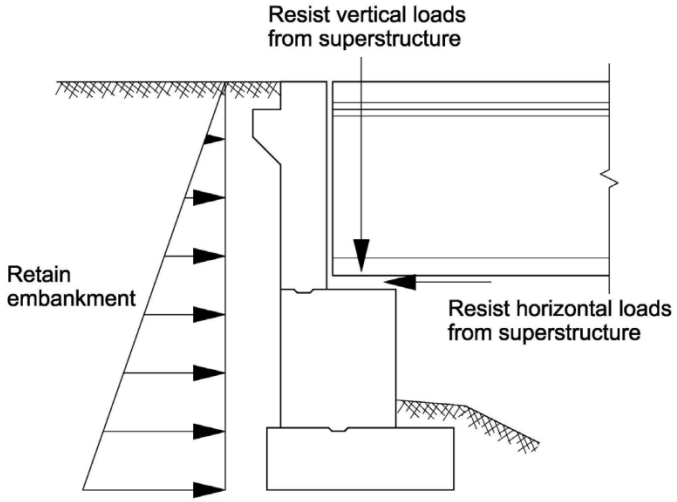

Figure 2.5: Example of an abutment in a viaduct [76]

The foundation transmits the load from the piers or abutments into the supporting soil. The main purpose of the foundation is to provide stability to the structure and distribute the loads over a large area of soil. Two types of foundations can be distinguished: shallow and deep foundations, as shown in Figure 2.6. Shallow foundations, also known as spread footings, are used for small and light structures. These foundations are placed close to the earth's surface and are easy to construct. In comparison, deep foundations are used for large and heavy structures and can be used on soft soils. The deep foundation uses piles that are drilled or driven into the ground to find a soil layer with sufficient bearing capacity. The load is mainly transmitted by the shaft or skin of the pile and partly by the base of the pile [73].

In the Netherlands, the soil is soft and does not have enough load-carrying capacity close to the surface. Therefore, mainly deep foundations with piles are used to transfer the load from the structure to a load-bearing soil layer (i.e. sand layer). Moreover, these piles can be drilled under a certain slope to create the optimal load distribution of horizontal and vertical forces.

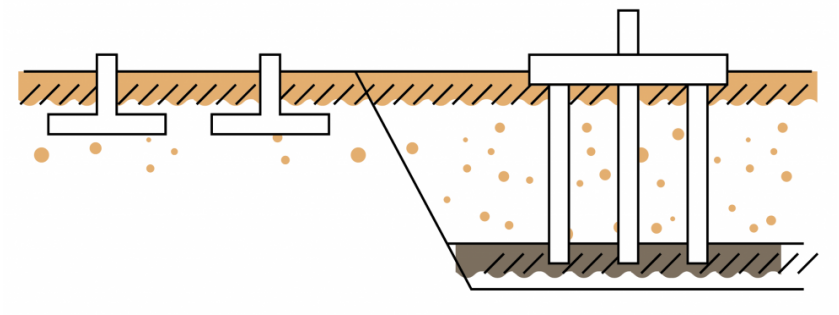

Figure 2.6: Shallow and deep foundations [29]

2.1.2. Structural system of superstructure

The most critical forces that a viaduct should withstand are the shear forces and moments. Shear forces primarily result from the structure's self-weight and variable loads on the deck. These loads are transmitted through the girders to the support via the bearings. Moments in the structure can occur around both transverse and longitudinal axes. Bending moments, arising around the transverse axis, are generated by loads causing the element to deflect. These bending moments play a crucial role in determining the structural integrity of the viaduct. Torsion moments around the longitudinal axis result from girders deforming independently. The stiffness of the entire structure provides resistance against these twisting forces and contributes to the overall stability of the structure.

Within structural mechanics, two main categories of structures are classified: statically determinate and statically indeterminate. Statically determinate structures have a known internal force system that can be analysed by using fundamental equilibrium equations [28]. In contrast, statically indeterminate structures involve more unknowns than can be solved with only equilibrium equations. Determining the internal force distribution requires additional conditions such as the compatibility conditions of deformations [28]. The prefabricated inverted T-girder system applies to both categories, but a statically determinate structure is often preferred due to lower hogging moments at the supports.

The type of bearings between the super- and substructure influences the stress distribution across the entire structure. For prefabricated inverted T-girders, the most commonly used structural system for the superstructure is the simply supported configuration. In this setup, each girder is individually supported by bearings at its end, requiring the incorporation of expansion joints at intermediate supports and between girders and abutments. This design permits almost all movements of the girders, preventing the generation of unnecessary stresses. Properly designed joints are crucial for preventing durability issues, such as the wear of bearings. The main advantages of simply supported decks include [79]:

- Girders installed directly on their final bearings
- Differential settlements do not affect the structural system
- Dimensioned joints accommodating thermal movements, creep, and shrinkage
- Results in durable structures

However, the main disadvantages of a simply supported superstructure are highlighted by [79]:

- Requirement for two rows of bearings at intermediate supports, resulting in increased expenses and the need for piers with larger surfaces
- Requirement for expansion joints, causing discomfort to traffic and susceptibility to durability issues in the presence of de-icing salt

The utilisation of multi-span bridges enables the spanning of larger distances. Initially, these bridges were designed with a series of simply supported girders. When H. Cross introduced the moment distribution of continuous beams in 1932 [12], the use of continuous decks commenced [56]. The continuity

of a deck plays a crucial role in the bending moment distribution over the girders, as illustrated in Figure 2.7. The implementation of continuous girders introduces a hogging moment at the intermediate support and a lower bending moment along the rest of the girders. This results in not only better structural performance but also allows for a reduction in the number of expansion joints and bearings, resulting in significant cost savings [56]. Nevertheless, the main disadvantages associated with a continuous deck system include increased complexity, higher construction costs, and the need for wider in-situ crossbeams [79].

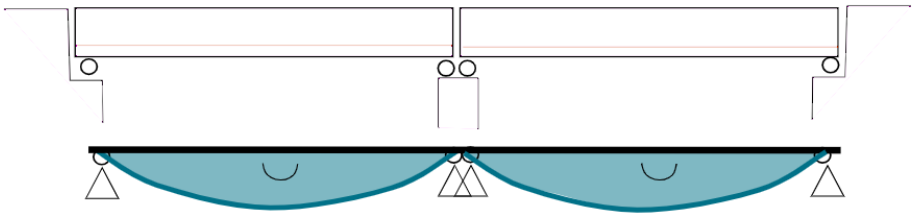

(a) Disjointed girders

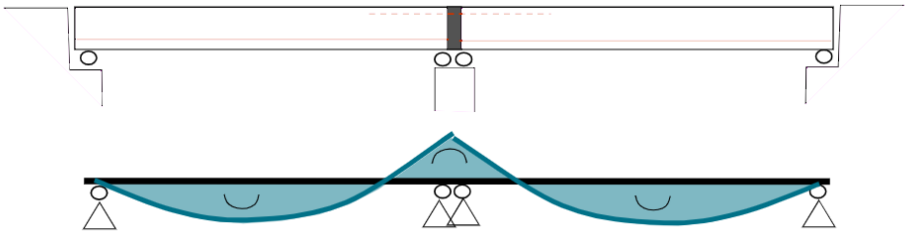

(b) Continuous girders

Figure 2.7: Impact of continuity spans on the moment distribution in multi-span structures [79]

Three solutions exist for providing continuity in the deck of a prefabricated inverted T-girder system. The first method involves expansion joints to only connect the deck. This approach results in a simply supported structure with separate girders and a discontinuous deck slab. The presence of joints in the deck slab not only results in discomfort for traffic but also requires frequent maintenance due to their susceptibility to wear and damage.

The second method addresses continuity in the deck by connecting adjacent girders using an integral reinforced crossbeam at the intermediate supports. Known as mechanical continuity, this connection establishes a continuous connection between the girders. It is important to note that this continuity only applies to additional loads, as the connection is constructed after the girders are simply supported. This statically indeterminate structure provides great structural performance, characterised by minimal moments and deflection [79].

The third method also uses simply supported girders as a starting point but provides continuity through the deck slab only. This approach referred to as partial continuity, includes the construction of the deck slab on top of the simply supported girders. However, it incorporates an elastic material to separate the deck slab from the crossbeams, allowing rotational movements. This debonded deck slab, illustrated in Figure 2.8 and referred to as the link slab, mitigates the effects of rotation by allowing the development of fine cracks within the link slab itself [66]. This method strikes a balance between the simplicity of a simply supported structure and the benefits of a jointless continuous deck slab. The incorporation of this method not only minimises maintenance requirements but also contributes to the overall structural performance by decreasing the continuous stress in the deck slab [74].

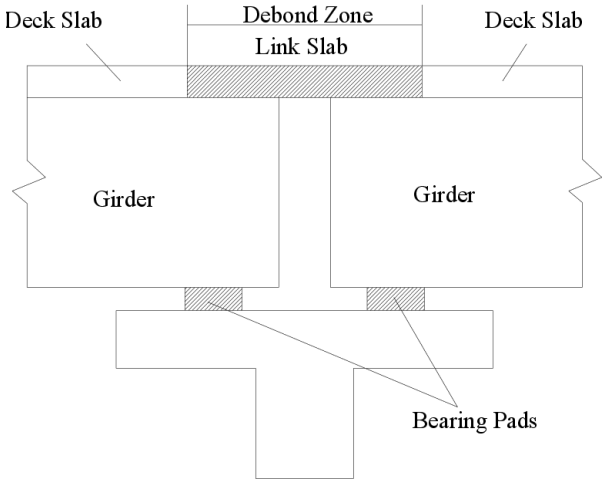

Figure 2.8: Partial continuity in prestressed girder bridges by using the link slab [48]

Eliminating the durability problems associated with bearings and enhancing structural efficiency, integral bridges are introduced as an alternative to conventional girder bridges. Distinguished by the absence of bearings and expansion joints, this design integrates the superstructure with the substructure. Rigid connections are established between the deck girders and the supports, as presented in Figure 2.9. This bridge design is suitable for both single- and multiple-span bridges. The resulting portal frame transfers all movements and rotations directly to the abutments, which are pushed into the soil. It is therefore accepted that these structures are subjected to secondary stresses induced by settlements, post-tensioning, and significant internal moments [7]. The simplicity of these structures contributes to faster and easier construction. However, the design can cause some problems related to the lack of flexibility in accommodating thermal expansion and contraction. Moreover, semi-integral bridges have been developed to optimise this bridge design by combining simplicity and necessary flexibility by incorporating bearings at specific locations.

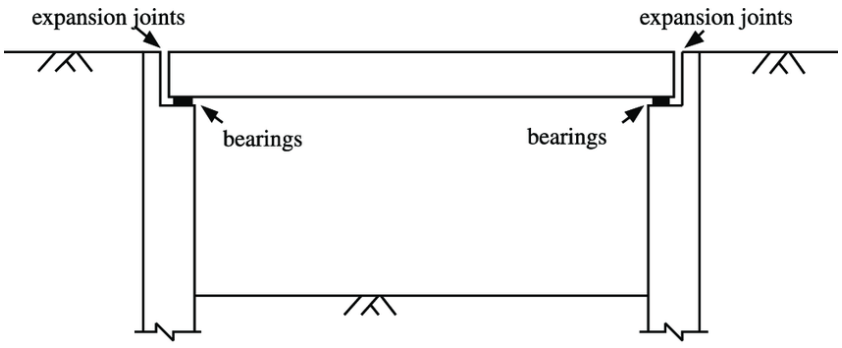

(a) Conventional bridge

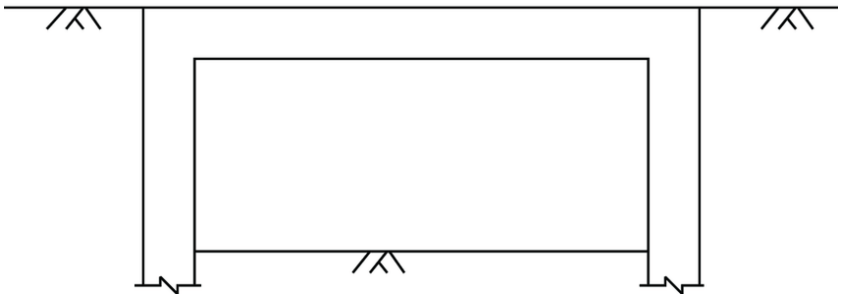

(b) Integral bridge

Figure 2.9: Comparison of a conventional bridge and integral bridge [77]

2.1.3. Different types of inverted T-girders

Over time, the inverted T-girder has found application in numerous infrastructure projects and has undergone various structural developments. Figure 2.10 shows the cross-sections of the predominant inverted T-girder types used in the Netherlands. The designs of Figure 2.10a till Figure 2.10d were designed by Spanbeton BV, whereas Haitsma designed the remaining cross-sections. Despite major differences in the girder's cross-sectional profiles, the structural principle of the inverted T-girder system remains unchanged, as discussed in Appendix A.1.3.

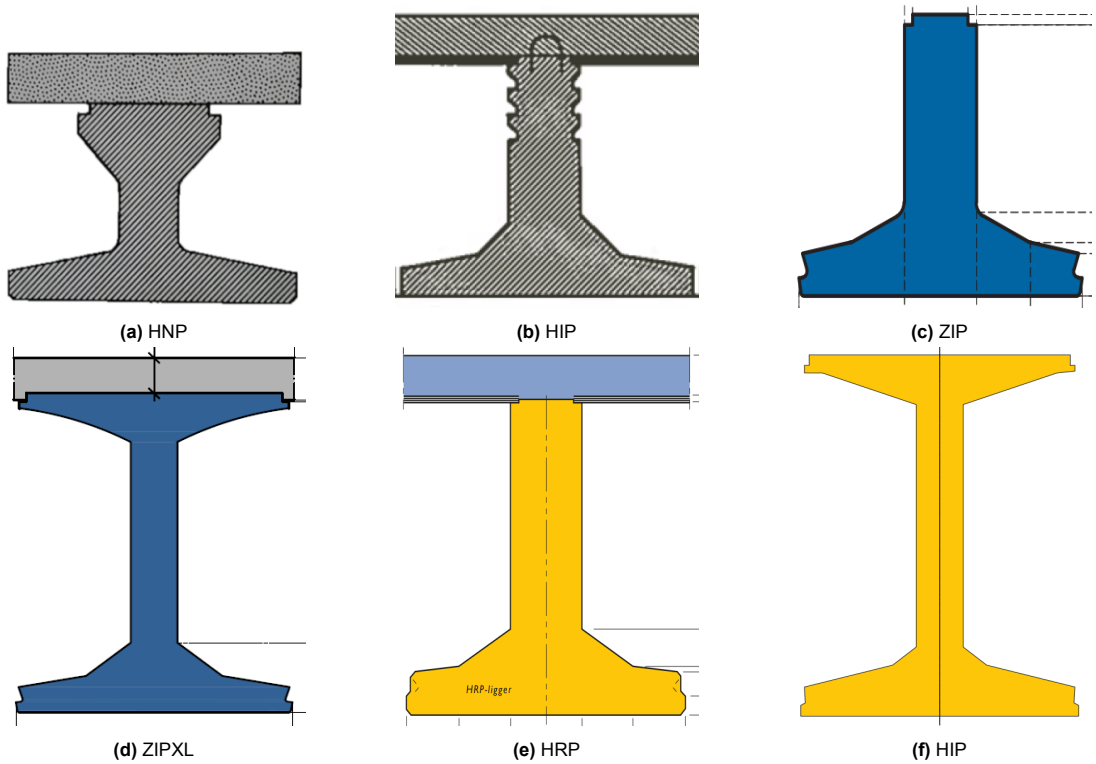

Figure 2.10: Cross-section of different prefabricated inverted T-girders [55] [10] [31]

HNP girder

The first generation of inverted T-girders was the HNP girder produced by Spanbeton BV from 1965 until 1972. These girders were used to span between 13 and 29 meters. The width of these girders was constant at 1000 millimeters and a varying height of 500 to 1000 millimeters. This profile has little to no shear reinforcement and is therefore incompatible regarding the required shear capacity with the more stringent standards nowadays [15].

HIP girder

The HIP girder introduced by Spanbeton BV in 1970 was the expansion to the HNP girder to fulfil the need for greater spans while concerning the economic interests [57]. With this girder spans up to 40 meters were possible. The girder has a constant width of 1200 millimeters and a variety in height between 500 and 1400 millimeters. In addition, the web of the girder was 300 millimeters and contained shear reinforcement [15].

ZIP girder

In 1973 Spanbeton BV introduced the ZIP girder which is identical to the HIP girder system but with some strengthening to withstand the collision load of the deck [57]. There are two types of this girder; ZIP and ZIPXL. The ZIP girder has a constant width of 1200 millimeters and a varying height between 500 and 900 millimeters. Spans up to 25 meters were possible to reach. The big brother, the ZIPXL, has a constant width of 1500 millimeters and a varying height of 1000 to 2400 millimeters. With this XL variant, spans up to 60 meters were available [10].

HRP girder
The HRP girder is designed by Haitsma and stands for 'Haitsma Rail Profiel' [31]. This girder is designed to span 15 to 45 meters. The standard width is 1200 millimeters and the construction height varies between 500 and 1600 millimeters [31].

HIP girder
The expansion of the HRP girder is the HIP girder which Haitsma also designs. The top and bottom flanges have the same width, making this an I-girder. These HIP profiles are suitable to span 40 to 65 meters and have a standard width of 1500 millimeters [31]. The construction height is varying between 1200 and 2000 millimeters [31].

An overview of all inverted T-girder profiles, along with their most important characteristics, is presented in Table 2.1.

Table 2.1: Overview of the key characteristics of various inverted T-girder profiles

Profile	Width [mm]	Height [mm]	Span [m]
HNP	1000	500-1000	13-29
HIP	1200	500-1400	13-40
ZIP	1200	500-900	13-25
ZIPXL	1500	1000-2400	10-60
HRP	1200	500-1000	15-45
HIP	1500	1200-2000	30-60

2.2. Structural behaviour of the inverted T-girder system

With the structural design of an inverted T-girder system described, a theoretical analysis of its structural behaviour can be performed. This section explores the structural behaviour of the entire superstructure, emphasising the interaction between structural components in terms of stiffness and efficient load distribution, using a single span simply supported at both ends. Subsequently, the stress distribution within an individual composite inverted T-girder is analysed and detailed.

2.2.1. Analysis of the systems structural response

Describing the structural behaviour of the inverted T-girder system involves understanding the response to external loads. These forces result in various internal stresses that can lead to failure if not adequately accounted for in the structural design. Especially, the ability to resist bending moments, shear forces, axial forces, and torsion moments is crucial to ensure the structural integrity and safety of the structure. Moreover, efficient load distribution significantly influences structural performance. By comprehending the behaviour of the complete system, one can evaluate the contributions of components and explore the feasibility of various design innovations.

In structural engineering, evaluating the load-bearing capacity of a structure involves two design criteria: the Ultimate Limit State (ULS) and the Serviceability Limit State (SLS). The ULS focuses on extreme conditions determining the maximum load a structure must withstand without failure, thereby ensuring its safety and reliability. Conversely, the SLS deals with normal operating conditions, ensuring that the structure remains functional and comfortable during regular use. This involves controlling factors such as vibrations, deflections, and crack widths to maintain the structure's durability and usability over time.

In the context of this research, the superstructure's system behaviour is analysed by evaluating the configuration of its structural components and assessing the system's stiffness and load distribution capabilities under ULS conditions. Specifically, the emphasis is on investigating the collaborative behaviour of all structural components when exposed to critical conditions.

Structural components

The superstructure of the prefabricated inverted T-girder system can be divided into four principal structural components:

1. Inverted T-girders
2. Edge girders
3. Deck
4. Transverse diaphragms

The primary load-carrying components within the inverted T-girder system consist of a series of simply supported prefabricated girders oriented in the longitudinal direction. Initially, these girders provide longitudinal stiffness without contributing to transverse stiffness due to their separation. Similarly, edge girders contribute to the system's stiffness but with different characteristics due to their distinct cross-sections. The in-situ deck slab connects the girders, creating a continuous composite system in both longitudinal and transverse directions. This integration enables applied loads at any point to be transferred through the girders to the supports. Furthermore, the deck slab enhances transverse stiffness by acting as a cross beam. The transverse diaphragms positioned at both ends of the girders further increase the transverse stiffness by rigidly connecting the girders in the transverse direction. Both the deck and transverse diaphragms play important roles in creating a unified system that facilitates bending in multiple directions.

Structural stiffness and arrangement in both directions

The superstructure of a viaduct or bridge is orthotropic and behaves distinctively in longitudinal and transversal directions due to varying stiffness and a different structural system. In the longitudinal direction, the bending stiffness is determined by the total cross-section of the combined girder and deck. In the transversal direction, the bending stiffness only relies on the height of the deck, resulting in lower stiffness than the longitudinal direction. In addition to the difference in stiffness, the presence of prestressing steel in the inverted T-girders further influences the longitudinal behaviour. Furthermore, the structural system varies in both directions, resulting in a different moment distribution, as illustrated in Figure 2.11. In the longitudinal direction, the girders are supported at both ends, resulting in a simply supported deck. Conversely, each girder forms a support in the transverse direction, resulting in a continuous deck slab with multiple supports. The corresponding moment distribution shows hogging moments above each girder and lower deflection moments between the girders.

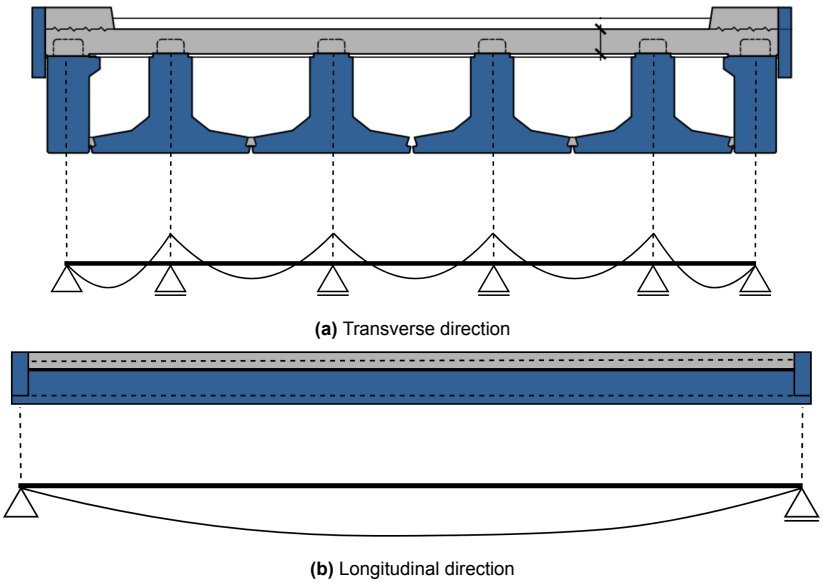

(a) Transverse direction

(b) Longitudinal direction

Figure 2.11: Cross-section of the superstructure in both directions with corresponding moment distribution

Load distribution

The behaviour of a structural system can be defined by the transfer of applied loads across its components toward the supports. Load distribution predominantly depends on the arrangement of girders and the system's stiffness in both longitudinal and transverse directions. As described, longitudinal stiffness mainly relies on the girders themselves, while the presence of the deck slab and transverse diaphragms enhances transverse stiffness. Greater transverse stiffness ensures a more efficient load distribution, ensuring uniform deformation of the deck slab, with multiple structural elements participating. Traditionally, multiple cross beams were installed along the span to provide sufficient transverse stiffness. However, these cross beams have been omitted for simplicity reasons and to mitigate labour-intensive processes, resulting in a less effective system [64]. Consequently, the torsional stiffness of principle structural components significantly influences transverse load distribution [81].

The load distribution of a concrete girder bridge can be analysed using the Guyon-Massonnet method, which details the distribution of moments and forces in slabs supported by a grid of beams. This semi-empirical approach determines the deflection of a deck slab in both longitudinal and transverse directions by describing the orthotropic slab behaviour with a fourth-order differential equation. Appendix B provides the background and derivation of this equation. The inputs for this equation include the geometry of the deck slab and its flexural and torsional stiffness. In linear elastic systems, the slab deflection is directly proportional to the load distribution.

The Guyon-Massonnet method demonstrates the influence of various structural properties on the load-bearing capacity of a slab. The method highlights that higher torsional stiffness enhances the slab's ability to distribute loads in the transverse direction. Additionally, the method shows that lower longitudinal flexural rigidity relative to transverse flexural rigidity further improves transverse load distribution. When cracking occurs in the slab or transverse cross beams, the transverse flexural rigidity decreases. According to the Guyon-Massonnet method, this reduction leads to an overall decrease in flexural stiffness, significantly affecting the transverse load distribution. Moreover, the method indicates that load distribution is independent of the slab's thickness, emphasising that the slab stiffness and structural properties over more critical than geometric dimensions in determining load distribution patterns.

Research on the effectiveness of component collaboration

Now that the system behaviour of the superstructure has been thoroughly clarified through theory, the importance of the contribution of all structural components has become clear. Although most concrete research tends to emphasise the capacity of individual components rather than the whole deck, there are a few relevant examples of studies that highlight the importance of system collaboration in girder systems.

One example is the research done by Ensink et al. (2018) [20] in which multiple experiments are conducted on a simply supported multi-span T-girder bridge, consisting of prestressed T-girders and cross-beams, subjected to an individual point load. A part of the experiments was carried out with the original structural system unchanged, consisting of connected T-girders. The other part of the experiments was carried out on the individual T-girder, separated by sawing the cast-in-situ deck in the longitudinal direction. The results from the experiments show that the bridge deck with connected T-girders can resist very high loads compared to the individual T-girder.

Another example is the research done by Murray et al. (2018) [50] and Murray et al. (2019) [49] in which prestressed I-beams are tested individually and compared to a bridge deck, consisting of similar prestressed I-beams connected by a cast-in-situ deck slab and transverse diaphragms. The experiments show that the bridge deck and transverse diaphragms provide additional load distribution after girder failure and allow two-way bending of the deck slab, suggesting different behaviour than typically assumed. These load transfer capabilities affect the failure mechanism of the bridge, potentially increasing the capacity.

Another example is the study done by Ensink (2024) [21], which provides an extensive analysis of the system behaviour in prestressed concrete T-beam bridges. The main part of this research is a case

study of a typical concrete T-beam bridge in the Netherlands. The study demonstrates how the interaction of elements within the structural system enhances the ultimate load capacity of the main T-beams. Using experimental, numerical, and analytical methods, including a full three-dimensional nonlinear finite element model, the research reveals that the system behaviour significantly differs from that of an individual T-beam due to the contribution of secondary load-bearing mechanisms. While traditional assessments of these bridges often overlook these mechanisms, Ensink's research highlights their role in increasing the bridge's overall capacity.

The studies conducted show the importance of cooperation among various structural components in enlarging the load-bearing capacity. This collaboration hinges upon the overall coherence of the system, which relies on the connections between the structural components. The transverse stiffness is therefore an important characteristic of the system. Its presence facilitates the transverse load distribution across the deck, resulting in the involvement of multiple girders. This more effective load distribution improves the structure's load-bearing capacity and durability [50].

As demonstrated by Ensink (2024) [21], the cooperation among structural components not only increases the system's structural capacity but also activates secondary load-bearing mechanisms that further enhance the overall capacity. These mechanisms involve compressive membrane action (CMA) in the deck and arch action in the girders. When structural deformations combine with lateral restraints, internal compressive arches form, generating compressive membrane forces, as illustrated by Figure 2.12. These mechanisms are identical for slabs and beams and can substantially enhance the load-bearing capacity of prestressed bridge decks [1]. This hidden residual capacity is traditionally not considered but could have a positive effect when reusing the girders.

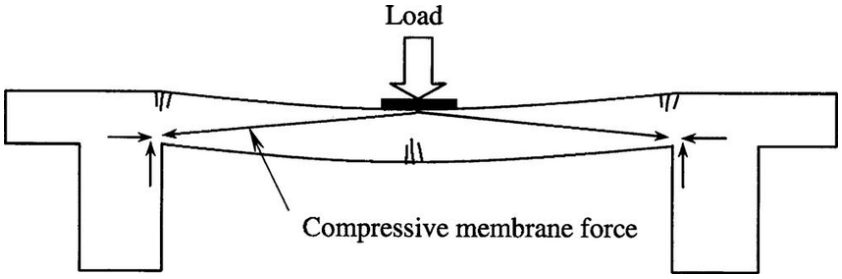

Figure 2.12: Visual representation of CMA in both concrete deck and girders [19]

2.2.2. Assessment of the individual inverted T-girder

The structural response of the individual composite inverted T-girder can be described using a statically determinate simply supported girder, as illustrated in Figure 2.13. This homogeneous concrete girder demonstrates linear-elastic behaviour, primarily experiencing dead loads, live loads, and prestressing forces. These loads induce internal forces expressed by shear forces, bending moments, and torsion moments. Consequently, internal stresses develop within the girder, comprising both normal and shear stresses. The normal stresses are oriented perpendicular to the cross-section, whereas shear stresses are oriented parallel to the cross-section. The internal forces always maintain equilibrium with the external forces along the entire length of the girder.

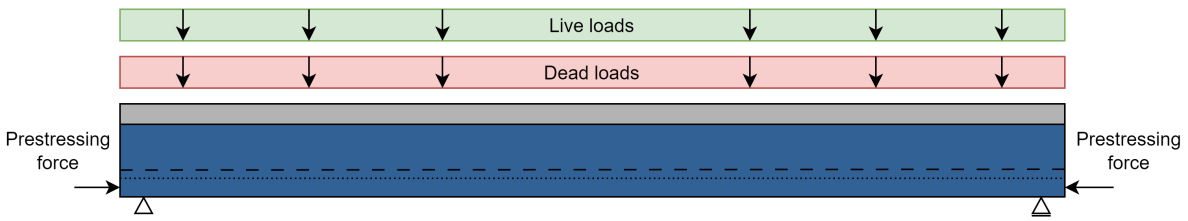

Figure 2.13: Overview of inverted T-girder subjected to dead loads, live loads, and prestressing forces

Inverted T-girder construction design

As a building material, concrete's material properties are much stronger in compression than in tension. The occurrence of tensile stresses should be therefore taken up by another material that is strong in tension such as steel. Moreover, different techniques such as arching or prestressing offer solutions to mitigate tensile stresses. The considered prefabricated inverted T-girders are both reinforced and prestressed to improve the structural integrity of the concrete girder. The method of prestressing that is mainly used for the production of prefabricated bridge girders is prestressing with pre-tensioned steel. This method stresses the steel tendons by elongating them at the ends before pouring the concrete into the inverted T-girder mould. After hardening the concrete, the tension in the tendons is released by cutting them at the girder's ends. The tendency of the steel tendons to return to their original state creates a firm connection by the expansion of the tendons. These tendons then exert a compressive force on the concrete over their entire length. The prestressing force is gradually transferred at both ends over a certain transmission length. Adjusting the transmission length by detaching prestressing steel and concrete can be used to optimise the bending moment distribution. Since the prestressing steel is concentrated below the centroidal axis of the girder, it naturally induces an upward curvature in the girder. Simultaneously with the release of the prestressing force, the self-weight of the girder is mobilised, resulting in the moment distribution, as illustrated in Figure 2.14a.

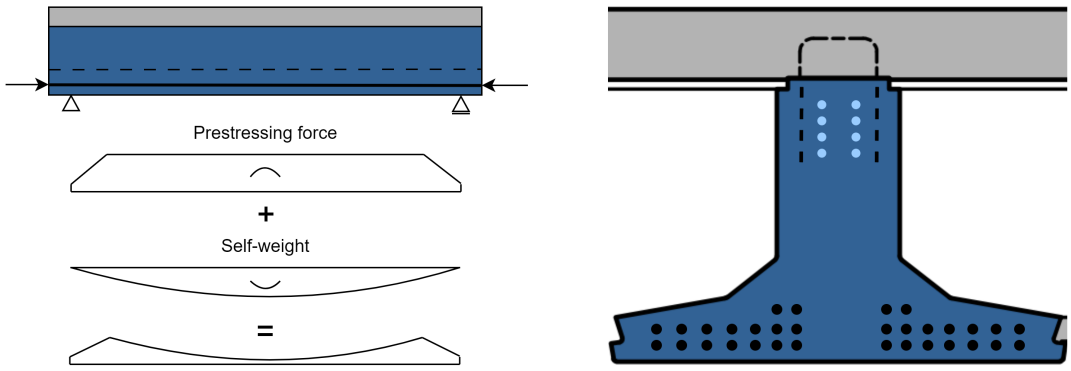

(a) Moment distribution due to prestressing force and self-weight

(b) Cross-section detailing prestressing steel and reinforcement

Figure 2.14: Structural design of individual inverted T-girder

The shape of the inverted T-girder is characterised by its optimal material usage and suitability for incorporating prestressing steel into the bottom flange due to the space availability. Typically, reinforced concrete girders start to crack at relatively low loads due to concrete's limited tensile strength. After cracking, the longitudinal reinforcement takes over the tensile stresses, withstanding bending moments, and controlling concrete crack width. However, this system diverges from the conventional approach as it operates mainly under compression during service conditions (SLS) due to the prestressing force. Consequently, longitudinal reinforcement may only be needed at the top to absorb potential tensile forces immediately after the release of the prestressing force. Additionally, split reinforcement at the supports within the bottom flange can be necessary due to concentrated forces for controlling the crack width. Figure 2.14b illustrates the layout of the longitudinal reinforcement and prestressing steel, marked by blue and black dots respectively, within the cross-section of the composite inverted T-girder. Notably, the stirrup reinforcement surrounding the longitudinal reinforcement is not shown; only the hairpins between the girder and the deck are presented.

Stress distribution within the composite girder

To provide a better understanding of the behaviour of the girder, the internal stress distribution within the composite girder is analysed. Normal stresses arise due to axial forces and bending moments, whereas shear stresses are generated by forces acting perpendicular to the girder's cross-section, involving shear forces and torsion moments. Figure 2.15 illustrates the stresses generated by bending and torsion moments in a cross-section.

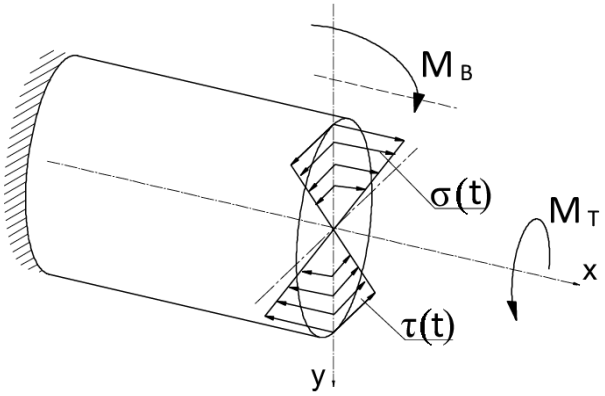

Figure 2.15: Normal and shear stresses due to bending and torsion moments [42]

The normal stress distribution of the composite girder is analysed by examining the stress development during various construction stages. Since this distribution varies along the length of the girder due to changes in internal bending moments, the cross-section is examined at mid-span. Furthermore, the equations for calculating the maximum stress values at the top and bottom of the girder are provided in the figures.

In the initial stage of the composite system's life, the prestressed inverted T-girder exists just a few days after fabrication in the factory. At this stage, the inverted T-girder is subjected only to the prestressing force and its self-weight. The eccentric compressive force exerted by the prestressing steel can be described as an axial force combined with a bending moment, inducing high compressive stresses at the bottom and minor tensile stresses at the top of the girder. Consequently, the resulting forces are primarily compressive, as illustrated in Figure 2.16.

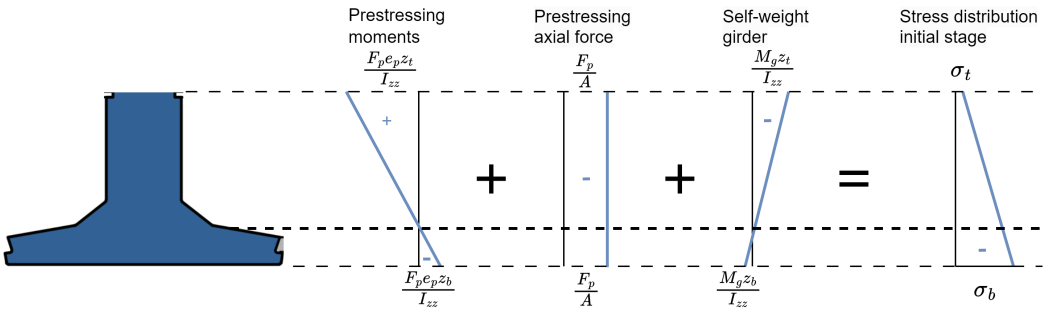

Figure 2.16: Normal stress distribution at the initial stage

The intermediate stage occurs during the casting of the compression layer, following the girder installation in the structure but before the cast-in-situ concrete has hardened. At this stage, the girders bear an additional load from the self-weight of the compression layer. The resulting stress distribution is presented in Figure 2.17.

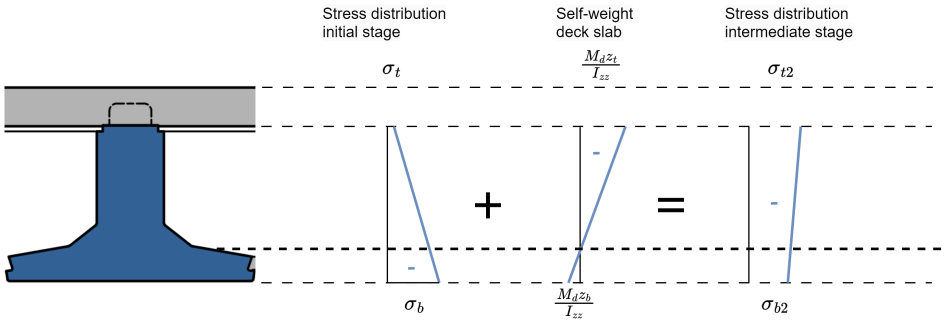

Figure 2.17: Normal stress distribution at the intermediate stage

The final stage involves the composite action of the system after the compression layer has hardened. At this stage, the components of the system function as a single cross-section, altering the position of the neutral axis. During service, the composite system must support additional dead loads from the asphalt layer and live loads from passing traffic. The stress distribution observed during service is illustrated in Figure 2.18. The discontinuity in the stress distribution is due to the varying stiffness between the compression layer and the girder. This variation in stiffness, combined with an equal strain, causes a jump in stress values at the connection.

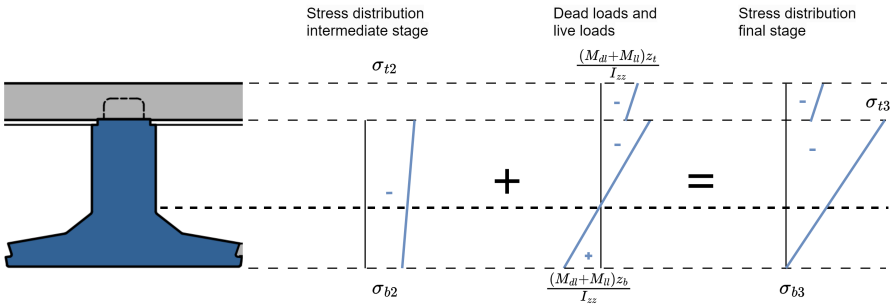

Figure 2.18: Normal stress distribution at the final stage

In addition to normal stresses, shear stresses arise due to shear forces and torsion moments, flowing parallel to the cross-section. The shear stress distribution from shear force is uniform across the width of the web, while shear stresses from torsion moments are linearly distributed, with extreme values at both ends. Figure 2.19 illustrates the flow parallel to the cross-section and shows the total shear stress distribution over the complete height of the composite girder. The maximum shear stress is observed in the middle of the cross-section and is primarily carried by the girder's web. These vertical shear stresses are complemented by horizontal shear stresses along the girder's length to maintain equilibrium. The shear stresses from torsion moments occur when the girder experiences torsion moments due to eccentric loading, the curvature of the alignment, or the skew angle of the girder. The magnitude of these shear stresses within composite girders is significant at the ends, where the girders are restrained against rotation. Both shear stresses develop concurrently within the girder and can influence each other, potentially leading to higher stress magnitudes within the cross-section. This could lead to higher shear stress magnitudes within the cross-section. Furthermore, the presence of the deck slab significantly increases the stiffness and torsional rigidity of the girder system. This results in a more uniform stress distribution along the length of the girder, reducing stress concentrations at specific locations.

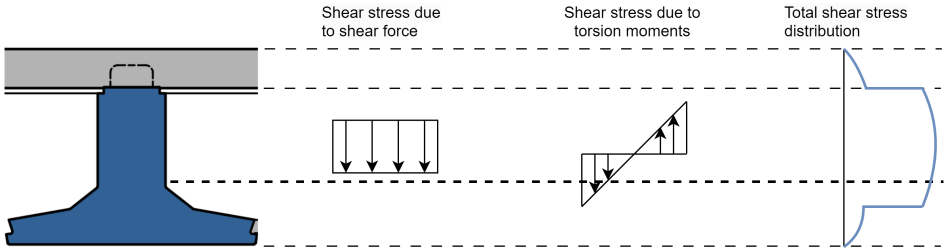

Figure 2.19: Shear stress distribution of the composite girder

Time-dependent effects

Besides the immediate response of a girder under load, time-dependent effects significantly influence concrete behaviour, especially shrinkage and creep. Shrinkage refers to the change in length or volume of a non-stressed concrete element caused by changes in moisture content or chemical reactions. Conversely, creep is defined as the gradual deformation of a concrete element over a long-term period under stress. Restraining these time-dependent effects through the supports or for example with the bonding of steel [27] or the casting of new to old concrete [59], introduces additional stresses within the cross-section of the composite system. These stresses could considerably impact the structural performance, causing substantial deflections and increasing crack widths, potentially leading to serviceability failures. Moreover, both shrinkage and creep contribute to a reduction in prestressing force over time. This effect is enhanced by relaxation, a time-dependent material property of steel characterised by stress reduction at a constant material strain.

Structural response during its operational lifespan (SLS)

The composite system formed by the prefabricated prestressed girder and the in-situ deck slab combines two distinct concrete elements into a single cross-section. Throughout its operational lifespan, the behaviour of the girder is influenced by various loads and time-dependent factors, resulting in changes to the stress distribution. Understanding the stress distribution within the composite system is crucial for ensuring durability when preparing the girders for a second service life.

Figure 2.20 - 2.22 provides an overview of the stress distribution within the composite inverted T-girder, showing key moments from its construction in the factory to the end of its initial service life and preparation for reuse. These figures aim to provide insight into the evolution of stress distribution during the life cycle of the composite girder and are conceptual rather than based on calculations.

Initially (at t=0), concrete is poured into the mould containing prestressing and reinforcing steel. Several days later (at t=3-5), the prestressing force is released, exerting a compressive force on the girder and mobilising its self-weight. The girder reaches its full strength after 30 days, allowing for its installation in a structure. In practice, the girder is often installed after approximately 50 - 60 days with the cast-in-situ compressive layer initially adding its self-weight as a distributed load before contributing to the system. After the hardening of the cast-in-situ concrete, the composite system begins to function collectively. Approximately 100 - 200 days into the process, the additional dead loads in the form of the asphalt layer are introduced, making the system ready for its service life.

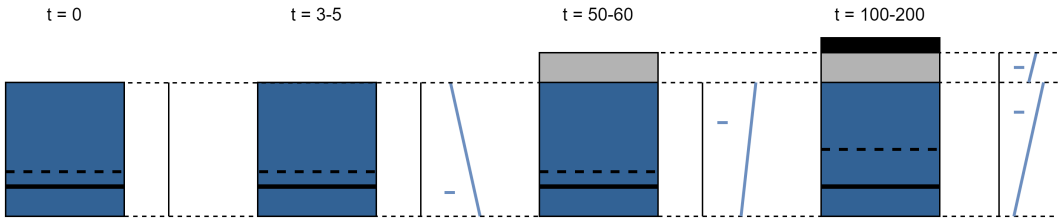

Figure 2.20: Stress distribution of the composite inverted T-girder during its construction

At the start of its service life at around 100 - 200 days, the composite girder is subjected to dead loads with minimal time-depend effects and live loads. As the service life progresses (t=∞), the time-dependent effects due to the dead loads become more present, leading to additional self-weight and a prestressing force in the compression layer due to creep. Additionally, the prestressing force on the girder decreases due to shrinkage and relaxation, leading to an overall assumption of decreasing compressive stress values on the top side of the composite girder. Figure 2.21 shows the stress distribution at the beginning and end of its lifespan with a distinction in the stress distribution due to the dead- and live loads.

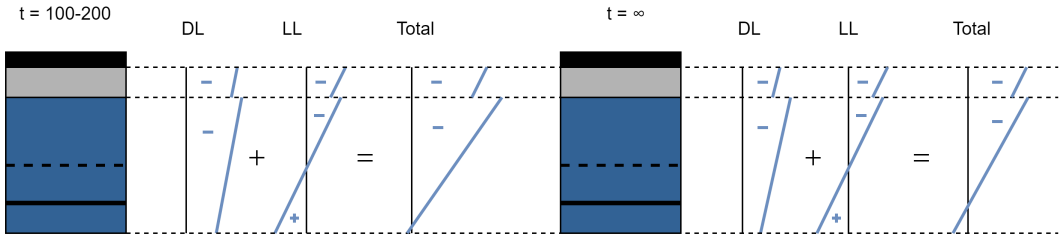

Figure 2.21: Stress distribution of the composite inverted T-girder during its service life

Figure 2.22 illustrates the stress distribution of the composite girder during the reuse process. Preparing the inverted T-girder for future use begins with the removal of the asphalt layer, which reduces distributed loads. Following the disassembly of the girder, the compression layer is partially removed, restoring the girder to its original shape with reduced compressive stresses from the unchanged prestressing force. When reusing these girders, it is important to consider the reduced compressive stress remaining in the girders, as it increases the potential risk of exceeding the concrete's tensile stress capacity.

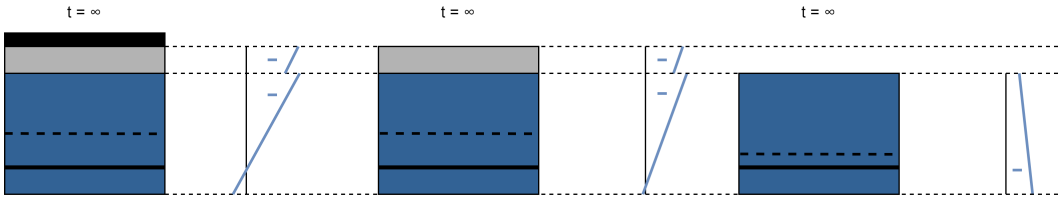

Figure 2.22: Stress distribution of the composite inverted T-girder during its reusing process

Structural response at failure (ULS)

The stress distributions of the composite girder, as shown in Figure 2.20 - Figure 2.22, help by understanding the structural behaviour under SLS conditions. However, the girder's stress distribution in the ULS could be decisive when ensuring its safety and reliability. Therefore, Figure 2.23 shows the stress distribution of the composite girder under ULS conditions, representing the behaviour of the structure when approaching failure. Here, a distinction is made between the consequences due to dead and live loads.

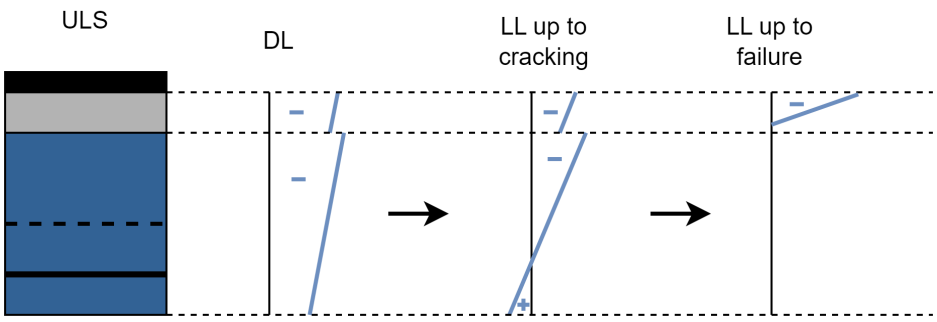

Figure 2.23: Stress distribution of the composite inverted T-girder under ULS conditions

2.3. Current methods to enable reuse of prefabricated girders

Improving the circularity of prefabricated inverted T-girders involves a shift in design considerations to facilitate future disassembly and reassembly processes. As described in Section 1.1, some girders have already been successfully reused after being disassembled from their original structures. This section outlines the current methodologies for disassembling, modifying, repairing, and strengthening prefabricated inverted T-girders.

2.3.1. Disassembling of prefabricated girders

The circularity process starts with the disassembly of various structural elements. This disassembly process shows similarities to the conventional demolition process of concrete structures, primarily driven by transport capacity considerations. However, in contrast to typical demolition, the disassembly process demands precision and accuracy. This is necessary to ensure that reusable elements retain their structural integrity and functionality. Throughout the process, the safety and stability of the structure should always be guaranteed. Numerous factors influence the disassembly process with hindrances to the surrounding environment being of primary concern. In the Dutch infrastructure, factors such as duration, noise, and traffic hindrances emerge as critical considerations. The ambient traffic should not be limited by supporting constructions or potential issues like the leakage of cooling water from the sawing process [71]. When dealing with a viaduct, a temporary sand layer is often applied to the underlying road to provide protection.

The traditional demolition process incorporates heavy machinery equipped with hammers, shears, and concrete crushers. It is important to note that this demolition process also requires structural analysis to remove a concrete structure safely and responsibly. The removal of each structural component changes the structural system and leads to different force distributions within the structure [3]. While the traditional process is cost-effective and fast, it limits the traffic hindrance. However, this method does not consider any reusable value of concrete elements. This approach results in the pulverisation of all demolished materials into debris. As this results in non-reusable girders, a more delicate approach is needed. The suitable approach can be described by the deconstruction process, which is defined by the disassembly of elements and material salvage [36].

The deconstruction of a prefabricated concrete viaduct involves the removal of non-structural elements, such as streetlights and guardrails, followed by the removal of the asphalt layer using milling machines [82]. Subsequently, the compression layer connecting the girders is sawn through to enable the longitudinal separation of the girders. The slab saw, as presented in Figure 2.24, is typically used on horizontal surfaces and provides clean, accurate cuts up to 700 millimeters deep [25]. Dust creation is mitigated by using water, ensuring the cleanest and most effective way to cut concrete [25].

Figure 2.24: Example of a slab saw being used in practice

Major challenges arise with the presence of crossbeams and end transverse diaphragms due to their robustness. The height of these end transverse diaphragms matches the construction height, which exceeds 900 millimeters for spans over 20 meters [71]. Detaching the transverse diaphragms requires specialised, time-consuming methods, such as wire cutting and stitch drilling [71]. Figure 2.25 shows practical examples of these methods. Wire cutting involves a wire wrapped around an element to make clean controlled cuts for elements with an out-of-reach depth for other methods. This method does not require as much space as other methods and can be controlled remotely, minimising risks. On the other hand, stitch drilling involves a sequence of overlapping vertical holes to form a 'cut'. This method is easy to perform but the result is an uneven cut and lost material between the girders. The complexity due to transverse diaphragms can extend the deconstruction process by up to one week. In contrast, other girder types without transverse diaphragms such as box beams are easier, faster, and cheaper to deconstruct [71].

(a) Example of a wire saw being used in practice

(b) Example of stitch drilling in practice

Figure 2.25: Special methods for detaching end transverse diaphragms [25] [64]

2.3.2. Modification of prefabricated girders

Following the disassembly of prefabricated girders from the original structure, they are transported via trucks or boats to a storage area or workplace. Here, the prefabricated girders are modified and prepared for future use. This process starts with the removal of residual cast-in-situ concrete parts from the compression layer and end transverse diaphragms. Subsequently, the girders are adapted to

meet the requirements for new constructions by shortening and adjusting the skew angle of the girders.

Eliminating the remaining cast-in-situ concrete parts from the compression layer and transverse diaphragms is achieved while maintaining the shear reinforcement within the girder's web. The most commonly used techniques include hydraulic hammering and hydro demolition. Hydraulic hammering is more often chosen due to its cost-effectiveness [71]. This method involves breaking concrete into smaller pieces, allowing for accurate removal and preservation of the girders and their reinforcement. However, the presence of high bond strength between concrete elements increases the risk of potential damage to other structural components. Mitigating the risk involves careful machine operation by limiting the power of the machines and extending the process time. It may suffice to expose a minimum of 60 millimeters of reinforcement instead of entirely removing the compression layer. An alternative approach is to retain the original compression layer and cast a new layer on top, which increases the bending moment and shear capacity. However, this also results in a greater overall construction height. A prerequisite for this method is the good condition of the compression layer, which requires an additional inspection to ensure its structural integrity.

Making the girders suitable for new constructions involves alignment adjustments in both length and angle. Shortening prefabricated prestressed girders is not straightforward due to potential changes in stress distribution, leading to the formation of cracks. The removal of splitting reinforcement, applied at the ends of the girders to counteract splitting stresses from prestressing, can lead to issues during shortening. Moreover, modifications to the skew angle may introduce additional stresses. Research shows that skew angle adjustments between 60 and 90 degrees can be effectively made using a wire saw [71]. However, these modifications may lead to insufficient coverage on reinforcing and prestressing steel or even expose these steel strands. To protect these steel strands from potential corrosion by their surroundings, the cover of concrete must be restored. During their service life, girders may sustain damage and require repairs to satisfy the standards and guidelines.

2.3.3. Repairs

Over the years, structural elements can suffer damage due to various factors, including weather conditions and vehicular collisions, ultimately leading to a potential decrease in load-bearing capacity. However, the long-term performance of infrastructural structures depends greatly on their ability to resist the degradation of materials [43]. Environmental influences can significantly affect the structural properties of reinforced concrete elements through multiple deterioration mechanisms, such as reinforcement corrosion. For the preservation and reuse of the girders, it is crucial to understand the current conditions of the materials to determine their properties and durability. Visual inspection, coupled with several testing techniques, could be used to measure structural properties and determine the remaining service life of the reinforced concrete element.

The cause of deterioration of a reinforced concrete element depends on the deterioration of the concrete itself and the deterioration of steel. One may lead to the other when, for example, physical damage to the concrete cover could expose the reinforcing steel directly to the environment. Concrete cracking is a source of concern as it can cause severe corrosion of reinforcement, which is the most critical factor in the durability of reinforced concrete structures [43]. The two major causes of reinforcement corrosion in structures within the infrastructure are:

1. Carbonation-induced corrosion
2. Chloride-induced corrosion

Carbonation of concrete denotes a chemical reaction occurring within the concrete, particularly in environments rich in carbon dioxide, such as the road network. This process causes embedded reinforcement to corrode resulting in the formation of expansion cracks and weakening the concrete. Additionally, the presence of chloride ions, primarily coming from deicing salts used on roads, could initiate chloride-induced corrosion in reinforcing steel. This type of corrosion diminishes the mechanical strength of steel, causing cracks and a decline in the bond between steel and concrete. Both deterioration mechanisms affect the durability of reinforced concrete structures, ultimately reducing their service life [43].

Ensuring the durability of structures involves timely repairs to restore structural integrity and prevent deterioration of materials. Concrete coverage is an important factor in preventing corrosion of steel. These relatively small procedures could have a significant impact on the structure's durability. Nevertheless, when repairs are inadequate, strengthening the girders is a feasible measure to maintain structural integrity to prescribed standards.

2.3.4. Strengthening of prefabricated girders

Due to various factors, the bearing capacity of existing prefabricated girders may no longer meet the requirements for future use. In these cases, various strengthening options are available to increase the bending moment capacity, shear capacity, or transverse stiffness. These options can be categorised into active and passive methods. Active methods immediately increase the structure or element's capacity after application. Whereas, passive methods only become active when the load exceeds a certain threshold.

The feasibility of strengthening methods for existing structures depends on several factors, including the amount of strength increase, constructability, accessibility, functionality, aesthetics, and available space. However, constructability and accessibility are less significant since the girders are strengthened after disassembly. Typically, strengthening methods are employed as a last resort to extend the service life of a structure without prioritising durability. In contrast, the existing girders will now be used in new structures and must meet durability standards with an expected lifespan of one hundred years. Additionally, the costs and environmental impact of the strengthening methods should not exceed those of producing a new girder.

Several methods are available to strengthen the superstructure of a bridge. Figure 2.26 provides an overview of the most common techniques for strengthening reinforced concrete girders. Following this overview, the suitability of each method for prefabricated concrete girders is evaluated and discussed.

(a) CFRP strips

(b) Steel strips

(c) External prestressing

(d) Concrete overlay

Figure 2.26: Overview of the most commonly used methods for strengthening concrete structures

The principles behind using CFRP (Carbon Fiber Reinforced Polymer) and steel strips for strengthening are quite similar. Attaching these strips to the concrete surface ensures that these strips absorb stresses, thereby enhancing the strength and stiffness of the reinforced members. Simultaneously applying these strips to both the tension and compression regions results in a substantial increase in flexural strength [35]. Additionally, attaching these strips to the sides of the girder's web increases its shear capacity. Due to their external application, these techniques are relatively easy to install and widely applicable. However, significant challenges are associated with debonding and anchoring the strips to the concrete surface.

Another strengthening technique to improve a structure's bearing capacity is external prestressing. This involves placing a reinforcement layout outside the structure, which transfers the prestressing force to the concrete through anchorages and steering blocks. This method can limit cracks and reduce the structure's deformation without increasing its dead load. Moreover, it is easy to set up and maintain, while also improving the effectiveness of the prestressing system by reducing friction loss [83]. However, the external tendons are susceptible to environmental exposure and potential damage.

In addition, applying a concrete overlay is another effective strengthening technique. This method involves adding a new layer of concrete over the existing surface, significantly enhancing the structural capacity and durability of the reinforced members. Beyond concrete repairing and correcting surface irregularities, the concrete overlay increases the cross-sectional area of the member, thereby improving its flexural and shear capacities. However, the effectiveness of a concrete overlay relies on the quality of the bond between the new and existing concrete. While this technique can be highly effective, the potential increase in structural height and dead load must be carefully considered.

2.4. Eliminating end transverse diaphragms from inverted T-girder systems

As described in Section 2.3.1, the primary challenges in reusing the inverted T-girders arise from the end transverse diaphragms. Considering the removal of the end transverse diaphragms presents significant opportunities to improve the reusability of the girders. Therefore, further investigation into the elimination of end transverse diaphragms in inverted T-girder systems is desirable.

Few relevant studies have been found on exploring the effects of eliminating transverse diaphragms in concrete girder bridges. The first section presents two international studies that investigate the effect of transverse diaphragms in prestressed T-girder bridges, comparing systems with and without diaphragms. Since the inverted T-girder system is similar, these findings may also be applicable.

Next, two studies specifically examine the effect of end transverse diaphragms in inverted T-girder systems. One study evaluates the advantages and disadvantages of excluding end transverse diaphragms by comparing systems with and without them. The other study investigates the feasibility of eliminating end transverse diaphragms, questioning their practical functionalities. Following the description of these significant studies, their findings are reviewed and discussed in detail.

2.4.1. Effect of transverse diaphragms in prestressed T-girder bridges

The research conducted by Ramos (2019) [58] aims to determine the effectiveness of closure pour connections and diaphragms between T-girders on the live-load distribution of a concrete girder bridge. Using a three-dimensional finite element model of a simply supported straight bridge representative of a typical T-girder bridge, the study investigates the moment distribution factors for both interior and exterior girders. The model incorporates longitudinal closure pour joints between the girders and various configurations of transverse diaphragms. Moments experienced by the girders were compared between models with and without transverse diaphragms.

The analysis reveals that the effects of transverse diaphragms on load distribution vary with the applied load configuration. Models without transverse diaphragms show higher design moments in all girders across different load cases. However, the differences are marginal, with a maximum deviation

of about 6% in the design moments between the models with and without transverse diaphragms. Consequently, the study concludes that intermediate transverse diaphragms could be eliminated in these types of bridges. Additionally, it finds no significant difference in performance between cracked and uncracked end transverse diaphragms under all loading cases.

Another relevant study by Saber et al. (2010) [61] investigates the effectiveness of continuity diaphragms for skewed continuous concrete girder bridges through field verification. This study examines the effects of continuity diaphragms on stresses and deflections in both the bridge deck and girders. Previous theoretical results from Saber et al. (2007) [62], derived from finite element models, suggested that continuity diaphragms could be eliminated as they were ineffective in reducing and controlling maximum stress and deflection.

Field verification confirms these theoretical findings, indicating that the impact of continuity diaphragms on skewed, continuous, precast concrete girder bridges is negligible. Comparisons of stresses, strains, and deflections in the concrete girders, as well as stresses in the bridge deck, show negligible variation. Therefore, continuity diaphragms may be omitted from the structural design of these bridges.

2.4.2. Effect of end transverse diaphragms in inverted T-girder systems

The research conducted by Minalu (2010) [45] presents appropriate finite element modelling techniques to predict the behaviour of skew bridges consisting of prefabricated inverted T-girders and a cast-in-situ concrete deck. Various numerical models were created, incorporating different structural modelling approaches and element types. The model utilising shell elements for the deck and eccentric beam elements for the girders was identified as the most suitable for engineering practice.

The study examined the sensitivity of skew bridge performance in two finite element models, both including and excluding end transverse diaphragms. The findings indicate that removing the stiffness provided by the end transverse diaphragms increases the live load longitudinal bending moments by 2% for orthogonal systems and up to 4% for skewed systems. Additionally, removing the end transverse diaphragms increases the torsion moments in the composite girders by approximately 35% for straight systems, with this increase reducing to about 20% as the skew angle decreases. Unlike the longitudinal bending moments in the girders, the maximum transverse bending moment in the deck slab increases by 7-12% for straight systems and 10-15% for skewed systems, depending on the finite element model used. These changes are accompanied by high torsion moments in the end transverse diaphragms, which are practically unsustainable. Given that shear stresses resulting from torsion moments and shear forces can be substantial, incorporating end transverse diaphragms in the finite element model could optimise the required stirrups. Conversely, for small-angle skew bridges, the contribution of end transverse diaphragms is negligible compared to the high torsion moments they induce, suggesting they can be omitted.

In addition, Van Vliet [68] highlights in his study on torsion in the ZIP bridge system that while the presence of end transverse diaphragms in a linear elastic model decreases stresses, it results in unrealistically high torsion moments in the end transverse diaphragms. Therefore, eliminating the diaphragms in calculations provides a more conservative and practical approach.

2.4.3. Practical functions of end transverse diaphragms in inverted T-girder systems

The memorandum by Vergoossen (2021) [72], which includes consultations with numerous experienced and reputable constructors, aims to investigate the necessity of end transverse diaphragms in inverted T-girder systems and explore whether their functions can be replaced. To assess the potential exclusion of end transverse diaphragms from the design, it is crucial to summarise their functions. This memorandum focuses exclusively on statically determinate spans and draws primarily on the expertise and experiences of several skilled and respected constructors. The six functions of the end transverse diaphragms are described and evaluated as follows:

1. Contribution to load distribution over the girders/supports
2. Transfer loads across single joint crossings

3. Fixation of girders during construction
4. Preservation of the girder head
5. Enhancing the robustness of the deck under special loads such as collisions and earthquakes
6. Load absorption during jacking for support replacement

Contribution to load distribution over the girders/supports

Based on the review of multiple calculations and the experience of specialists, it turns out that the transverse diaphragms are often not modelled or with negligible torsion stiffness to avoid high torsion moments. Also, the assessment of existing bridges does not consider transverse diaphragms in the models. In addition, few international studies show a marginal contribution of the transverse diaphragms in the load distribution within precast girder bridges. From this, it can be concluded that the end cross beams function for the load distribution can be omitted.

Transfer loads across single joint crossings

At the intermediate supports, a flexural joint can be applied in the compression layer to transfer the loads. Wheel loads acting between the precast inverted T-girders are transferred via the joint transition to the compression layer. It is expected that a joint beam of 600 mm width and 400 mm height is required to meet the coverage and detailing requirements of the Eurocode. This does not require a recess in the precast girders.

Fixation of girders during construction

During the construction phase, inverted T-girders are supported by bearing pads only, which can lead to an unstable situation. Especially, horizontal loads at the top of the girders could compromise the stability of the beam. However, this can be solved with temporary fixation, consisting of a pair of steel bars connecting the beams in the transverse direction. It can be concluded that the function of fixating the girders during construction can be taken over with simple measures.

Preservation of the girder head

Near an expansion joint, the components located under this joint must be additionally protected against the penetration of de-icing salts. This is because, in practice, joint transitions do not remain permanently watertight throughout the entire design life. By hydrophobing the surfaces of the girder heads over the last meter, the requirements of the ROK[1] can be met. Therefore, the presence of end cross beams to preserve the girder heads is not necessary.

Enhancing the robustness of the deck under special loads such as collisions and earthquakes

Apart from variable loads, special loads such as collision and seismic loads can occur. However, in the Netherlands, the magnitude of seismic loads is so low that the resulting loads are not significant compared to normal loads. Therefore, it is assumed that the compression layer provides sufficient shear action even in the absence of end cross beams. In the case of collision loads, the load is applied on the edge girder. When reusing precast beams, it is assumed that the edge girders are always remade since they are often specific to a structure and difficult to disassemble. These new edge girders are designed to withstand impact load, and as with new viaducts, the impact loads can be distributed through the connections of the lower flanges. Therefore, the end cross beams have negligible contribution in absorbing frontal impact loads.

Load absorption during jacking for support replacement

According to the ROK guidelines, the supports of a separate support system for the superstructure should be replaceable. With an end cross beam, it is not necessary to support each beam with a jack. However, if the end cross beam is excluded, the deck can be lifted using staggered jacks positioned under each beam. There is sufficient space at the abutments to accommodate jacks under each girder. Conversely, at the intermediate abutments, the absence of end cross beams presents a challenge. This can be easily solved by facilitating temporary jacking through the construction of an auxiliary structure, a method commonly employed with precast box girders. Meeting the ROK's requirement regarding the jacking capacity for support replacement demonstrates that an end cross beam is not required.

[1]The guideline 'Richtlijnen Ontwerp Kunstwerken' (ROK) by Rijkswaterstaat sets out the requirements for the design and construction of new structures.

2.4.4. Conclusions

The studies conducted by Ramos (2019) [58] and Saber et al. (2010) [61] suggest that the effectiveness of transverse diaphragms in concrete girder bridges could be questionable. Comparisons of girder bridge models with and without transverse diaphragms show only minor differences in longitudinal bending moments, while the effect of continuity diaphragms on stresses, strains, and deflections in the bridge girders and deck is negligible.

Additionally, research by Minalu (2010) [45] concludes that the contribution of end transverse diaphragms is insignificant compared to the stresses generated within the transverse diaphragms themselves. Consequently, Minalu suggests that wide reinforced concrete end transverse diaphragms can be excluded from the finite element model for straight girder bridges.

Furthermore, the memorandum by Vergoossen (2021) [72] proposes alternative solutions to fulfil the functions of the end transverse diaphragms. Drawing from practical experiences, the memorandum suggests that all functionalities of end transverse diaphragms are either negligible or can be taken over by other structural members.

The conclusions drawn from these references suggest the feasibility of eliminating end transverse diaphragms from inverted T-girder systems. This revelation provides opportunities to substitute the functionality of end transverse diaphragms with other structural and non-structural elements. Incorporating this principle in new viaducts enhances the potential for reusing these girder types in future projects.

However, these studies only address the negligible influence of transverse diaphragms in similar systems to the inverted T-girder system and do not provide definitive solutions for substituting the end transverse diaphragms.

2.5. Conclusions from literature

The literature review has provided a comprehensive overview of the design details of an inverted T-girder system, focusing on the arrangement of its structural components and the construction processes involved. Employing a theoretical approach to understanding the systems' structural response has provided valuable insights into its orthotropic properties and the cooperative behaviour of its structural components. The incorporation of the deck slab and cross beams significantly enhances transverse stiffness, optimising load distribution throughout the structure. As a result, multiple structural elements participate, improving the system's overall load-bearing capacity.

The theoretical assessment of individual inverted T-girders, including aspects of structural design and stress distribution, has revealed potential deficiencies and weaknesses. Integrating time-dependent effects into the stress distribution analysis has shown the expected residual stresses at the end of its lifespan. After preparing the girders for reuse, the presence of prestressing force has moderately decreased compared to the original. This leads to higher potential risks for tensile stresses occurring during the construction of new structures using reused elements.

Examination of current disassembly methods for the girders has identified challenges primarily associated with transverse elements such as the deck slab and end transverse diaphragms. Addressing these challenges creates various opportunities for improving the circularity of the girders. With the relatively straightforward removal of the deck slab due to its limited thickness, the focus will be on removing the transverse end diaphragms.

Considering the removal of end transverse diaphragms in the inverted T-girder system, limited research has been found investigating the effect of eliminating end transverse diaphragms in girder bridges. In all studies addressed, the absence of end transverse diaphragms has little to negligible impact on the moments and stress distribution of the girders and a slightly higher impact on the moments in the deck slab. Overall, the findings suggest that eliminating the end transverse diaphragms in the inverted T-girder system could be feasible.

The findings from the literature review form the foundation for this research. This thesis specifically examines the contribution of end transverse diaphragms to the system's load distribution. Additionally, it investigates the impact of various design adjustments aimed at enhancing the circularity of the girders on the load-bearing capacity of the inverted T-girder system.

3

Case Study

This chapter provides a detailed description of the case study used to construct the numerical model. First, the structure's geometry, supporting conditions, and material properties are described. Then, the chapter presents the loading conditions, which include dead loads and critical live load configurations based on Load Model 1 from the Eurocode.

3.1. Introduction

The case study selected to investigate the system's structural behaviour, as well as the feasibility and impact of various design adjustments, features a single-span inverted T-girder system. To facilitate a comprehensive understanding of structural components and the potential impact of design improvements, the complexity of geometries within the structure has been minimised. Several simplified assumptions have been adopted, considering the entire structure to be straight and no distinction is made between sides. These simplifications aim to ease modelling and facilitate the analysis of structural adjustments.

The inverted T-girder system, known as the underpass Stayerhofweg, is located within the area development 'Ooijen-Wanssum' in Limburg, the Netherlands. The underpass features a statically determinate structure, utilising prefabricated and prestressed inverted T-girders with edge girders. It includes a cast-in-situ deck slab and transverse diaphragms, ensuring a cohesive and well-integrated system. Additionally, the material properties are assumed to conform to the values prescribed in the Eurocodes [22].

3.2. Geometry

The dimensions of the bridge are detailed in Figure 3.1 and Figure 3.2. The single span of the concrete structure spans 31730 millimeters in length, while the total width of the bridge deck measures 13760 millimeters. Comprising a total of 12 girders arranged side by side, the bridge features ten inverted T-girders of type HRP1150 and two edge girders of type RH. The combined width of the prefabricated girders counts up to 13005 millimeters. A reinforced cast-in-situ compression layer on top of the girders and transverse diaphragms at both ends facilitate the transverse connection of the girders. The composite girders have a construction height of 1350 millimeters, resulting in a construction thickness of the compression layer of 200 millimeters. For simplification, it is assumed that the girders are constructed perpendicular to the abutments, maintaining a skew angle of 90 degrees. The transverse diaphragms are cast-in-situ on top of the bottom flanges of the inverted T-girders, with a height of 987 millimeters and a width of 850 millimeters.

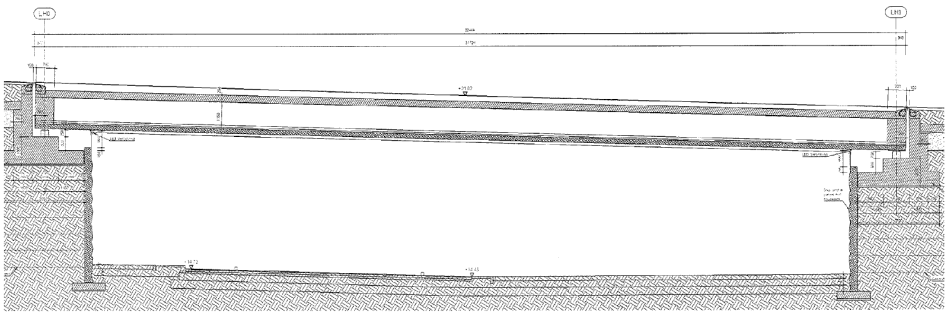

Figure 3.1: Longitudinal cross-section of the structure

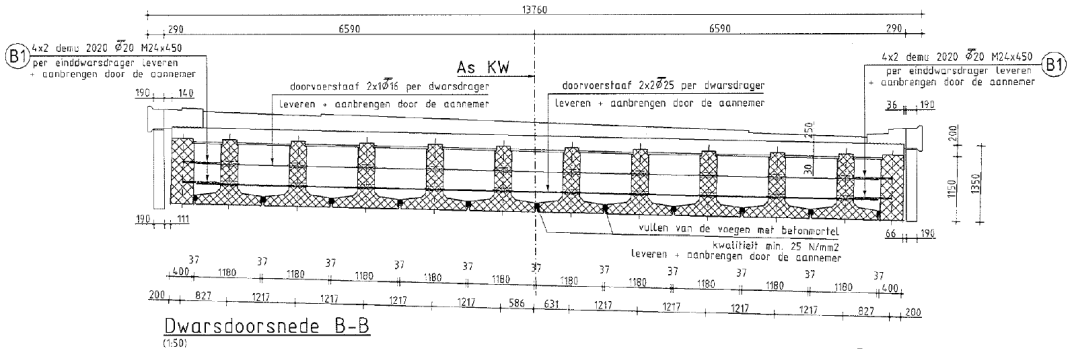

Figure 3.2: Transverse cross-section of the structure

Figure 3.3 and Figure 3.4 illustrate the geometry of the middle and edge girders, respectively, along with the arrangement of prestressing strands and stirrups. As shown by the figures, both girders mainly contain prestressing steel in their configurations. As elaborated in Section 2.2.2, the prestressing steel strands are strategically positioned primarily at the bottom of the cross-section, inducing an upward deflection effect. Additionally, ten steel strands are detached from the concrete to optimise the bending moment distribution from the prestressing force. This adjustment ensures an effective counteract of external loads without arising additional stresses at the supports.

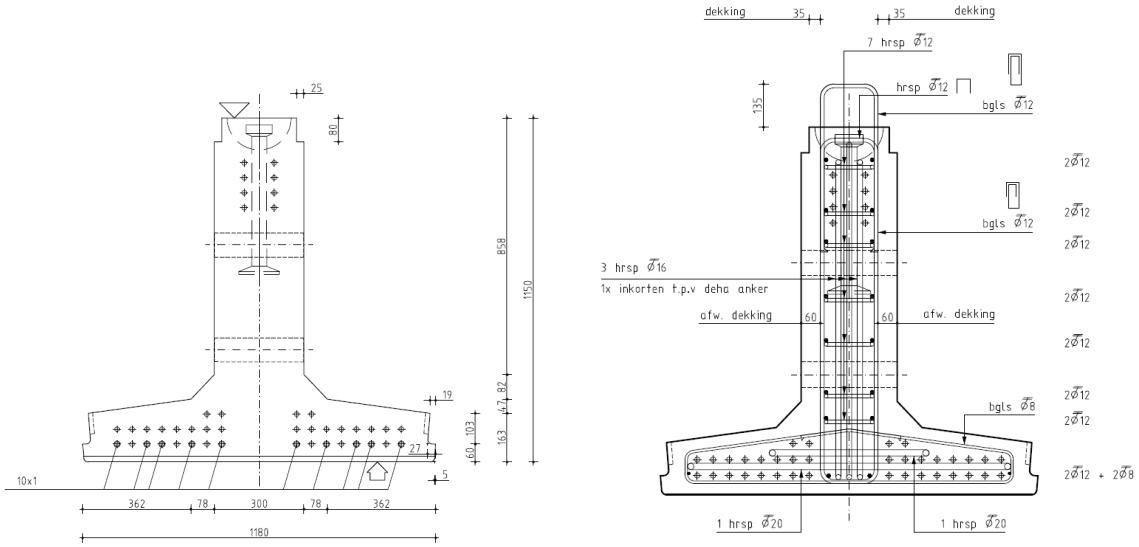

(a) Prestressing steel configuration **(b)** All steel strands configuration

Figure 3.3: Cross-section of the HRP1150 girder profile

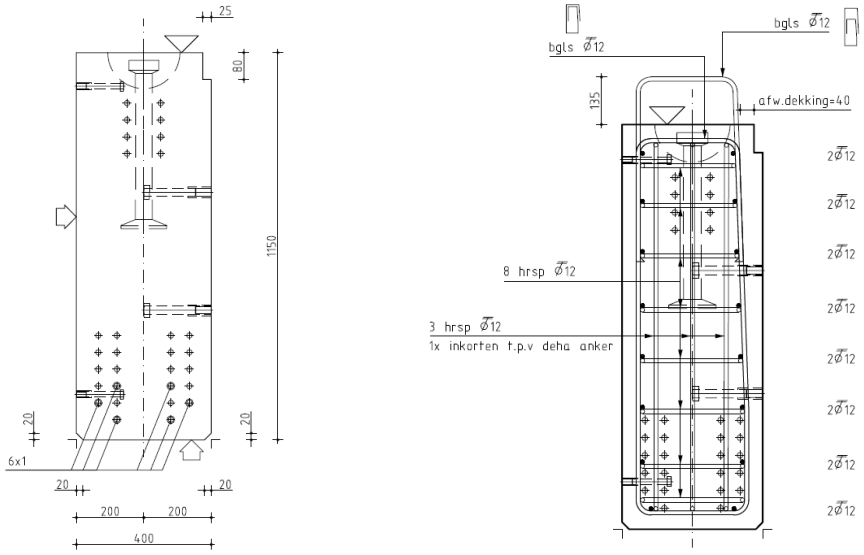

(a) Prestressing steel configuration **(b)** All steel strands configuration

Figure 3.4: Cross-section of RH girder profile

As illustrated in Figure 3.2, the edge girders are similarly part of the system as the middle girders, but contribute differently due to different dimensions.

3.3. Supporting conditions

The supporting conditions of a structure play a significant role in determining its force and stress distribution. In the case of the examined bridge, each girder is supported at its ends by elastomeric bearing pads, creating a statically determinate structure. These bearing pads, comprised of rubber layers separated by steel plates, are designed to accommodate slight structural movements in longitudinal, transverse, and rotational directions. While the rubber layers permit these movements through shear deformation, their stiffness restricts excessive displacements. The vertical stiffness of these bearing pads significantly surpasses their lateral stiffness, ensuring robust support under varying loading conditions. The dimensions of the bearing pads are measured to be 300 millimeters in length, 250 millimeters in width, and 75 millimeters in height.

3.4. Materials

The structure is a composite system that comprises several structural components consisting of concrete and steel. According to the Eurocode, the concrete components are classified into different concrete classes with varying material properties. In all classes, the Poisson ratio is equal to 0.2.

- Prefabricated girders: C60/70
- Cast-in-situ deck slab: C35/45
- Cast-in-situ end transverse diaphragms: C35/45

The prestressing steel strands, consisting of 7 tendons, feature a steel grade of FeP 1860. Additionally, the reinforcing steel used in the reinforced deck slab and as shear reinforcement in the prefabricated girders is of steel grade B500B.

3.5. Loads

The structural integrity of structures depends on their ability to endure various loads throughout their lifespan. A structural analysis evaluates how well a structure withstands different load types and combinations. The modelling approach employed for these loads significantly influences the accuracy of the analysis results. The Eurocode and National Annexes provide load models for simulating traffic loads

with a certain degree of accuracy.

This research focuses exclusively on vertical loads due to dead and live loads. Determining dead loads involves making simplified assumptions about the structure's geometry, assuming both longitudinal edges are identical, resulting in a symmetrical structure. The live loads simulate the action of vehicles over the deck at worst-case locations, as prescribed by Eurocode's Traffic Load Model 1. The structure's resilience to permanent and variable loads is tested under SLS conditions to evaluate its capacity during service. Several critical cases involving the most unfavourable load configurations due to traffic positions are determined to test the behaviour of the structure. These critical cases are assumed to result in the maximum bending moments in both longitudinal and transverse directions, shear forces, and torsion moments.

Regarding other types of loads, the effect of thermal loads can be expressed as imposed deformations. In the assessment of a statically determinate structure, it is assumed that imposed deformations can occur freely without generating additional stress. However, in the case of simply supported structures, horizontal movements are partially constrained due to the stiffness of the bearing pads. Therefore, it is considered that the supports can fully accommodate the deformation in both longitudinal and transverse directions. Furthermore, the horizontal force components in the longitudinal and transverse direction from braking loads, seismic activities, and wind loads are excluded from the analysis, as it is assumed that these forces have a negligible impact. Additionally, it is assumed that the edge structures absorb collision loads and therefore do not critically impact the rest of the structure. Consequently, these loads are not considered in this study.

3.5.1. Dead loads

The dead loads indicate permanent or static loads with a constant magnitude over time. This includes the self-weight of the structural concrete components, the asphalt layer, and the additional elements. Figure 3.5 illustrates the distribution of the structure's dead loads on the modelled deck slab. It is assumed that the dead loads are symmetrical, with the same dimensions and distribution applied to the opposite side.

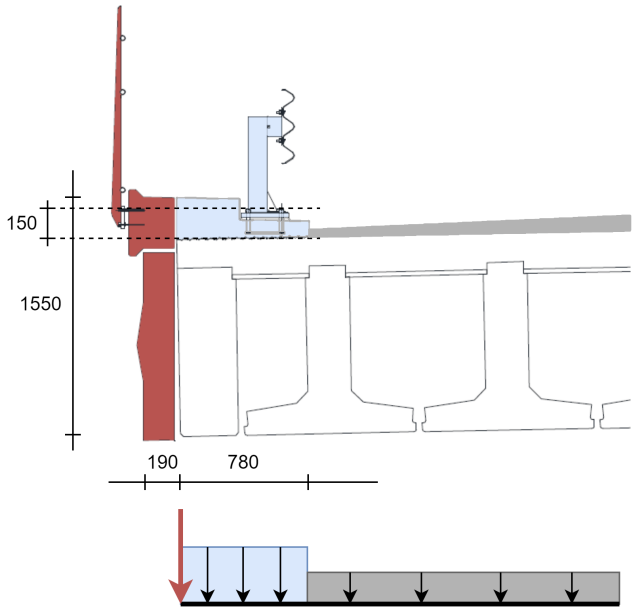

Figure 3.5: Dimensions and load distribution of the structure's dead loads

Concrete components

As described in Section 2.2.2, the stress distribution within the girders changes during the construction phase of the structure. Initially, the prestressed girders must be capable of carrying their self-weight

and the weight of the deck slab. After hardening the cast-in-situ concrete deck slab, the prefabricated girders start to act as a single system during its service life. Due to this sequence in the construction phase, the stress distribution obtained by the self-weight of the girders and deck is not taken into account.

Asphalt layer

The cast-in-situ concrete deck slab is covered by an asphalt layer, which does not contribute to the structural performance but only imposes a permanent load. Assuming an average thickness of 120 millimeters, and a self-weight of 23 kN/m^3, the resulting distributed load of the asphalt layer is calculated as $23 * 0.12 = 1.955$ kN/m^2.

Additional dead loads

Additional permanent loads arise from concrete elements such as the edge structure, scrap strips, and other elements like traffic barriers. The concrete scrap strips, depicted in light blue in Figure 3.5, exert a distributed load over a width of 780 millimeters along the deck slab's entire length. With an average thickness of 150 millimeters, plus a distributed load from the traffic barriers of 1 kN/m, the total load is $(0.15 * 0.78 * 25) + 1.0 = 3.925$ kN/m.

The concrete edge structure, highlighted in red in Figure 3.5, is located on the outside of the system and is considered to be entirely taken by the deck slab. Its self-weight is estimated based on approximate dimensions and self-weight. Including the contribution of the railing (0.5 kN/m), the total dead load along the longitudinal edges of the deck slab is calculated as $(1.55 * 0.19 * 24) + 0.5 = 7.568$ kN/m.

3.5.2. Prestressing force

The prefabricated girders were prestressed using the method with pre-tensioned steel, which utilises horizontally applied strands. As elaborated in Section 3.2, the prefabricated girders contain 44 steel strands with a diameter of 12.5 millimeters, made of steel class FeP1860. However, prestressing force introduces nonlinear effects, such as geometric, material, and time-dependent effects, which cannot be adequately accounted for in a linear analysis. Additionally, this study focuses on a comparison of structural behaviour under various loading conditions where including nonlinear effects is beyond its scope. The analysis remains focused on the primary objectives by excluding the complexities introduced by prestressing.

3.5.3. Live loads

The live loads refer to the dynamic and transient loads that structures experience during service. For bridges, these live loads mainly consist of traffic loads. These live loads do not have a fixed position and may vary over time. Various factors such as bridge composition, traffic density, and vehicle types could influence the traffic loads on bridges. Because of these variable traffic actions and dynamic load characteristics, load models are created in the Eurocode to reproduce real values induced by traffic loads [23]. Most of the effects of traffic are covered by Load Model 1 comprising concentrated and uniformly distributed loads.

The representation of the traffic action on the structure starts by dividing the carriageway into notional lanes and a remaining area. The total number of lanes and their width is determined using table 3.1.

Table 3.1: Number and width of notional lanes [23]

Carriageway width w	**Number of Notional lanes**	**Width of a notional lane** w_l	**Width of the Remaining area**
$w < 5,4$m	$n_1 = 1$	3 m	$w - 3$m
$5,4$m $\leq w < 6$m	$n_1 = 2$	$\frac{w}{2}$	0
6m $< w$	$n_1 = Int\left(\frac{w}{3}\right)$	3 m	$w - 3 * n_1$
NOTE For example, for a carriageway width equal to 11m, $n_1 = Int\left(\frac{w}{3}\right) = 3$, and the width of the remaining area is $11 - 3 * 3 = 2$m			

Following the divisions of the carriageway into notional lanes, the location and numbering of these lanes are assigned based on the most adverse effects from the loads. Notional lane number 1 represents the lane with the most unfavourable effects, followed by notional Lane number 2 and so on, as depicted in Figure 3.6.

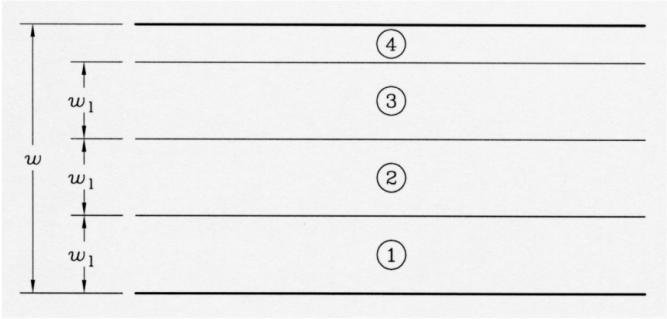

Key
w Carriageway width
w_1 Notional lane width
1 Notional Lane Nr. 1
2 Notional Lane Nr. 2
3 Notional Lane Nr. 3
4 Remaining area

Figure 3.6: Example of the Lane Numbering [23]

Load Model 1

Vertical loads due to normal vehicles are generally represented by Load Model 1, incorporating concentrated and uniformly distributed loads. This model consists of two partial systems: Double-axle concentrated loads, referred to as the Tandem System (TS), and the Uniformly Distributed Loads (UDL system). The characteristic values of the load model are presented in Table 3.2.

Table 3.2: Characteristics values of Load Model 1 [23]

Location	**Tandem system TS Axle loads Q_{ik} [kN]**	**UDL system q_{ik} or q_{rk} [kN/m^2]**
Lane Number 1	300	9
Lane Number 2	200	2.5
Lane Number 3	100	2.5
Other lanes	0	2.5
Remaining area (q_{rk})	0	2.5

The carriageway, typically comprising multiple traffic lanes, is divided into notional lanes, as depicted in Figure 3.7a. These notional lanes correspond to specific loading configurations, including concentrated and uniformly distributed loads. The concentrated loads, consisting of a tandem system with two axle loads, are applied to a 400 by 400 millimeter surface area, representing the wheels of the vehicles. These axle loads are considered at their most critical position, with minimal dimensions outlined in Figure 3.7b.

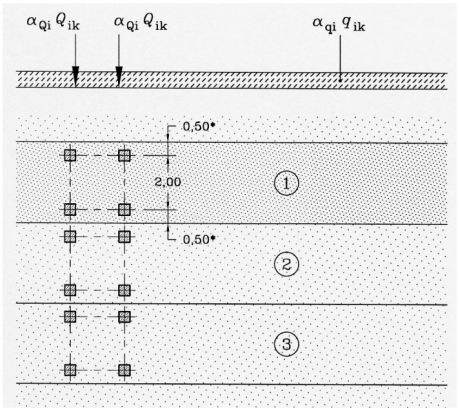

Key
(1) Lane Nr. 1 : $Q_{1k} = 300$ kN ; $q_{1k} = 9$ kN/m^2
(2) Lane Nr. 2 : $Q_{2k} = 200$ kN ; $q_{2k} = 2{,}5$ kN/m^2
(3) Lane Nr. 3 : $Q_{3k} = 100$ kN ; $q_{3k} = 2{,}5$ kN/m^2
* For $w_l = 3{,}00$ m

(a) Application of Load Model 1

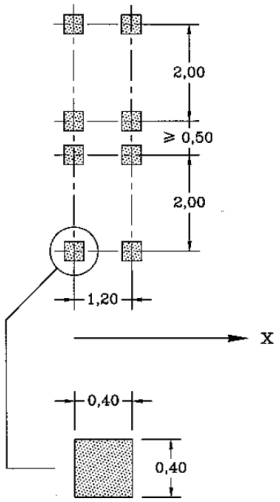

(b) Application of tandem systems for local verifications Load Model 1

Figure 3.7: Application of Load Model 1, according to the Eurocode[23]

The concentrated axle loads from the tandem systems should be taken as uniformly distributed on their contact area for local verifications, according to Eurocode [23]. The dispersal of these concentrated loads goes through the asphalt layer until reaching the centroidal axis of the compression layer, as illustrated in Figure 3.8. With a thickness of 120 millimeters for the asphalt layer and 200 millimeters for the compression layer, the total contact area of the concentrated loads from the tandem system is 840 by 840 millimeters.

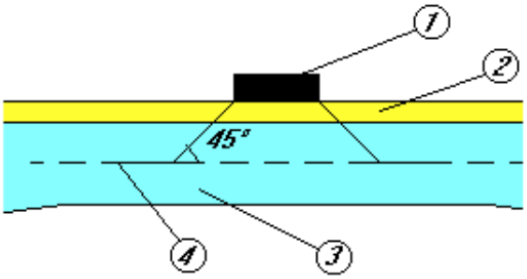

Key
1 Wheel contact pressure
2 Pavement
3 Concrete slab
4 Middle surface of concrete slab

Figure 3.8: Dispersal of concentrated loads through asphalt layer and concrete deck [23]

3.5.4. Critical load configurations

The structural integrity of the inverted T-girder system is assessed through the examination of various critical scenarios, each designed to generate maximum internal stresses. Four different load configurations, strategically positioned to produce peak moments in longitudinal bending, transverse bending, shear force, and torsion moment are thoroughly investigated. These critical load cases are designed

to simulate the most demanding conditions, accounting for both dead and live loads during the operational life of the structure.

The selection of critical load configurations is based on Eurocode's Load Model 1, further refined by modification factors specified in the Dutch National Annex to obtain characteristic design loads. These characteristic design loads for each notional lane are shown in Table 3.3. Each tandem system consists of two axle loads evenly distributed over four contact surfaces, while the UDL system is uniformly distributed over the entire notional lane surface.

Table 3.3: Characteristic design loads used in the numerical model

Location	Tandem system TS [kN]	UDL system [kN/m^2]
Lane Number 1	600	10.35
Lane Number 2	400	3.5
Lane Number 3	200	3.5
Rest	0	3.5

Maximum bending moment

The critical load cases yielding maximum bending moment in both longitudinal and transverse directions are closely related to those for maximum deflection. For a simply supported structure, maximum deflection typically occurs at the midpoint of the span. Consequently, the greatest moments occur when loads are applied at mid-span. In the longitudinal direction, the girders positioned near the edges experience a bigger moment due to their constrained ability to transfer loads to adjacent girders. In the transverse direction, the maximum bending moment arises at the center of the deck's surface. In this direction, each girder acts as a spring support for the deck slab, with the highest impact occurring when a load is applied between two adjacent girder. The critical load arrangements that cause maximum bending moments in both longitudinal and transverse directions are presented in Figure 3.9 and Figure 3.10, respectively.

Figure 3.9: Traffic load arrangement for maximum longitudinal bending moment

Figure 3.10: Traffic load arrangement for maximum transverse bending moment

Maximum shear force

The critical position for axle loads, resulting in the highest shear stresses, typically occurs near the edges close to the supports. In slab bridges, loads naturally follow the shortest path to the supports,

resulting in a 45-degree load distribution pattern. Maximum shear stresses are only observed when loads are applied at a distance from the supports, as shear forces are primarily absorbed by the supports otherwise. According to the Eurocode standards [22] and the study conducted by Lantsoght et al. (2012) [40], the maximum shear contribution from loads in slabs is observed at a minimum distance of twice the effective depth ($2d_{eff}$) between the faces of the first axle load and the support. In this study, determining the exact effective depth of the composite girder is outside the scope, so a depth of 1.2 meters is assumed. Although this assumption may overestimate the effective depth, it provides a conservative approach to ensuring that the shear forces in the girder are adequately considered. Additionally, research by Van Vliet (2012) [68] notes that Spanbeton employs this load arrangement in daily practice to generate maximum shear stresses. The load configuration that results in maximum shear forces is illustrated in Figure 3.11.

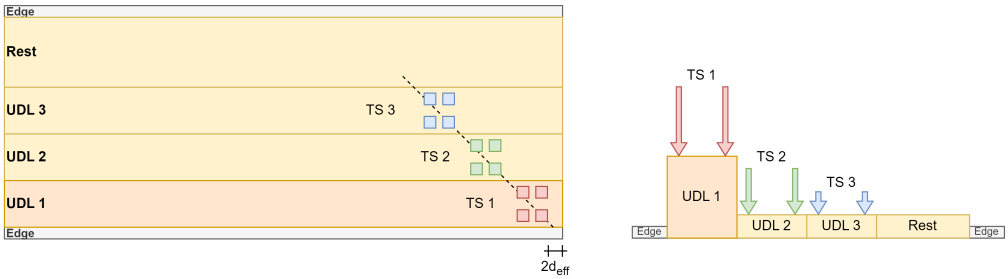

Figure 3.11: Traffic load arrangement for maximum shear force

Maximum torsion moment

The critical load case for maximum torsion moments in the system is determined by the angular rotation of the girders. A girder clamped at both ends experiences the maximum torsion moment when the relative angular rotation is maximised. After considering several loading configurations that could lead to the greatest rotation of one of the girders, the decisive load configuration was identified. The critical load case is created by maximally loading the first notional lane while unloading the remaining lanes. The load arrangement resulting in the maximum torsion moments is presented in Figure 3.12.

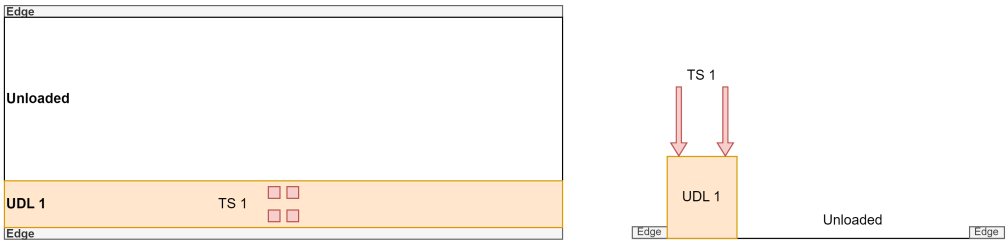

Figure 3.12: Traffic load arrangement for maximum torsion moment

3.5.5. Load combinations

The load combinations used in the model include both dead and live loads, as previously described. Table 3.4 presents the load combinations applicable to various critical scenarios. These combinations are designed to generate critical stresses, providing valuable insights into the overall system capacity.

Table 3.4: Load combinations employed in the numerical model

Load combination	Dead loads	Live loads
LC 1	asphalt layer + additional dead loads	critical load case 1
LC 2	asphalt layer + additional dead loads	critical load case 2
LC 3	asphalt layer + additional dead loads	critical load case 3
LC 4	asphalt layer + additional dead loads	critical load case 4

4

Finite Element Analysis (FEA)

This chapter delves into the numerical considerations essential for developing the finite element model of the case study. It provides a detailed description of the modelling approach, boundary conditions, and critical loading input, clarifying the construction of the numerical model. Additionally, it elaborates on the method employed for processing the results and details the analysis settings used in this study.

4.1. Global analysis

Various design approaches with different element types can be employed to accurately model the inverted T-girder system. In practice, two typical approaches are commonly used for modelling prefabricated decks: the orthotropic plate or the plate with ribs. These approaches involve simplifications in the stiffness of structural elements and may not fully capture the influence of the various structural components. A more comprehensive analysis can be achieved by employing shell or solid elements. This allows for considering several factors, including design and calculation time, accuracy of results, available modelling options, and complexity of the analysis. Appendix C provides more information on the characteristics and options of different element types within the DIANA FEA software.

Research conducted by A. Noukari in 2021 [54] highlights that employing shell elements to model the inverted T-girder system offers a precise representation of bridge geometry and a variety of modelling options. This approach demonstrates remarkable efficiency in computational time and practical application compared to solid elements. The accuracy and reliability of the modelling approach were validated using a detached individual inverted T-girder, including part of the compression layer. Appendix D presents the model validation, comprising an analytical comparison between several design approaches to accurately model the system geometry and component interactions. The primary challenge in this modelling approach is accurately connecting the horizontal and vertical shell elements due to the complex arrangement of structural components.

Considering the connectivity of diverse structural components and the results presented in Appendix D, a combination of vertical and horizontal curved shell elements with an eccentric connection has been identified as the most suitable approach for this study. Moreover, this type of connection is also expected to accurately represent the interaction between the end transverse diaphragms and the girders and deck slab.

4.1.1. Modelling structural components

The structural components constituting the inverted T-girder system are represented in the numerical model using shell elements. The distinct planes of various structural components are illustrated using different colours in Figure 4.1, showing their orthogonal configuration.

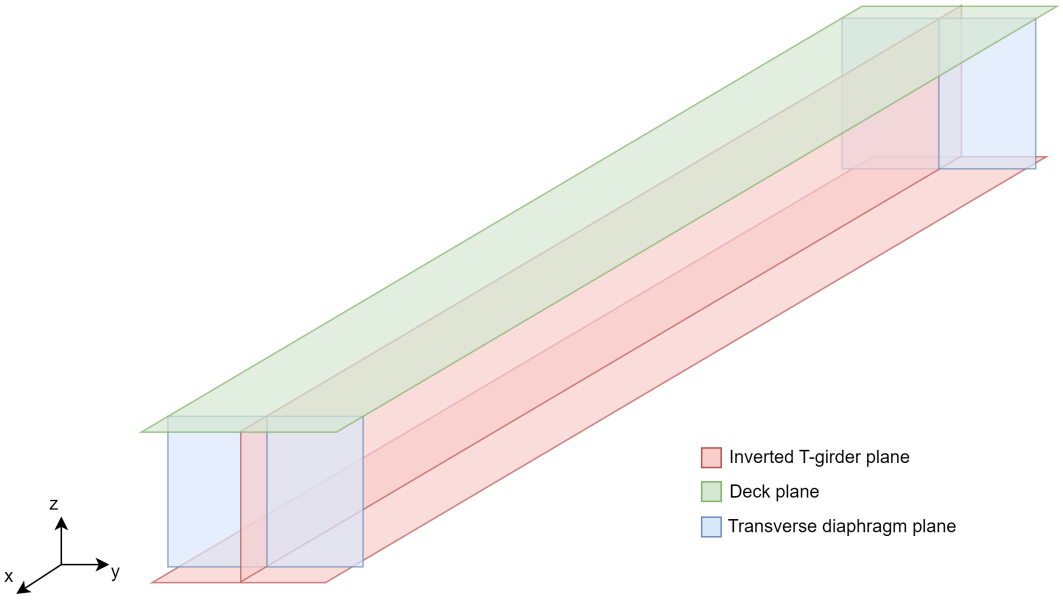

Figure 4.1: Orthogonal configuration of the planes used for modelling the structural components

Given the complexity arising from the intersection of these components, compatibility among shared nodes becomes challenging. A special type of curved shell element incorporating drilling rotation is employed within the model. This additional drilling rotation allows for rotation around the z-axis of the shell element, affording six degrees of freedom at each node, as depicted in Figure 4.2. This approach achieves compatibility among shell elements originating from orthogonal planes.

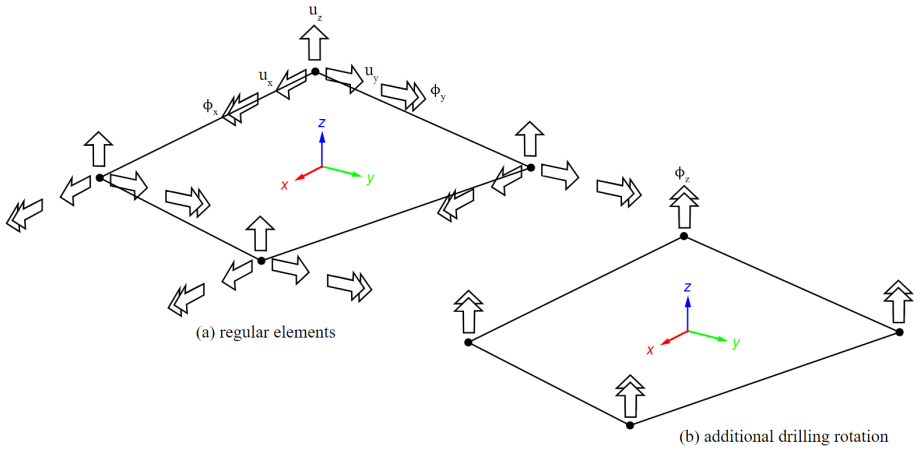

Figure 4.2: Degrees of freedom of a) regular shell elements and b) additional drilling rotation [17]

Prefabricated inverted T-girders and edge girders

The prefabricated inverted T-girders and edge girders are modelled using horizontal and vertical shell elements with constant and variable thicknesses matching the girders' cross-section. The inverted T-girder has been divided into five parts, with the bottom flange represented by horizontal shell elements and the web by vertical shell elements, as depicted in Figure 4.3a. The thickness of the horizontal shell elements, representing the bottom flange, is eccentrically positioned to avoid overlapping of material. The non-uniform thickness of some vertical elements is achieved using tapered shell elements defined by spatial functions. These spatial functions are specified grid-wise by using a multiplication factor and the gradient between the points. Conversely, the cross-section of the edge girder is matched by using

only one uniform thickness, as illustrated by Figure 4.3b.

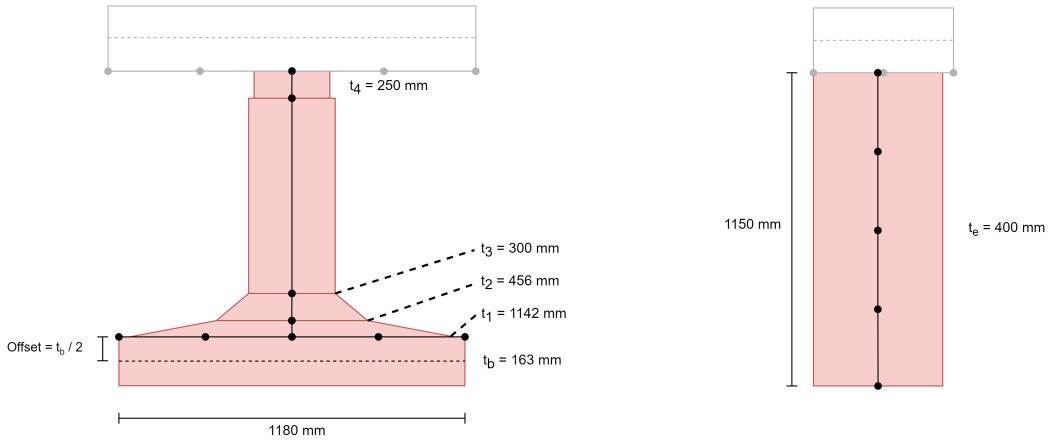

(a) Inverted T-girder **(b)** Edge girder

Figure 4.3: Arrangement of shell elements and dimensions for modelling inverted T-girders and edge girders

Furthermore, due to the presence of prestressing force in the longitudinal direction, the girders and deck slab remain in constant compression and are considered uncracked. The linear material properties of the prefabricated girders are specified as follows:

- $E_{C60/70} = 39100$ N/mm^2
- $v = 0.2$

Cast-in-situ deck slab

The cast-in-situ deck slab is modelled using horizontal curved shell elements with a constant thickness. This orthogonal shape has a uniform thickness across its entire surface and is positioned on top of the girders, as illustrated by Figure 4.4. To achieve a shared node connection without material overlap, the deck slab's thickness is eccentrically positioned by half of the deck slab's thickness.

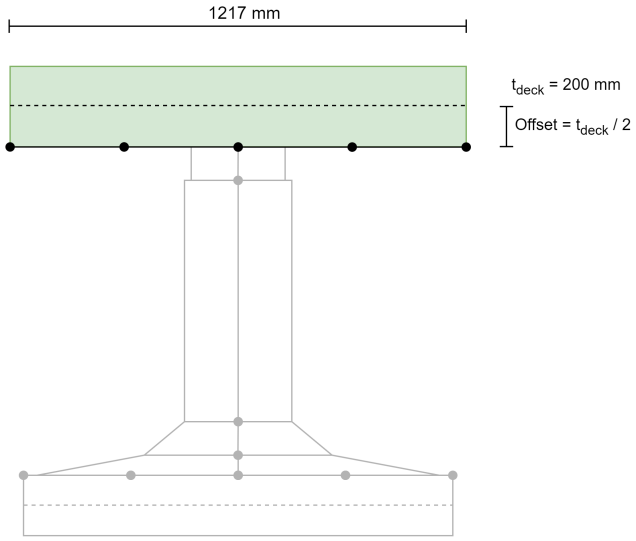

Figure 4.4: Arrangement of shell elements and dimensions for modelling the deck slab

Additionally, initial results indicate that a portion of the deck slab in the transverse direction exceeds the tensile strength of concrete. In linear analysis, the impact of cracking can be simulated by reducing

the stiffness of the cracked element. Consequently, this results in an elastic orthotropic deck slab with full stiffness in the longitudinal direction and reduced stiffness in the transverse direction. Since the analysis is linearly elastic, the steel reinforcement is excluded from the structural members. The linear material properties of the orthotropic cast-in-situ concrete deck slab are specified as follows:

- $E_{C35/45} = 34077$ N/mm^2
- $E_{C35/45,cracked} = \frac{E_{C35/45}}{3} = \frac{34077}{3} = 11359$ N/mm^2
- $v = 0.2$
- $v_{cracked} = 0$

End transverse diaphragms

The end transverse diaphragms are modelled using vertical curved shell elements positioned perpendicularly to both the girders and deck slab. This orthogonal configuration and its interface with other elements presents several challenges. Due to the complex geometry of the inverted T-girders, accurately representing the shape of the cast-in-situ transverse diaphragms along their connection with the girders is difficult. Given the extensive design time required to match the girders' geometry, precisely modelling these diaphragms is not considered worthwhile. Therefore, a conservative approach is taken by overlapping the girders' web, as illustrated by Figure 4.5a. Moreover, the transverse diaphragms are modelled using shell elements with a thickness equal to the width of the end transverse diaphragms, as depicted in Figure 4.5b.

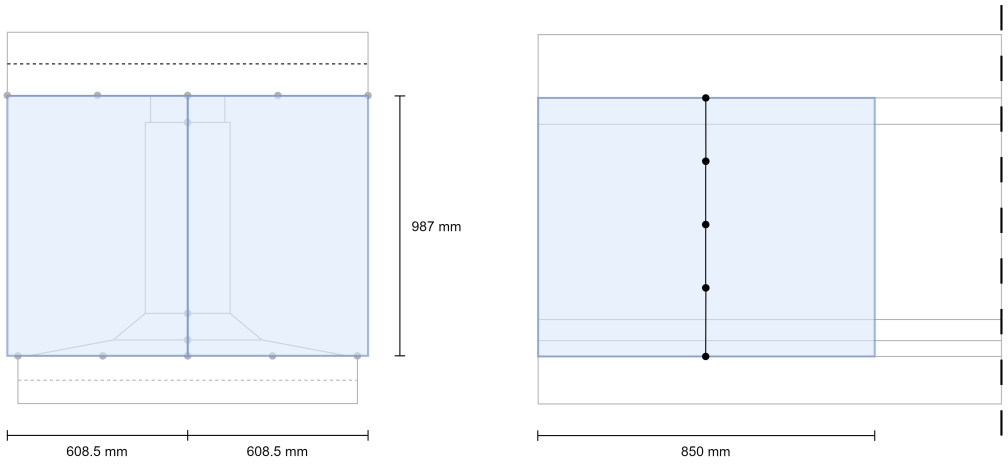

(a) Front view **(b)** Side view

Figure 4.5: Arrangement of shell elements and dimensions for modelling the end transverse diaphragms

Furthermore, there is an ongoing debate about whether to consider the end transverse diaphragms as cracked or uncracked. Since this study investigates the influence of the diaphragms by comparing the system with and without their presence, their full stiffness is assumed to obtain the clearest possible results. The material properties of the cast-in-situ concrete end transverse diaphragms are specified as follows:

- $E_{C35/45} = 34077$ N/mm^2
- $v = 0.2$

4.1.2. Boundary conditions

The examined superstructure is supported by bearing pads at each girder's ends. As explained in Section 2.1, these supports allow movements in all directions while possessing specific translational and rotational stiffness. Since this research focuses solely on the assessment of the superstructure,

the supports can be modelled using boundary springs connected to the environment. In the model, the one-node generic spring element type N6SPR is employed, which features three translational and three rotational degrees of freedom, as illustrated in Figure 4.6.

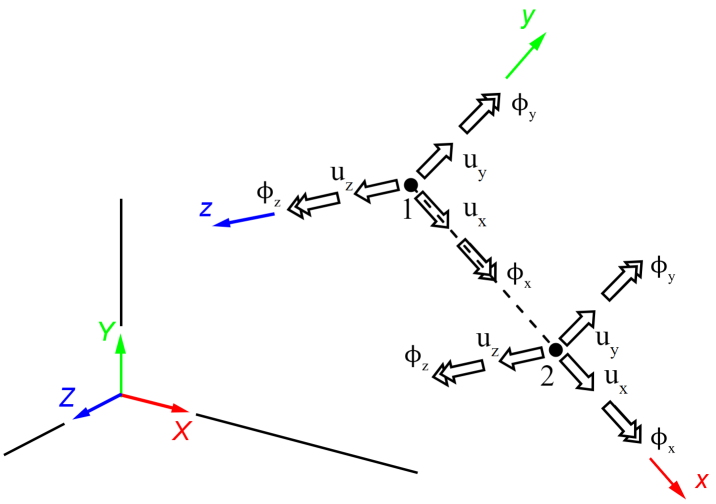

Figure 4.6: Degrees of freedom of matrix spring element type N6SPR [17]

The N6SPR element type is classified as a matrix or nodal spring element. This element is defined in a matrix form based on stress-strain relations, with or without cross terms. Since there is no coupling between the six degrees of freedom in the model, the nodal springs are implemented without cross terms [17].

The boundary springs are attached to the bottom of the girders and are positioned at the locations of the bearing pads. These springs are connected to a single node rather than being distributed over an area equal to that of the bearing pad. The stiffness of the supports is determined using values from the case study, as presented in Table 4.1. Additionally, it is assumed that the elastomeric bearing pads do not restrain any rotational movements.

Table 4.1: Overview boundary spring stiffness for all degrees of freedom

Spring stiffness	Stress [N/mm^2]
k_x	1250
k_y	1250
k_z	417000
k_r	0

4.1.3. Loads

The numerical model employs several load classes to accurately represent all actual loads, incorporating loads distributed over surfaces and along lines. As outlined by Section 3.5.4, four distinct load cases generating maximum stresses are considered to assess the impact of various design adaptations. These load cases involve specific load arrangements for the UDL and tandem systems. Each load within the UDL and tandem systems is applied using quadrilateral force loads. This feature in DIANA FEA allows a force to be distributed across a quadrilateral surface regardless of the underlying element areas. Internally, the load is converted to element surface or point loads without generally matching the element edges. This method is particularly useful when imprinting the surface load is impractical or time-consuming due to numerous loading points. This approach facilitates diverse load arrangements that enable precise user-defined positioning and values without disrupting the mesh of

the structural components.

Table 4.2 provides an overview of the load inputs used in the numerical model. The quadrilateral force loads are applied per surface area, resulting in input values that may differ from those specified in Section 3.5. The load input is validated by checking the external force equilibrium and the total maximum bending moments of the entire system, as described in Appendix D.

Table 4.2: Overview of load inputs in the numerical model

Load case	Load type	Input	Unit
Asphalt	Quadrilateral force	1026.16	[kN]
Edge loads	Quadrilateral force	127.48	[kN]
Edge structure	Distributed edge load	7.57	[kN/m]
UDL lane 1	Quadrilateral force	1008.50	[kN]
UDL lane 2	Quadrilateral force	341.04	[kN]
UDL lane 3	Quadrilateral force	341.04	[kN]
UDL rest	Quadrilateral force	278.17	[kN]
TS 1	Quadrilateral force	150.00	[kN]
TS 2	Quadrilateral force	100.00	[kN]
TS 3	Quadrilateral force	50.00	[kN]

4.1.4. Result processing

Before interpreting the analysis results, it is imperative to post-process the result outputs generated by the model. This process involves transforming the numerical data into visually understandable figures, facilitating the findings of this research. This section describes the model's orientation, the utilisation of composed lines, and the determination of mesh element size to achieve the desired result accuracy. Each aspect is crucial in ensuring the accuracy and reliability of the obtained results.

Model orientation

The structure's coordinate system is illustrated in Figure 4.7. This orientation affects the identification of the structural components in the analysis. The global x-axis runs parallel to the longitudinal direction of the structure, whereas the global y-axis is parallel to its transverse direction. The inverted T-girders are positioned with the first inverted T-girder at y=0, meaning that one of the edge girders is located on the negative y-axis. The vertical z-axis indicates positive values in the upward direction.

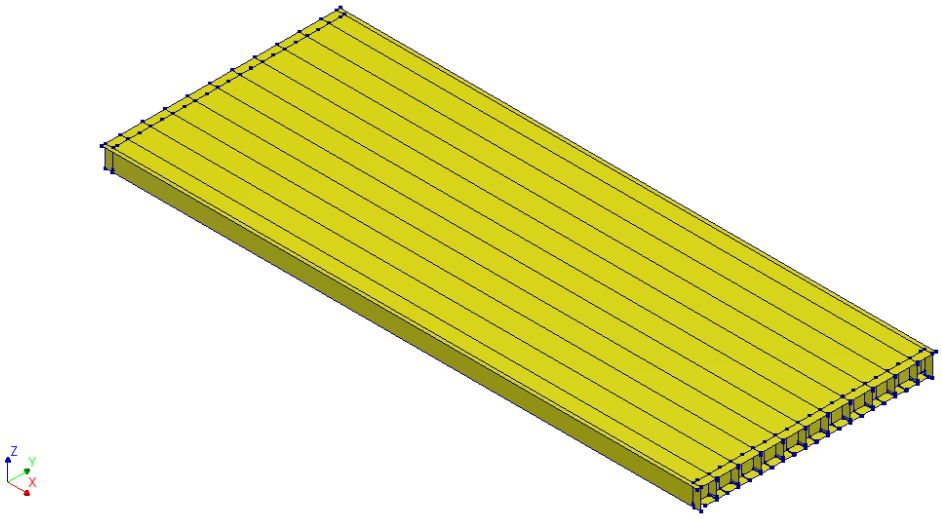

Figure 4.7: Coordinate system of the complete inverted T-girder system

In DIANA FEA, the axis orientation convention results in negative values for downward deflection. Additionally, sagging moments, characterised by tension on the bottom side and compression on the top side, are displayed as negative bending moments, while hogging moments are shown as positive values. Although this sign convention differs from the more commonly used standards, it is consistently applied throughout this report to ensure uniformity. Additionally, stress values follow the standard convention, with tensile stresses indicated by positive values and compressive stresses by negative values.

Furthermore, the structural components are modelled using both vertical and horizontal curved shell elements with varying thicknesses, as detailed in Section 4.1.1. The thickness of each shell element is divided into three layers, with layers 1 and 3 serving as the outer layers and layer 2 as the middle layer. The layer order is determined by the local axis of the shell elements. In the cross-section of the composite girder, the extreme values at the bottom are located in layer 1, while the extreme values at the top are in layer 3. Figure 4.8 illustrates the arrangement of these layers for both vertical and horizontal shell elements.

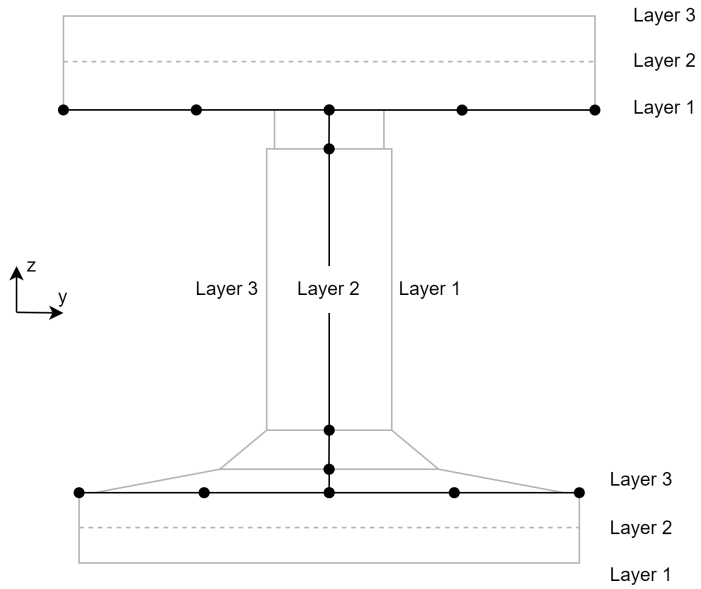

Figure 4.8: Layer arrangement for both vertical and horizontal shell elements

Composed lines

The results of a shell element model should be integrated over the entire cross-section to find internal forces and moments of the composite system. In DIANA FEA, the composed line elements feature can be used to automatically calculate the local forces and bending moments of a specified cross-section in the model. The composed line elements are created parallel to the prefabricated inverted T-girders using a line, as illustrated in Figure 4.9. The dimensions of the cross-sectional plane normal to the reference line are determined by two values that define the width and height. All nodes within these dimensions are included in the calculation. The composed line element is used as a reference line and is automatically shifted to the centroidal axis of the composite cross-section by the software. Moreover, the composed line elements do not have mechanical properties, therefore these elements do not affect the model's results.

Additionally, composed lines can be used to calculate forces and bending moments in specific areas within the complete structure. For instance, when examining the transverse direction, the internal forces in the compression layer are of particular interest. A composed line can be constructed in the transverse direction at the centroid of the compression layer. By specifying the height and width of this area, it is possible to determine the internal forces and bending moments specifically in the deck slab within this region. This method makes it possible to highlight the forces in different structural elements or other parts of interest, facilitating an understanding of the contributions of structural elements to the

overall system. When using elements with different orientations, it is important to consider their local axes, as this can cause some disturbances in the calculation of internal forces and moments.

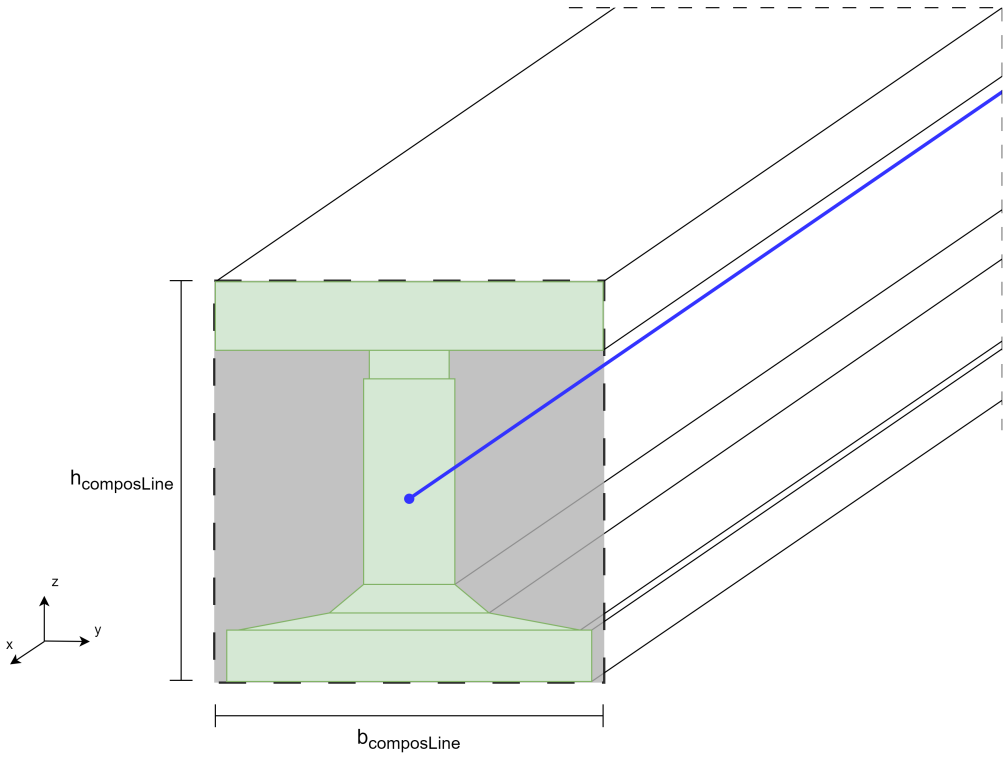

Figure 4.9: Principle and dimensions of the composed lines

Multiple critical load scenarios generate diverse maximum internal stresses within the system. These critical stresses are accessible in the model through various results outputs within the software. Therefore, Table 4.3 provides an overview of each critical load case alongside its corresponding result output in DIANA FEA. The maximum transversal bending moment can be determined by employing composed lines aligned in the transverse direction. These composed lines only consider the thickness of the deck slab since it exclusively contributes to the stiffness in this direction.

Table 4.3: Overview of critical load cases and associated composed line results

Critical load case	Result output
Maximum longitudinal bending moments	M_y
Maximum transverse bending moments	M_y
Maximum shear forces	Q_z
Maximum torsional moments	M_x

Mesh

The numerical model utilises two types of finite elements: four-node quadrilateral (Q24SH) and three-node triangular (T18SH) isoparametric curved shell elements, as illustrated in Figure 4.10. Figure 4.11 demonstrates the application of both element types in the mesh generated by DIANA FEA. Both element types employ linear interpolation and the Gauss integration scheme over the element area. These elements possess degrees of freedom for translation in all three directions and rotation in three directions. The average mesh size is set to 0.2 by 0.2 meters, which is considered sufficient to yield precise results for the model. Detailed information on the finite element types used in the model is provided in Table 4.4.

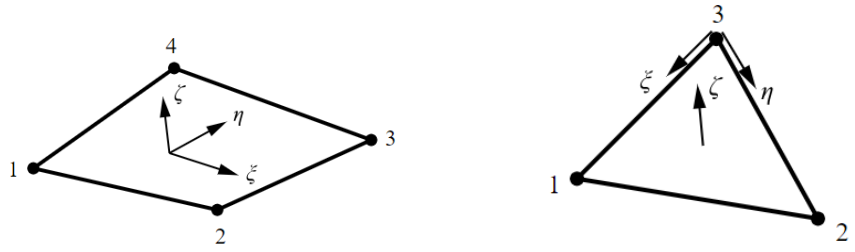

(a) Four-node quadrilateral element type (Q24SH) **(b)** Three-node triangular element type (T18SH)

Figure 4.10: Illustrations of the curved shell finite element types [17]

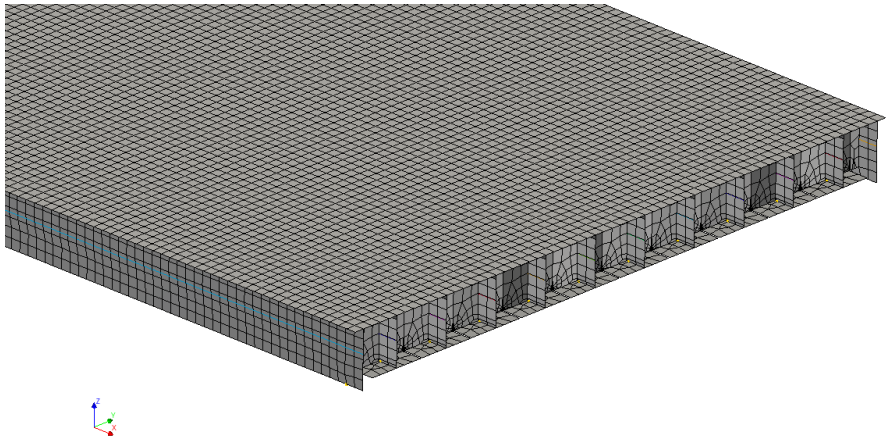

Figure 4.11: Finite element mesh generated by DIANA FEA

Table 4.4: Detailed information of the curved shell element types

Curved shell elements		
Finite element type	C24SH	T18SH
Degrees of freedom	6 $(u_x, u_y, u_z, \phi_x, \phi_y, \phi_z)$	6 $(u_x, u_y, u_z, \phi_x, \phi_y, \phi_z)$
Interpolation scheme	Linear	Linear
Integration scheme	2x2 Gauss	2x2 Gauss
Average element size [m]	0.2 x 0.2	0.2 x 0.2

Analysis settings

The numerical model employs linear analysis to evaluate the structural dynamic properties and responses under various loads. This analysis is performed using a force-based method known as linear static analysis. This approach is valid under specific critical conditions, including the absence of time variance, linear elastic material properties, and no significant deformations. While these simplifications prevent the model from capturing the actual behaviour of the structure, they allow for the determination of the maximum bearing capacity. The outputs of the linear analysis focus on forces, moments, displacements, stresses, and strains of the structural elements.

5

Structural Performance of the Inverted T-Girder System

In this chapter, the structural performance of the inverted T-girder system is examined by analysing its response in critical scenarios. This analysis of the base system evaluates the force and moment distribution, along with the normal and shear stresses, to clarify the contribution of various components to the overall structural capacity.

5.1. Base system

To assess the effects of various design adjustments, the results are compared to the structural performance of the base system. The structural performance of this base system is obtained and evaluated using the finite element analysis described in Chapter 4. The prefabricated inverted T-girder system comprises four main components: inverted T-girders, edge girders, deck slab, and end transverse diaphragms. This system exhibits inherent stiffness in longitudinal and transverse directions, enabling efficient load transfer to the supports. The structural performance and interaction of the various components are evaluated using four different load configurations, each simulating critical scenarios regarding forces and moments. To elucidate the distinct roles of each structural element, the system's performance is analysed by examining deflection, force distribution, and moment distribution. It is important to note that the load combination depicted at the top of the contour plots generated by DIANA FEA does not match the four distinct load combinations outlined in Table 3.4.

5.1.1. Bending moments

Before analysing the bending moments within the complete system, it is crucial to consider the vertical deformation of the system. The maximum vertical deflection occurs at mid-span under load combination 1, as presented in Figure 5.1. This figure shows that the vertical deformation begins at approximately zero at the supports and reaches its maximum at mid-span.

This load combination also results in the largest longitudinal bending moments, which are absorbed by both the girder and deck slab. Figure 5.2 presents the longitudinal bending moments in each composite girder, created by composed lines over the area of a single girder. The distribution of longitudinal bending moments is similar to that of vertical deflection, peaking in the middle of the first inverted T-girder. These moments are highly dependent on the longitudinal flexural stiffness of the composite girder, indicating greater stiffness in the inverted T-girder compared to the edge girder. This increased stiffness can be attributed to the advantageous size and shape of the inverted T-girder for incorporating bending moments.

In the transverse direction, the bending moments reach their maximum under load combination 2. Figure 5.3 shows the maximum bending moments at mid-span in the transverse direction, integrated over a meter width. As explained in Chapter 2, the system's stiffness in the transverse direction is solely

provided by the deck slab. With the girders acting as spring supports, the bending moments are highly dependent on the position of the applied TS loads. The largest transverse bending moments occur when the TS loads are applied both at mid-span and precisely between two girders. This positioning maximises the bending effects on the deck slab, highlighting the flexural stiffness of the system in the transverse direction. The large difference between the maximum bending moments in both directions indicates the great flexural stiffness of the composite girder in the longitudinal direction.

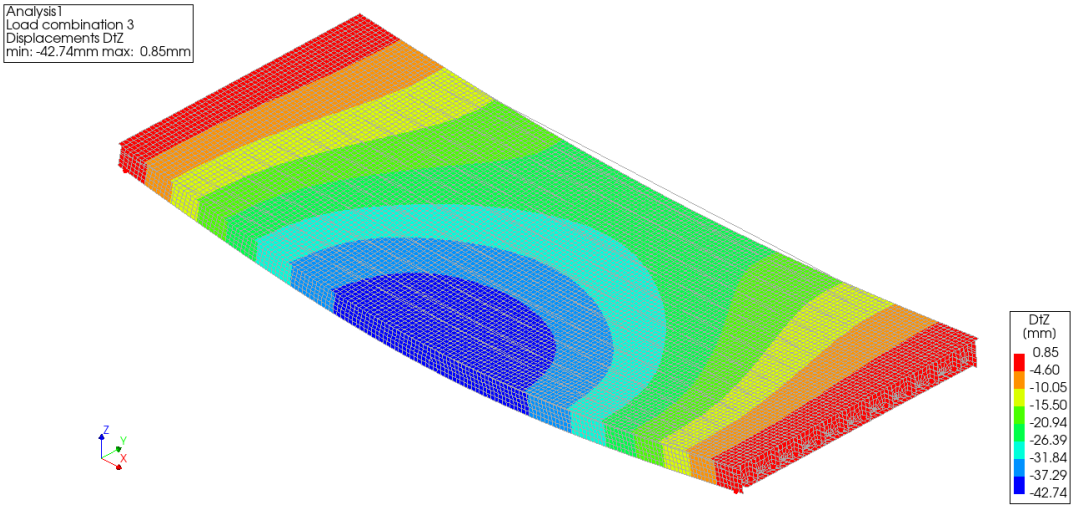

Figure 5.1: Vertical deformation of the system under LC1

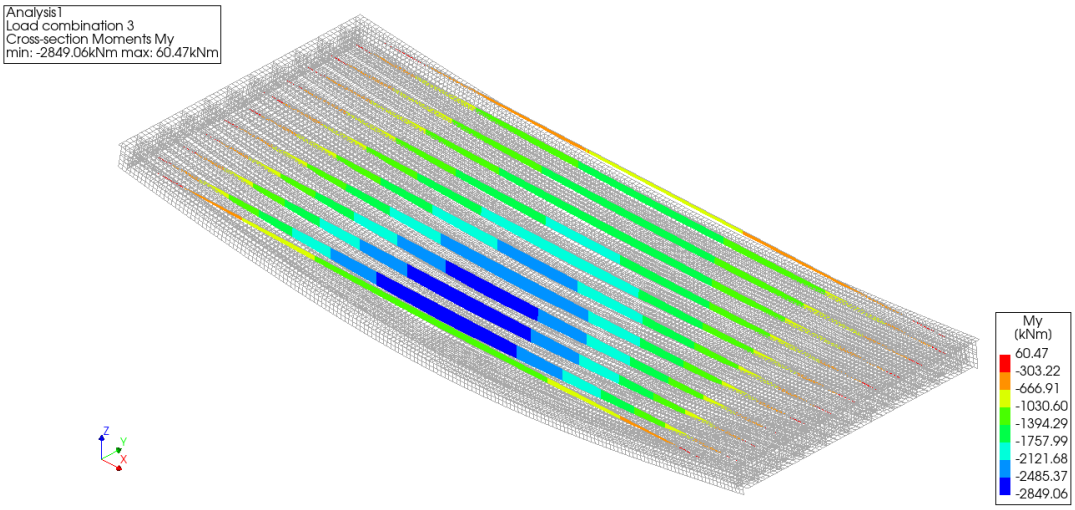

Figure 5.2: Longitudinal bending moments in each composite girder under LC1

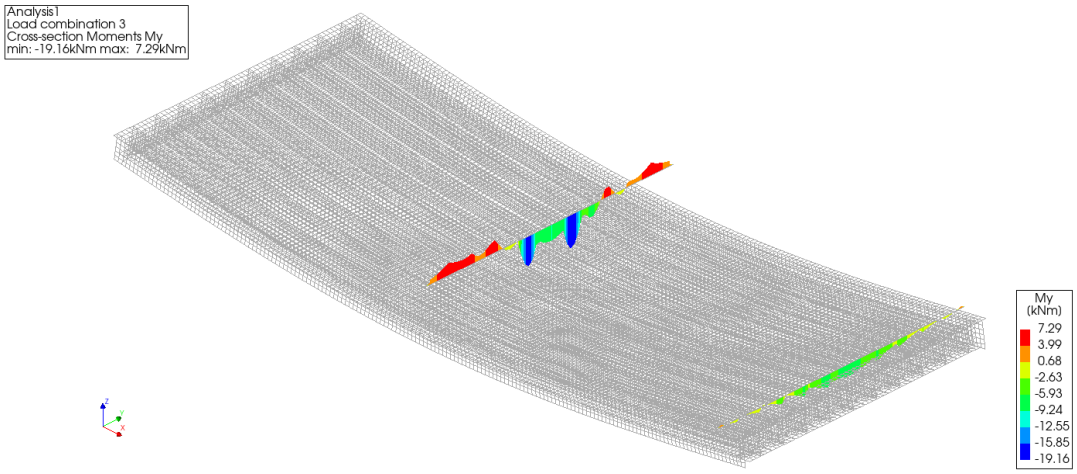

Figure 5.3: Transverse bending moments in the system at mid-span under LC2

5.1.2. Shear forces

In addition to bending moments, the inverted T-girder system must also transfer shear forces to the supports. These vertical shear forces are carried by both the deck slab and the girders. The governing shear forces in the composite girder arise when load combination 3 is applied to the system. Figure 5.4 presents the shear force distribution in each composite girder under load combination 3. This figure shows that the shear forces decrease as the distance from the supports increases, with the maximum shear forces occurring in regions near the supports where the applied loads are concentrated.

Moreover, the shear force distribution demonstrates effective load transfer in the transverse direction, enabling multiple girders to resist the applied loads. This highlights the importance of the composite action between the deck slab and the girders in distributing shear forces across the system.

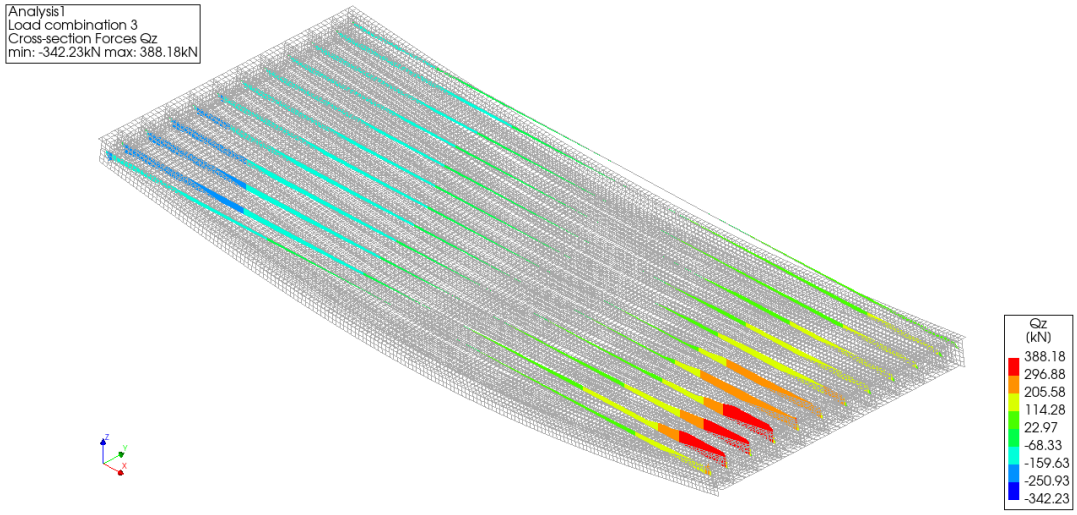

Figure 5.4: Maximum shear force in each composite girder under LC3

5.1.3. Torsion moments

Due to the applied loads, torsion moments also arise in the composite girders. Eccentric loading and asymmetrical characteristics create uneven load distribution, leading to torsional moments in the system. These torsion moments are directly related to the angular rotation of the girders, reaching their maximum at positions where this rotation is restrained. Figure 5.5 shows the torsion moments in each composite girder under load combination 4. The largest torsional moments are observed in the girders located adjacent to the applied loads. This indicates that these girders experience the highest imposed

rotation. Additionally, the peak values of torsion moments occur near the end transverse diaphragms, which prevent the rotation of the girders.

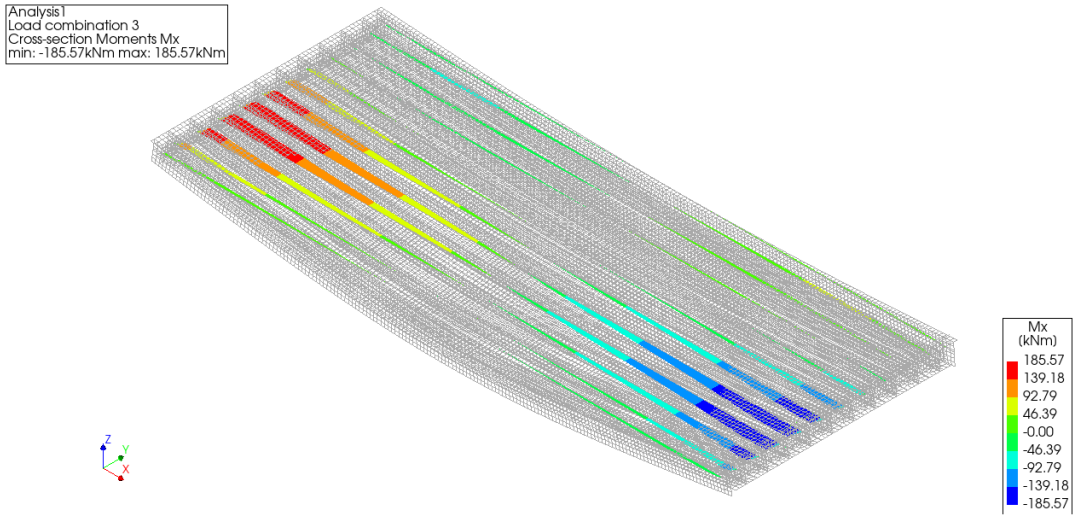

Figure 5.5: Maximum torsion moment in each composite girder under LC4

5.2. Stress distribution

After analysing the distribution of forces and moments, a more detailed analysis is conducted to highlight the stress distribution within the different structural elements. Therefore, this analysis focuses on the normal and shear stress distribution under the critical load cases. Maximum bending moments result in maximum normal stresses, while maximum shear stresses occur due to a combination of maximum shear forces and torsion moments.

5.2.1. Normal stresses

The normal stresses in the girders are oriented in the axial direction and can be either compressive or tensile. The maximum normal stress in the longitudinal direction occurs in the girder subjected to the largest longitudinal bending moments. Figure 5.6 presents the normal stress distribution in the longitudinal direction over the height of the governing composite girder. This is represented by a three-dimensional visualisation of the stress values in the middle layer, along with a stress diagram over the entire cross-section. The stress diagram displays the stress values for the vertical shell elements in the middle layer and the extreme values at the top and bottom, corresponding to layer 3 and layer 1, respectively, for the horizontal shell elements. The figure shows that longitudinal bending moments induce tensile stress in the bottom part of the cross-section and compressive stress in the top part. The stress distribution over the height of the cross-section is linear, with zero stress at the neutral axis and maximum stress at the extreme fibres. A shift occurs in this stress distribution between the prefabricated concrete girder and cast-in-situ concrete deck slab due to their differing material properties. For equal strains, the variation in the modulus of elasticity between these materials results in different stresses, leading to a shift in the stress distribution.

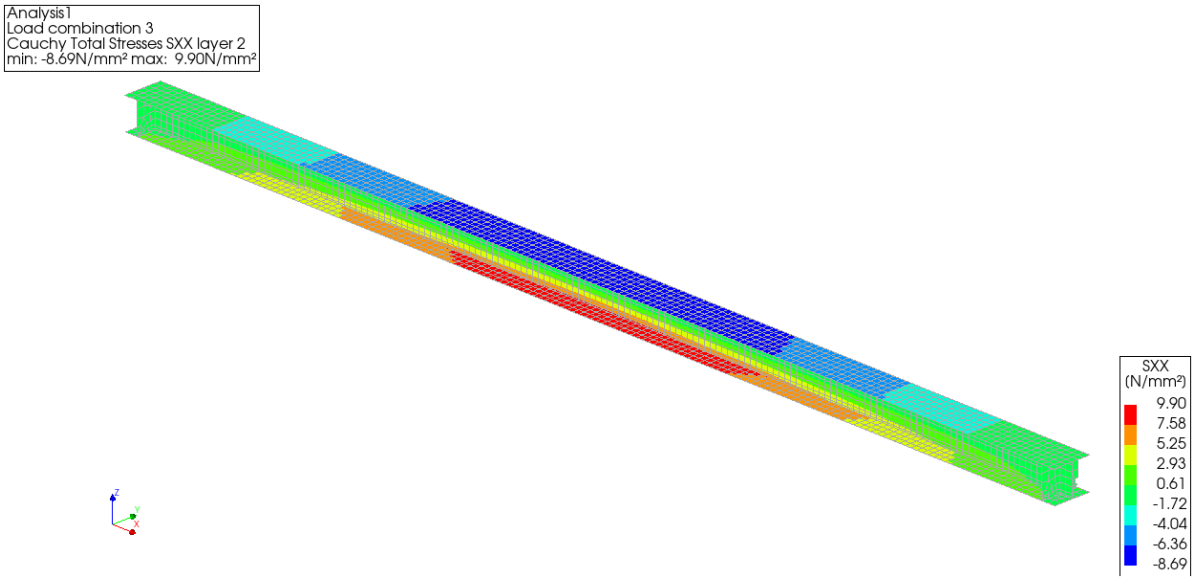

(a) Three dimensional representation of the stress distribution in the governing girder of layer 2

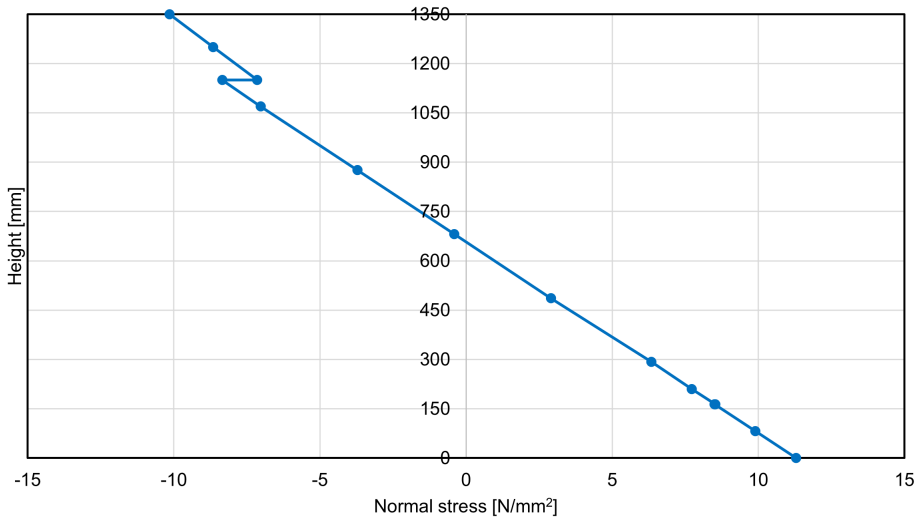

(b) Normal stress distribution over the height of the cross-section

Figure 5.6: Normal longitudinal stress distribution in the first inverted T-girder under LC1

In the transverse direction, only the deck slab contributes to the system's flexural stiffness. Figure 5.7a and Figure 2.15b present the normal transverse stress distribution in the bottom and top layers of the deck slab, respectively. Figure 2.15c illustrates the stress distribution over the height of the deck slab at the critical node. At t his critical node, the normal stresses cause tension at the bottom and compression at the top of the cross-section. Closer to the free edges of the structure, the deck slab experiences tension in the top layer and compression in the bottom layer, resulting in hogging moments. Similar to the longitudinal direction, the normal stress in the transverse direction is distributed linearly over the height of the deck slab, reaching its maximum values at the outer fibres.

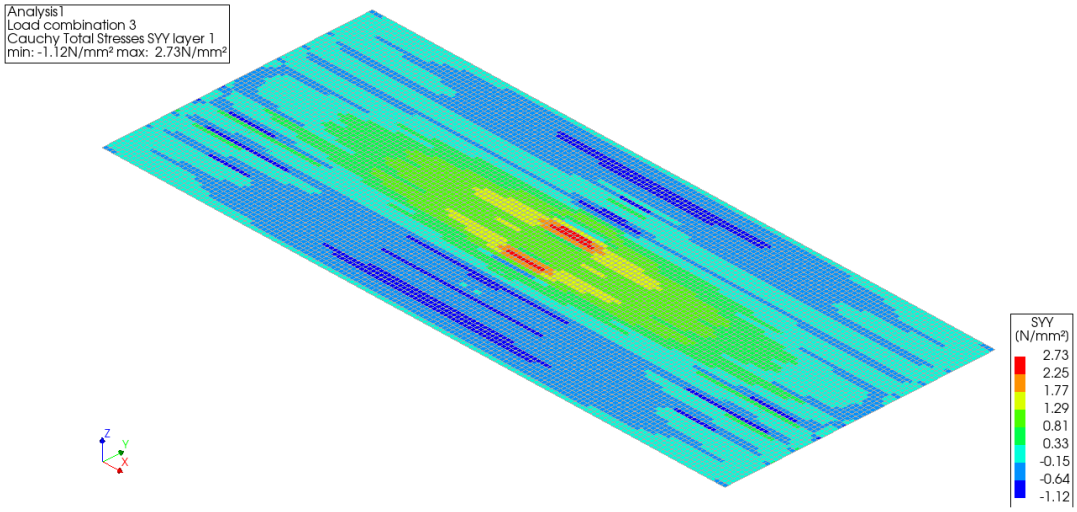

(a) Stress distribution in the bottom layer

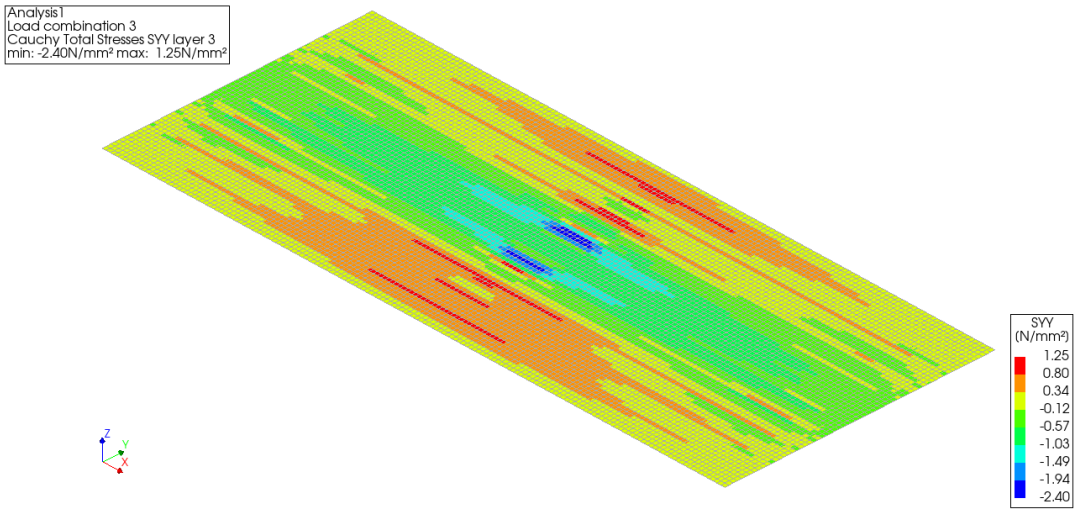

(b) Stress distribution in the top layer

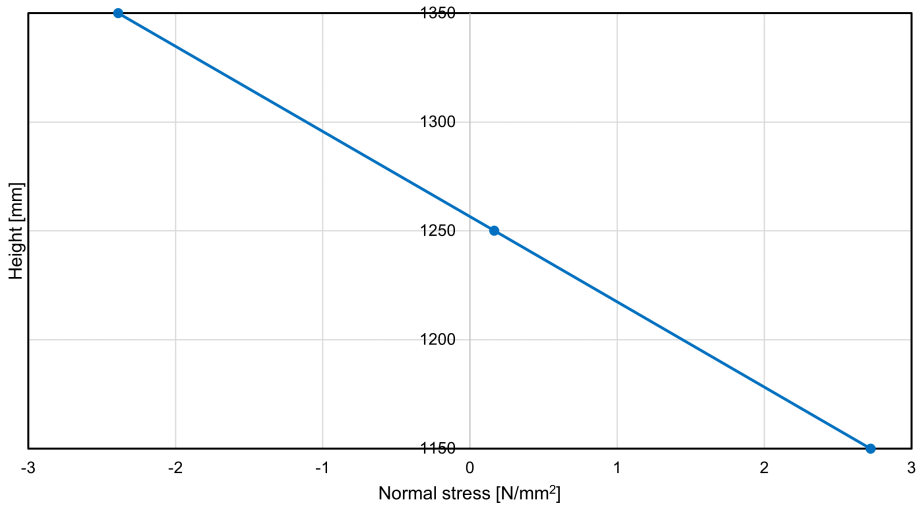

(c) Stress distribution over the height of the deck slab in the critical node

Figure 5.7: Normal transverse stress distribution in the deck slab under LC1

5.2.2. Shear stresses

The shear stresses arise due to shear forces and torsion moments and are primarily present in the girder's web, as explained by Section 2.2.2. Figure 5.8 presents the vertical shear stress distribution over the height of the web in a critical cross-section for shear forces by LC3 and torsion moments by LC4. As shown by the blue lines in the figure, the shear stresses produced by shear forces are similar in the three distinct layers over the height, indicating that these stresses are uniformly distributed across the width of the web. Conversely, the orange lines which represent the shear stresses in different layers of the governing girder subjected to torsion, show significant differences between the layers with positive and negative values. These shear stresses with opposite directions demonstrate that the vertical shear forces produced by torsion flow through the cross-section.

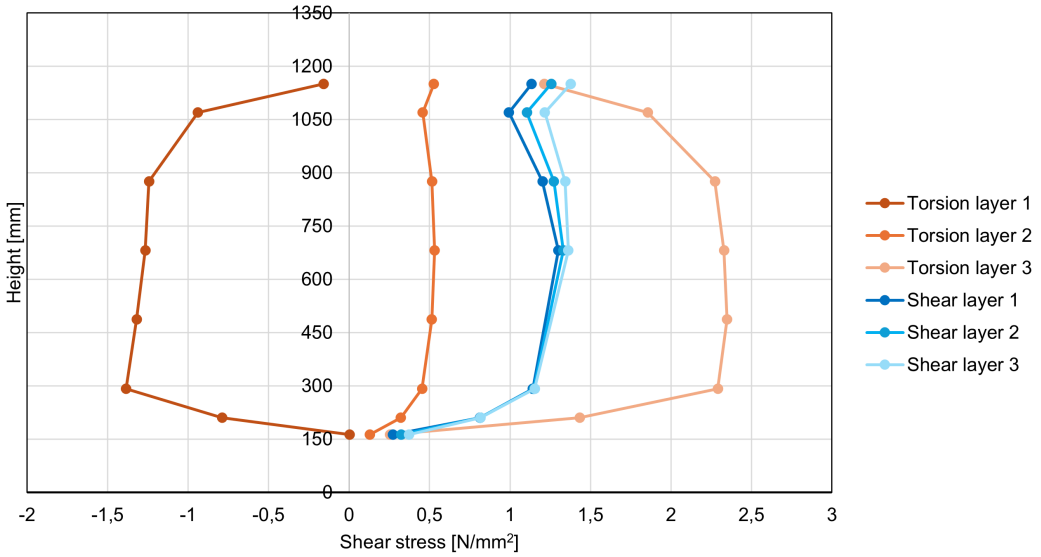

Figure 5.8: Comparison between shear stresses due to shear force and torsion moments at the critical nodes under LC3 and LC4

6

Effect of Design Adjustments

This chapter examines the impact of various design adjustments on the inverted T-girder system, focusing on their behaviour under critical load cases. Initially, the structural performance of different design configurations is compared under these critical load conditions. Following this, an in-depth analysis is conducted on key points of interest. Finally, conclusions are drawn based on the results obtained from these analyses.

6.1. Design adjustments

The structural performance of the original base system is demonstrated by Chapter 5, highlighting how the applied loads are transferred to the supports and identifying the components that contribute to both longitudinal and transverse stiffness. The global operation of the system is elucidated, allowing for the evaluation of several design adjustments.

This research specifically examines the effect of eliminating the end transverse diaphragms from the inverted T-girder system. Recognising the potential reduction in transverse stiffness due to this modification, the study also explores the impact of increasing the deck slab thickness in the absence of the end transverse diaphragms. The additional load that is significant when increasing the full-width deck slab thickness automatically results in higher maximum values. However, the purpose of this adjustment is to increase stiffness and therefore the contribution of the additional self-weight is only indicated in this part of the study.

The results of these modified systems are compared to those of the original system, providing a comprehensive understanding of their impact on overall structural performance. This comparative analysis clarifies the feasibility of various design adjustments, guiding potential improvements in the structural performance of the inverted T-girder system.

6.2. Comparison of distribution in transverse direction

Since eliminating the end transverse diaphragms primarily affects the transverse stiffness of the system, the comparison focuses on load distribution in the transverse direction. Figure 6.1 - Figure 6.4 present the maximum values in the composite girders or deck slab distributed over the width of the system for each critical load case. This comparison only considers values in the girders and deck slab, excluding those in and near the end transverse diaphragms. These figures provide valuable insight into how the design adjustments affect load distribution across the entire system. By analysing these differences, we can assess the impact of removing the end transverse diaphragms and increasing deck slab thickness on load distribution and overall structural integrity.

In these figures, the maximum values of each composite girder are connected with lines for visualisation purposes, even though these values are not related to each other. The graphical representations include:

- Blue lines representing the original system.
- Orange lines representing the system without the end transverse diaphragms.
- Green lines representing the system without the end transverse diaphragms and with an increased deck slab thickness of 350 millimeters.
- Green dashed lines indicating the additional load from the increased deck slab thickness, added to the dead loads.

The maximum longitudinal bending moment per composite girder for each system is presented in Figure 6.1. According to the results, maximum bending moments occur in the inverted T-girders directly beneath the applied loads. The figure shows minor differences between the system with and without the end transverse diaphragms, with a maximum increase of 2% for the peak values in the system without end transverse diaphragms. The maximum bending moments in the system incorporating end transverse diaphragms are more evenly distributed, indicating a slightly better load distribution in the transverse direction. Additionally, in systems without transverse diaphragms, increasing the deck slab thickness shows a minor improvement in transverse load distribution. However, the potential extra weight leads to a significant 20-40% increase in the bending moments per girder.

More significant differences between the systems are observed in the transverse bending moments per meter width in the deck slab at mid-span, as presented by Figure 6.2. The figure shows that all various systems experience hogging moments near the edges and sagging moments under the applied TS loads. The peak values after each dip indicate the support of the deck slab by the girders in the transverse direction. This figure highlights differences between systems with and without transverse diaphragms, with the system incorporating increased deck slab thickness deviating even further. Specifically, the maximum transverse bending moment at mid-span in the deck slab increases by 16% in the system without end transverse diaphragms compared to the base system. Furthermore, the system with an increased deck slab thickness exhibits an approximate 100% increase in maximum bending moment relative to the base system. Notably, the potential extra weight of the thicker deck slab has limited impact on the transverse bending moments.

In Figure 6.3, the maximum shear forces per composite girder are shown with positive values, along with the associated support forces on the negative y-axis. The highest shear forces are observed in composite girders 3 and 4, where TS loads 1 and 2 are closely positioned. No significant differences are observed in the shear force distribution across the different systems. However, two peaks appear in the shear force distribution of the base system due to the concentration of the applied TS loads. This concentration of forces most significantly affects the shear force distribution of the base system, indicating sensitivity to shear force concentrations. Conversely, the distribution of support forces demonstrates more differences in which the base system shows a more levelled transverse load distribution compared to the others. When omitting the end transverse diaphragms, the maximum support force increases by approximately 17%. Additionally, the support forces closely resemble the maximum shear forces but show small differences at the locations where loads are applied. These differences can be attributed to the distance between the location of the maximum shear forces and the supports. The potential extra weight of the thicker deck slab indicates in both the shear and support force distribution a substantial 20-50% increase per girder.

Figure 6.4 presents the maximum torsion moments per composite girder for each system. The location of each girder's maximum torsion moment varies along its length. At the side opposite to where the loads are applied, the torsion moments flow in the opposite direction. However, the highest torsion moments are observed in composite girders 4 and 5, which are adjacent to the girders directly beneath the applied loads. Significant differences are observed between the various systems when comparing the maximum torsion moments. Eliminating the end transverse diaphragms leads to a better distribution of the maximum torsion moments across different composite girders. This modification results in lower torsion moments in the girders near the applied loads, while the girders on the opposite side experience higher torsion moments. Overall, the maximum torsion moments across all composite girders decrease by approximately 22.6% in the system without end transverse diaphragms compared to the base system. Additionally, increasing the thickness of the deck slab ensures a more uniform

distribution of torsion moments over the composite girders, resulting in 36.8% lower peak values. The potential extra load from the increased deck slab thickness does not significantly affect the maximum torsion moments in the composite girders.

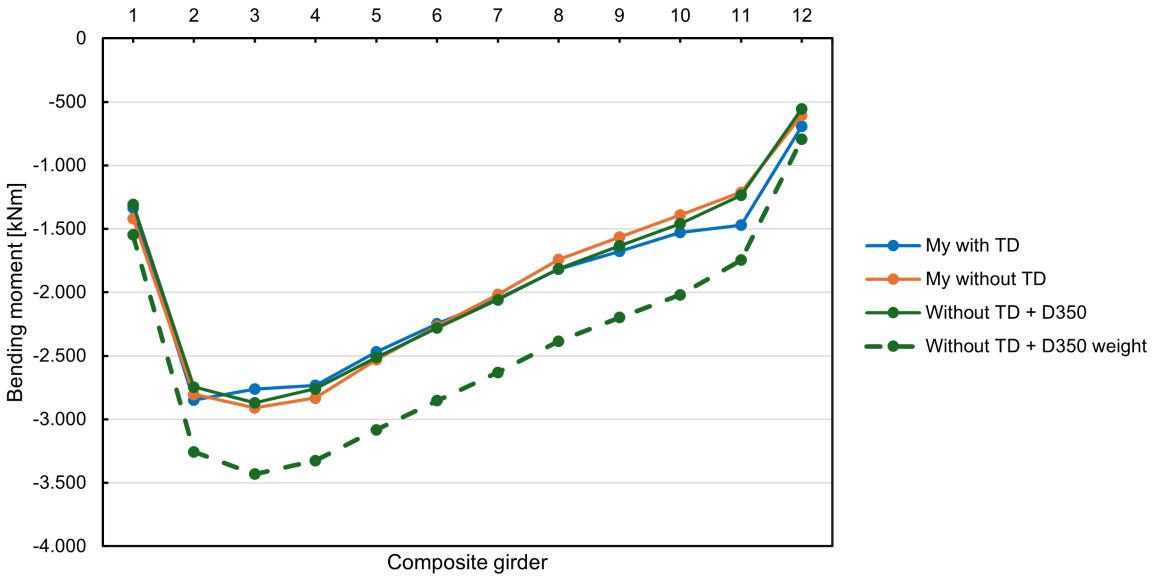

Figure 6.1: Maximum longitudinal bending moments in each composite girder per system (LC1)

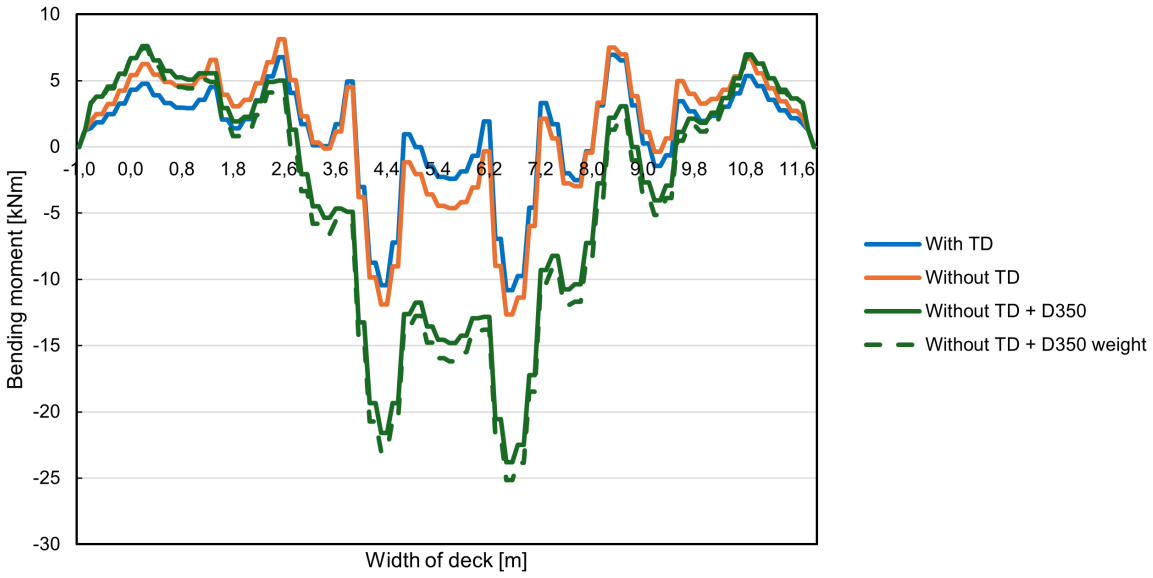

Figure 6.2: Transverse bending moments at mid-span in the deck slab per system (LC2)

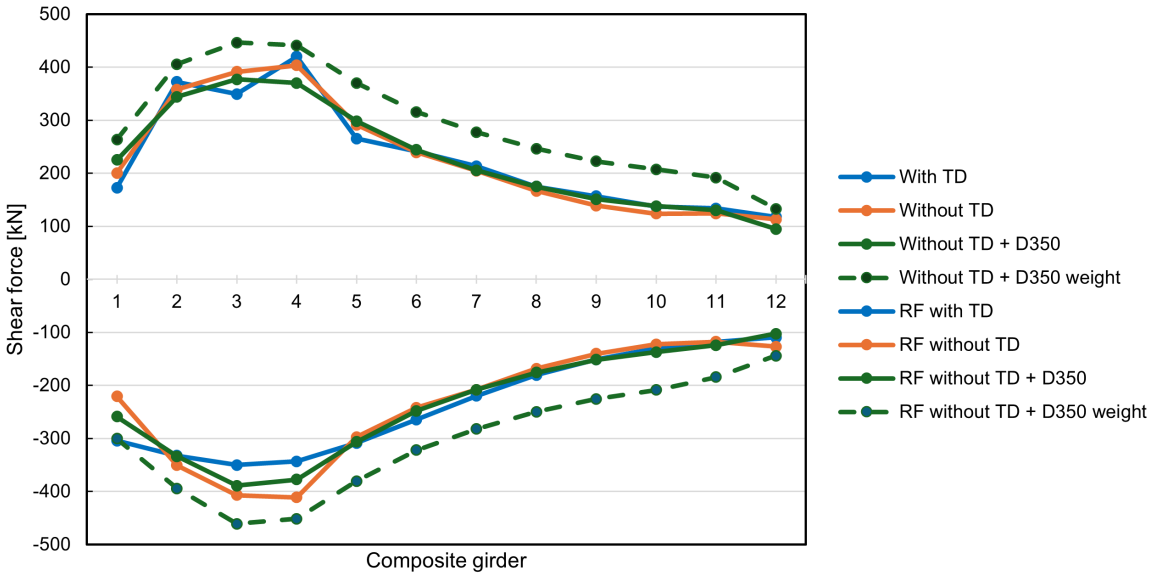

Figure 6.3: Maximum shear forces on the positive y-axis and associated support forces (RF) on the negative y-axis of each composite girder per system (LC3)

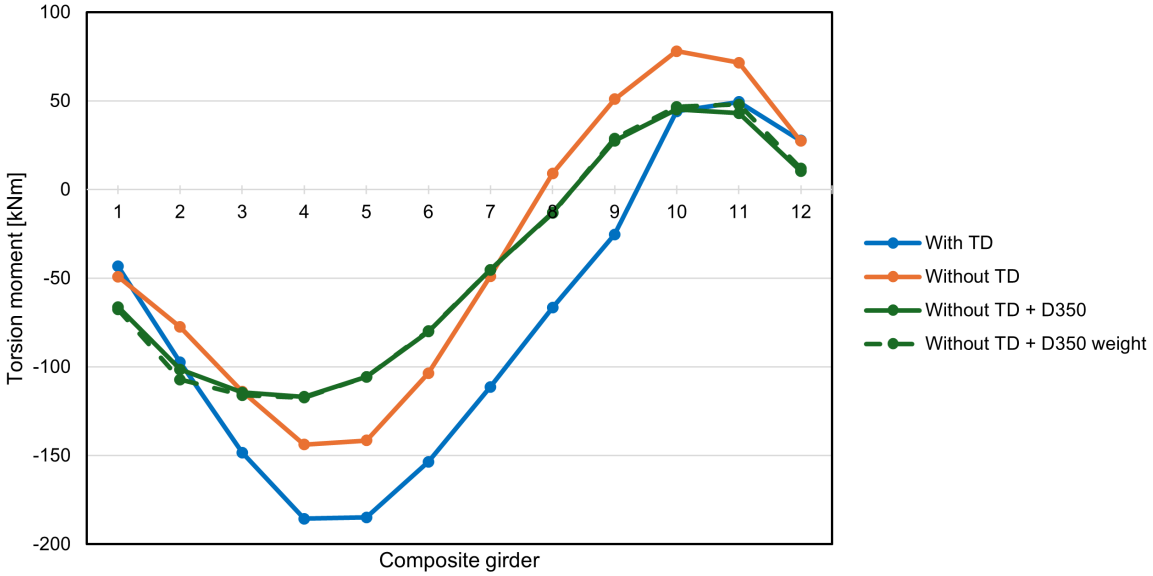

Figure 6.4: Maximum torsion moments in each composite girder per system (LC4)

As indicated by Figure 6.1 - Figure 6.4, the most significant differences between the modified systems are observed when comparing the transverse bending moment at mid-span in the deck slab and the maximum torsion moments in the composite girders. Therefore, further investigation into these load cases is conducted to determine the causes of these differences.

6.3. In-depth analysis of transverse bending moments and torsion moments

The most notable differences between the distinct systems emerge when considering the transverse bending moments in the deck slab and the torsion moments in the composite girders. To assess these differences, an in-depth analysis of these critical cases is conducted. Given the disproportionate in-

crease of nearly 100% in the transverse bending moment, coupled with only minor improvements in the longitudinal bending moment and shear force distribution, increasing the deck slab thickness does not appear advantageous. Although the capacity of the deck slab increases with its thickness, this modification offers no substantial benefit. This conclusion, further elaborated at the end of this chapter, leads to the exclusion of this system from the in-depth analysis. Consequently, the focus will be on comparing the systems with and without the end transverse diaphragms.

Eliminating the end transverse diaphragms results in a 16% increase in the maximum transverse bending moment in the deck slab compared to the base system. This indicates that the deck slab must compensate for the lack of stiffness due to the removal of the end transverse diaphragms. This is likely because the deck slab remains the only transverse connection between the girders. Additionally, the torsion moments in the composite girders decrease by nearly 23% when the end transverse diaphragms are removed. While this reduction seems advantageous, there may be drawbacks not immediately apparent from these results. Therefore, this section will further investigate the impact of eliminating the end transverse diaphragms on other system characteristics for these two critical cases.

6.3.1. Transverse bending moments in the deck slab

The difference in the transverse bending moments in the deck slab between the systems suggests that normal transverse stresses in the deck slab increase when the end transverse diaphragms are eliminated. The normal stresses in the deck slab are displayed over three layers, with the bottom and top layers showing the peak values that are evaluated and compared. Figure 6.5 shows the transverse normal stresses in the bottom layer of the deck slab, while Figure 6.6 presents the normal stresses in the top layer of the deck slab for both systems.

For the bottom and top layers, the distribution of transverse normal stresses across the deck slab is nearly identical for both systems. However, the system without end transverse diaphragms exhibits higher stress values near the supported edges in both layers. Additionally, the modified system experiences larger maximum stresses, aligning with the larger observed moments. The maximum tensile stresses are found in the bottom layer of the deck slab at the location of the largest TS loads. Removing the end transverse diaphragms results in a 15% increase in maximum tensile stresses. Similarly, in the top layer of the deck slab, maximum compressive stresses occur at the same location, showing a 16% increase when end transverse diaphragms are eliminated. These results are consistent with the trends observed in the transverse bending moments in the deck slab.

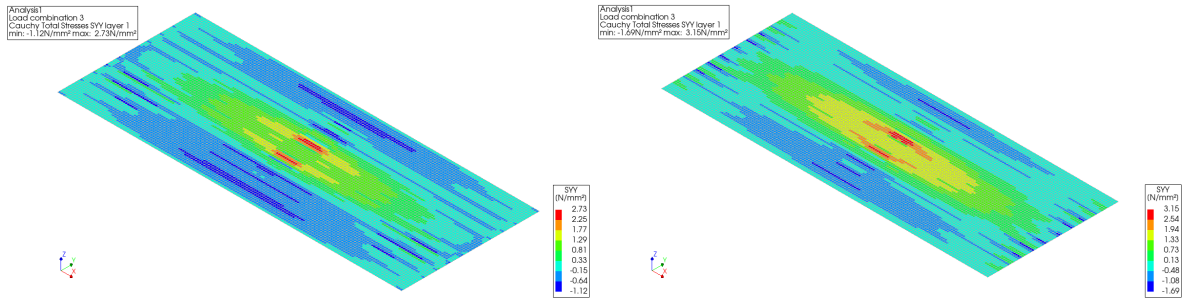

(a) System with end transverse diaphragms

(b) System without end transverse diaphragms

Figure 6.5: Transverse normal stress in the bottom layer of the deck slab for both systems

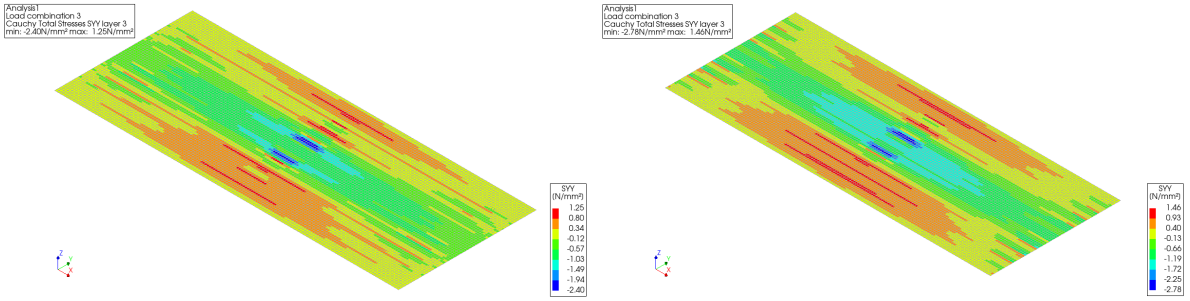

(a) System with end transverse diaphragms

(b) System without end transverse diaphragms

Figure 6.6: Transverse normal stress in the top layer of the deck slab for both systems

6.3.2. Torsion moments in the girders

To further clarify the difference in torsion moments, Figure 6.7 presents the complete distribution of torsion moments along the length of the governing composite girder for both systems. Considering an orthogonal system with centrally applied loads, both systems display a symmetrical distribution along the length of the girder. The primary distinction between the torsion moment distributions is observed in the peak values near the edges. As described by Section 2.2.2, torsion moments occur when rotation is restrained, resulting in shear stresses within the composite girders. In the base system, torsion moments reach their maximum values near the edges at the location of the end transverse diaphragms. In contrast, the modified system shows nearly zero torsion moments at the girder ends.

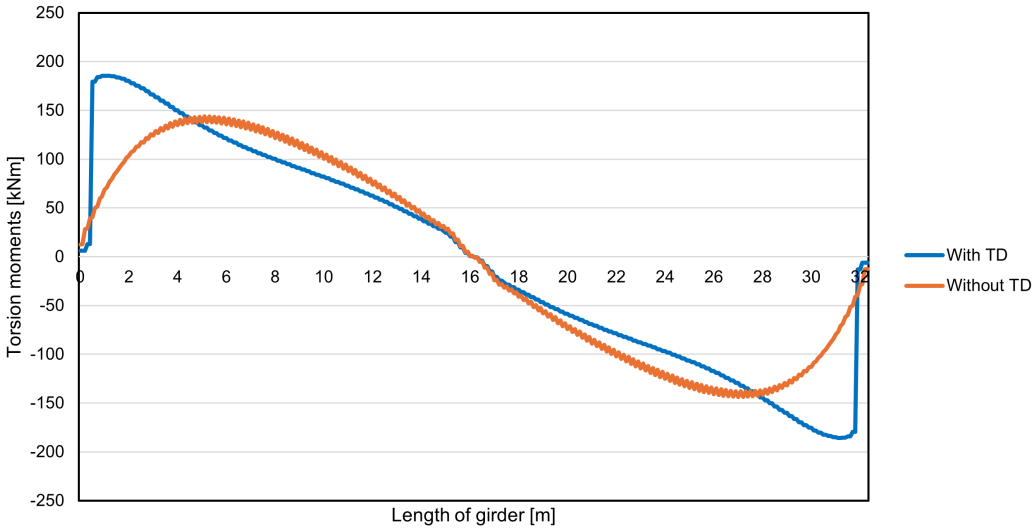

Figure 6.7: Distributed torsion moment along the length of the governing girder for each system

Since the deck slab remains the only transverse connection between the girders, the reduction of torsion moments in the composite girders is expected to impact the moments in the deck slab. This effect can be analysed by examining the twisting moments in the deck slab for both systems. Given that the twisting moments in the deck slab are symmetrical, Figure 6.8 focuses on the moments on one side. As shown in the figure, the twisting moments in the deck slab increase by approximately 28%. Moreover, the locations of these increased twisting moments correspond to the regions where the peak values of the torsion moments in the girders decrease.

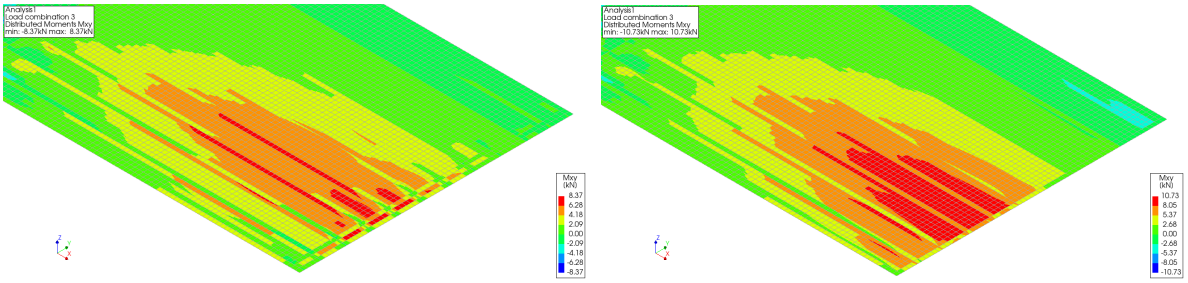

(a) System with end transverse diaphragms **(b)** System without end transverse diaphragms

Figure 6.8: Twisting moments in the deck slab of both systems

Furthermore, variations in torsion moments within the composite girders could influence the maximum shear stresses. Therefore, the shear stresses within the cross-section of the composite girders are analysed at the location of the critical torsion moments, which occur at x = 27.85 and x = 31.25. Figure 6.9 illustrates the size and direction of the shear stresses across the cross-section of the composite girder for both systems at 27.85 m, whereas Figure 6.10 shows the shear stresses at 31.25 m.

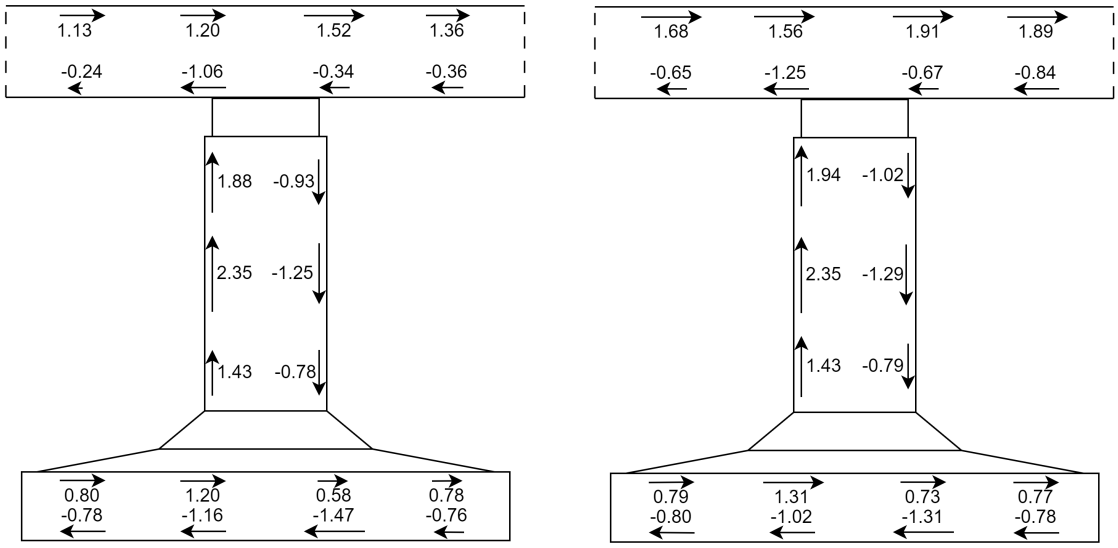

(a) System with end transverse diaphragms **(b)** System without end transverse diaphragms

Figure 6.9: Shear stresses in cross-section composite girder for different systems at x = 27.85 m

As shown by Figure 6.7, the torsion moments at x = 27.85 m are identical for both systems, with the maximum value observed in the system without end transverse diaphragms. Figure 6.9 compares the shear stresses in the composite girders for both configurations, illustrating that the shear stresses in the bottom flange and the girder web are similar for both systems. However, there is a slight increase in the shear stresses of the deck slab.

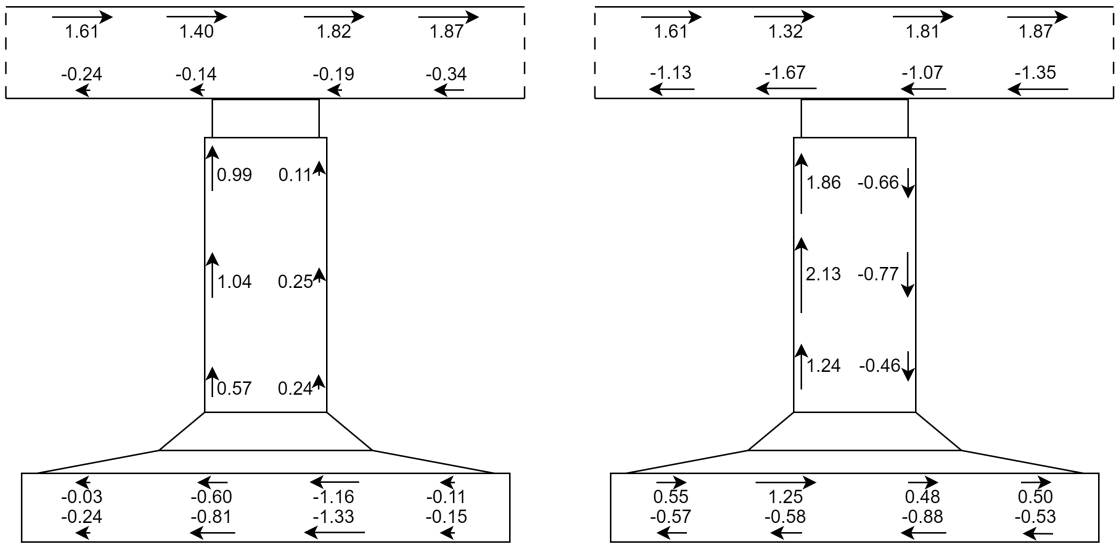

(a) System with end transverse diaphragms

(b) System without end transverse diaphragms

Figure 6.10: Shear stresses in cross-section composite girder for different systems at x = 31.25 m

Additionally, Figure 6.7 highlights significant differences in torsion moments between the two systems at x = 31.25 m. At this location, the governing girder from the base system experiences the maximum torsion moment, whereas the governing girder from the modified system exhibits a significantly smaller torsion moment. This discrepancy can also be observed in the shear stresses within the cross-sections, as presented by Figure 6.10. The large difference in torsion moments can be attributed to the alignment of shear stresses in the base system's girder. In this system, the shear stresses in the bottom flange and the web of the girder are oriented in the same direction. Additionally, the shear stresses in the deck slab are predominantly aligned in one direction, enhancing the overall torsion moment around the cross-section's centre of torsion. Conversely, in the modified system, the shear stresses are oriented oppositely. Although the shear stresses are higher in absolute terms, they effectively cancel each other out, resulting in smaller torsion moments. Therefore, a decrease in torsion moments in a composite girder does not necessarily lead to lower shear stresses.

The elimination of the end transverse diaphragms from the system decreases the torsion moments in the composite girders, impacting the shear stress distribution within the girder's cross-section. However, this change does not significantly affect the maximum shear stress across the entire system. While the torsion moments in the girder decrease, the absolute maximum shear stress remains unchanged, as for both systems the maximum shear stresses occur around x = 27.85 m.

6.4. Conclusion

The impact of various design adjustments on the inverted T-girder system is examined by comparing their structural performance with the base system. Through an in-depth analysis of the most critical points, significant findings are revealed, allowing for conclusions to be drawn.

Eliminating the end transverse diaphragms from the inverted T-girder system generally has minimal impact on the transverse distribution of longitudinal bending moments and shear forces across different composite girders. However, it results in a 17% increase in the maximum support force at one of the girder supports, leading to a locally heavier load on the substructure. This increase is not expected to cause issues, as the total load on the substructure remains unchanged. Additionally, practical experiences suggests that substructures are generally designed with additional capacity beyond what is ultimately required. Significant differences are observed in the deck slab when the end transverse diaphragms are removed. The deck slab must compensate for the loss of stiffness, leading to a positive impact on the maximum torsion moments in the composite girders, though maximum shear stresses remain unchanged. The transverse bending moment in the deck slab increases by 16%, leading to a

corresponding rise in maximum normal stresses in the transverse direction. Additionally, the twisting moments in the deck slab increase by 17%. Both increases in bending and twisting moments can be managed by increasing the reinforcement in the deck slab. Despite the limitations of this study, removing the end transverse diaphragms requires the deck slab to handle greater bending and twisting moments. However, this is achievable with minor adjustments, primarily through additional reinforcement. While these adjustments might lead to increased material usage, the advantages of eliminating the end transverse diaphragms are anticipated to outweigh the drawbacks.

Increasing the deck slab thickness to compensate for the reduction in transverse stiffness caused by the removal of end transverse diaphragms is not advantageous for several reasons. The added rigidity from a thicker deck slab has minimal impact on balancing the maximum longitudinal bending moments and shear forces in the composite girders. Moreover, this adjustment nearly doubles the transverse bending moments in the deck slab. While the capacity of the deck slab increases with thickening, this significant increase will not directly lead to excessive stresses. However, given that the adjustment requires significantly more material and only offers minor improvements, it does not provide a meaningful advantage over a thinner deck slab. Additionally, the increased material usage negatively impacts the environment. The only notable benefit of a thicker deck slab is a reduction in the maximum torsion moments in the composite girders, with these maximum values becoming more evenly distributed among the various girders. When the potential additional weight of the increased deck slab is also considered, the overall outcomes argue against this solution.

Furthermore, the impact of increasing the thickness is more pronounced in the transverse direction compared to the longitudinal direction, due to the relatively larger increase in thickness. The results indicate that deformation in the longitudinal direction is predominant over the transverse direction, suggesting that the deck slab experiences imposed deformation in the transverse direction. A thicker, more rigid deck slab has greater difficulty accommodating this imposed deformation, leading to higher internal moments. Although the capacity of the deck slab increases with thickness, these higher moments do not pose a problem but also offer no significant advantages. Overall, these findings suggest that increasing deck slab thickness is neither feasible nor beneficial for improving the system's performance.

The potential additional weight of the increased deck slab indicates that an increase in self-weight or distributed loads over the entire structure primarily affects the maximum longitudinal bending moments and shear forces. Conversely, the maximum torsion moments remain unaffected, suggesting that the torsion moments in the composite girders are generated by asymmetrical axle loads. Additionally, the transverse bending moments in the deck slab are highly dependent on the position of the axle loads between the girders. These findings offer valuable insights into the specific types of loads that cause particular stresses, leading to more effective structural design and analysis.

7

Effect of Skewness on the Behaviour of Inverted T-Girder Systems

This chapter assesses the applicability of findings from the orthogonal system comparison by examining the effects of various skew angles on the modified systems used in this study. It begins by reviewing relevant studies, followed by the modelling approach and loading conditions used to evaluate the impact of different skew angles. The results of this evaluation are then outlined and discussed, leading to the formulation of conclusions.

7.1. Introduction

As mentioned in Chapter 2, most viaducts or bridges are not constructed orthogonally but with a certain skew angle to better fit into the available space of the surroundings. The skew angle of a structure is defined as the angle between the abutments and the longitudinal centerline of the girders, represented by θ in Figure 7.1 - Figure 7.4. With this convention, an orthogonal system corresponds to a skew angle of 90 degrees.

For simplicity reasons, this study initially considered an orthogonal system as a test case. However, previous research indicates that a skew angle in a girder system significantly influences the load transfer mechanisms. As the skew angle increases, the system exhibits asymmetric responses due to the non-orthogonal alignment of the supporting lines with the girders. This misalignment results in different structural behaviours, with load concentrations typically occurring in the obtuse corners [16]. Several relevant studies have highlighted the effects of skewness on girder bridges.

One example is the research conducted by Menassa et al. (2007) [44], in which the effect of skew angle on multiple configurations of reinforced concrete slab bridges was investigated. This research incorporated multiple skewed simply supported one-span slab bridges with uniform material properties subjected to live loads by trucks over the complete span. The results of this study indicate that the longitudinal bending moments decrease as the skew angle decreases. Conversely, the transverse bending moments increase with a reduction of the skew angle. Significant differences are only observed when the skew angle is less than 70 degrees, suggesting that bridges with skew angles between 90 and 70 degrees can be designed as straight bridges.

Another relevant study is by Nagashekhar et al. (2016) [51], which examined the effect of skew angle on the behaviour of precast I-girder bridges by considering the maximum bending moment, shear force, and torsion moment. This study compared the results of skewed bridges with non-skewed bridges for both dead loads and live loads. The findings indicate that the maximum bending moments decrease as the skew angle decreases, while the maximum shear forces increase. Additionally, the maximum torsional moment initially increases with a smaller skew angle but then decreases, indicating dependence on span and skew angle. Furthermore, bridges with skew angles up to 75 degrees can be analysed as

non-skewed bridges.

Another study by Harba (2011) [32] addresses the impact of skew angles by conducting a three-dimensional finite element method to examine the behaviour of simply supported T-beam girder bridges. The model represents a simply supported T-beam bridge with uniform material properties subjected to edge truck loading. The results indicate that bending moments and deflections decrease, while torsion moments increase with a smaller skew angle. Shear forces and support forces in the girders either increase or decrease depending on the girder's location as the skew angle increases. Consequently, this study challenges the recommendation to consider skewed systems up to 70 degrees as straight systems.

The study by Minalu (2010) [45] addresses the effect of skew angles on the behaviour of an inverted T-girder bridge. Minalu employs two different finite element modelling techniques: one based on the orthotropic plate model with eccentric beam elements, and the other without. These models are used to analyse bending moments and torsion moments in the first composite girders, transverse bending moments in the deck slab, and torsion moments in the end transverse diaphragms. The model accounts for cracked stiffness in the end transverse diaphragms and the transverse direction of the deck slab by reducing the elastic modulus of these cast in-situ concrete elements. The findings indicate that as the skew angle decreases, the longitudinal bending moments in the reference girder decrease, while the torsion moments increase at the obtuse corner of the system. Additionally, the transverse bending moments in the deck slab increase as the skew angle decreases.

These studies present consistent findings of the impact of skew angles on longitudinal and transverse bending moments. However, despite not all studies incorporating these design parameters, the results for shear forces and torsion moments are inconclusive in some cases. Minalu's study aligns most closely with this research, as it tested systems under maximum design conditions according to the Eurocode [22] and accounted for the orthotropic material properties of the deck slab. Consequently, the findings of this research will be primarily compared with those of Minalu's study in Section 8.2.

The effect of skew angles on systems is examined using the same test case and critical load configurations previously employed in this study, maintaining the same geometries and assumptions. Critical load cases are ensured by adjusting the load arrangements with the same skew angle of the system. In addition to the orthogonal system with a 90-degree skew angle, three other skew angles of 75, 60, and 45 degrees are considered. This approach allows for a comprehensive analysis of the impact of skew angles on the load distribution in the modified systems. The objective is to evaluate the applicability of findings from the orthogonal test system to systems with varying skew angles.

7.2. Critical load cases for different skew angle bridges

The effect of skewness on the structural integrity of the system is assessed using the same critical scenarios as with the orthogonal system. The load configurations selected to generate maximum values for longitudinal bending moment, transverse bending moment, shear force, and torsion moments are adjusted for each skew angle. Note that the TS loads are transformed relative to the center of the four-axle loads, resulting in loads not being exactly in the middle of the span. This effect increases with the skew angle. Figure 7.1 - Figure 7.4 illustrate the transformation of both the system and load arrangements with the skew angle, depicted by θ.

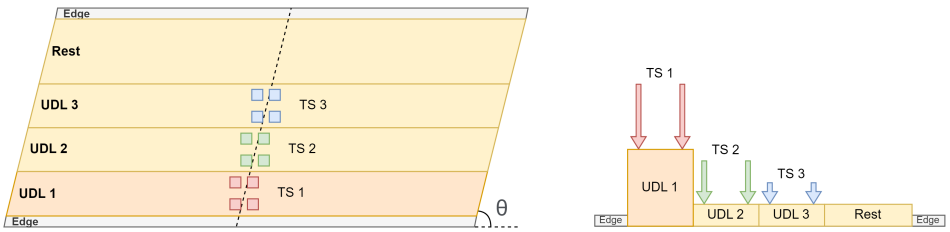

Figure 7.1: Traffic load arrangement for maximum longitudinal bending moment in skewed systems

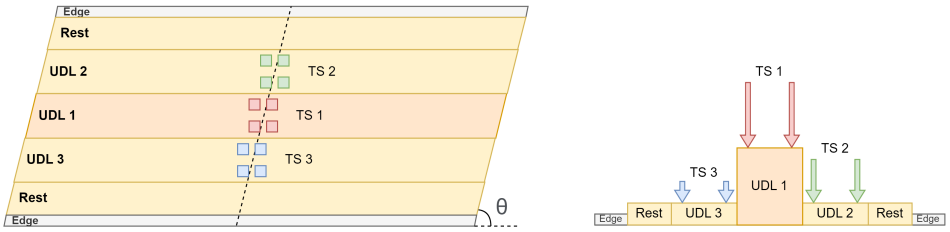

Figure 7.2: Traffic load arrangement for maximum transverse bending moment in skewed systems

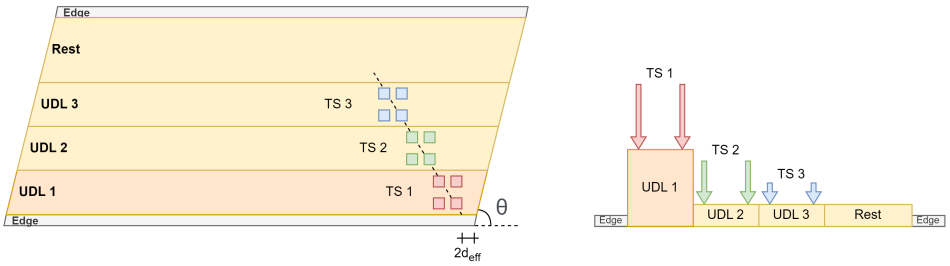

Figure 7.3: Traffic load arrangement for maximum shear force in skewed systems

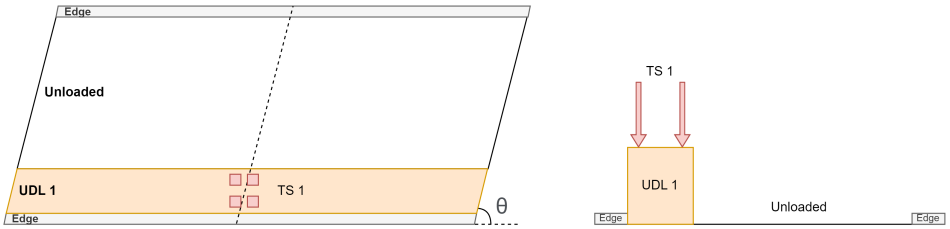

Figure 7.4: Traffic load arrangement for maximum torsion moment in skewed systems

In addition to the live loads, the permanent loads from the asphalt layer, scrap strips, and edge structures are considered in the model. As with the orthogonal system, each traffic load arrangement is combined with the dead loads to form a load combination. The load combinations applicable to each critical scenario are provided in Table 7.1.

Table 7.1: Load combinations employed in the numerical model for skewed systems

Load combination	Dead loads	Live loads
LC 5	asphalt layer + additional dead loads	critical load case 5
LC 6	asphalt layer + additional dead loads	critical load case 6
LC 7	asphalt layer + additional dead loads	critical load case 7
LC 8	asphalt layer + additional dead loads	critical load case 8

7.3. Model results

The impact of the skew angle on the behaviour of the modified systems is evaluated by comparing the maximum values of the key design parameters. Since the transverse direction of the system changes with the skew angle, and the composed lines integrate elements perpendicular to this line, the results from the composed lines no longer correspond accurately. Therefore, to ensure consistent comparisons across all systems with different skew angles, distributed moments in the deck slab are used.

Unlike the transverse bending moments from the composed lines, these values are expressed per element and not integrated over a meter width. Furthermore, building on the conclusion from Chapter 6 that torsion moments in the composite girders are related to twisting moments in the deck slab, both parameters are analysed to evaluate the effect of the skew angle on the system's torsion moments. The maximum values for the design parameters are determined by subjecting the skewed modified system to their most critical load cases, as detailed in Section 7.2.

Table 7.2 - Table 7.4 detail the maximum values observed for each design parameter in each system with a certain skew angle. Subsequently, the effect of the skew angle on each design parameter is highlighted and further explained. It is important to note that only the maximum values are considered, which may cause the locations where these maximum values occur to vary for each skew angle.

Table 7.2: Maximum value per critical load case in the original system for each skew angle

Skew angle	Max. longitudinal bending moment [kNm]	Max. transverse bending moment [kNm/m]	Max. shear force [kN]	Max. torsion moment [kNm]	Max. twisting moment [kNm/m]
90	2848.9	17.1	419.8	185.6	8.4
75	2842.6	17.2	410.7	188.5	8.6
60	2818.6	17.8	399.9	181.3	9.8
45	2751.6	18.6	384.7	162.8	10.4

Table 7.3: Maximum value per critical load case in the system without end transverse diaphragms for each skew angle

Skew angle	Max. longitudinal bending moment [kNm]	Max. transverse bending moment [kNm/m]	Max. shear force [kN] [kN]	Max. torsion moment [kNm] [kNm]	Max. twisting moment [kNm/m]
90	2910.2	19.7	403.6	143.7	10.7
75	2910.1	19.9	404.4	145.9	11.3
60	2828.9	19.9	384.2	133.8	12.6
45	2871.0	21.3	370.5	129.8	13.8

Table 7.4: Maximum value per critical load case in the system without end transverse diaphragms and increased deck slab thickness for each skew angle

Skew angle	Max. longitudinal bending moment [kNm]	Max. transverse bending moment [kNm/m]	Max. shear force [kN]	Max. torsion moment [kNm]	Max. twisting moment [kNm/m]
90	2870.8	32.6	377.3	117.1	31.8
75	2859.9	32.9	375.3	126.0	35.3
60	2748.1	34.0	384.5	120.9	41.3
45	2778.4	37.3	345.2	134.2	50.7

7.3.1. Effect of skewness for the maximum longitudinal bending moment

The maximum longitudinal bending moments for each modified system at different skew angles are presented in Figure 7.5. The overall trend indicates a decrease in the maximum longitudinal bending moments as the skew angle decreases. This observation aligns with the conclusions of the studies cited in the introduction of this chapter. All maximum values are observed at the mid-span of the second composite girder.

For skew angles 90 and 75 degrees, the maximum values for each system remain nearly equal. Between skew angles of 75 and 45 degrees, the maximum values of the base system decrease further, leading to a maximum reduction of 3.4% compared to the orthogonal system. The systems without end transverse diaphragms show a decrease of 1.3% and 3.2% for the 45-degree skewed system relative to the orthogonal system. Although all systems follow a similar trend, the systems without end transverse diaphragms exhibit a significantly lower maximum bending moment at the 60-degree skew angle. The position of the maximum values remains unchanged, suggesting that this drop could be due to a change in the load transfer mechanism, resulting in a better distribution of moments along the girders than expected.

Furthermore, excluding the values from the 60-degree skewed systems, the differences between the distinct systems for each skew angle increase as the skew angle decreases. The difference between the systems with and without end transverse diaphragms increases from 2.2% for the orthogonal system to 4.3% for the 45-degree skewed systems. The differences between the base system and thick deck slab system follow a similar trend but remain within a 1.0% deviation.

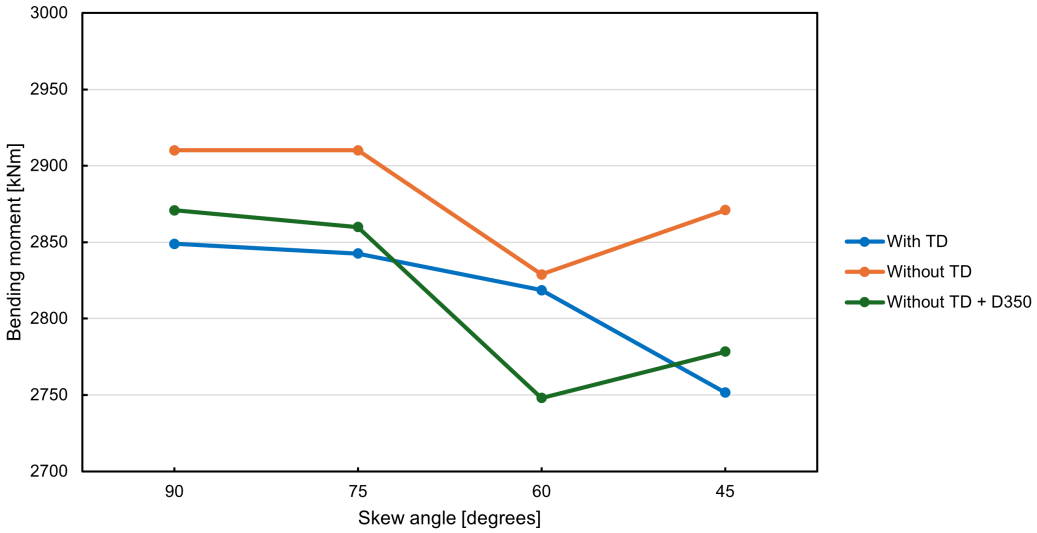

Figure 7.5: Maximum longitudinal bending moment in the composite girder per system for different skew angles

7.3.2. Effect of skewness for the maximum transverse bending moment

The maximum transverse bending moments in the deck slab of each system for different skew angles are presented in Figure 7.6. These maximum values are located beneath one of the TS loads in the middle of the deck slab and are consistent for all systems and skew angles.

For skew angles of 90 and 75 degrees, the values remain consistent across all systems. However, as the skew angle decreases further, the maximum values increase, reaching a peak increase of 8.1% and 8.7% for the system with and without end transverse diaphragms, respectively. The system with a thick deck slab demonstrates a significant increase, with a maximum of 14.4% for a 45-degree skewed system relative to the orthogonal configuration.

The mutual differences between the systems with and without end transverse diaphragms remain nearly constant across different skew angles, ranging from 13.2% for the orthogonal system to 10.6% for the 60-degree skewed systems. The system with the increased deck slab thickness shows a notable increase of at least 88% relative to the base system, with this increase becoming more pronounced as the skew angle decreases.

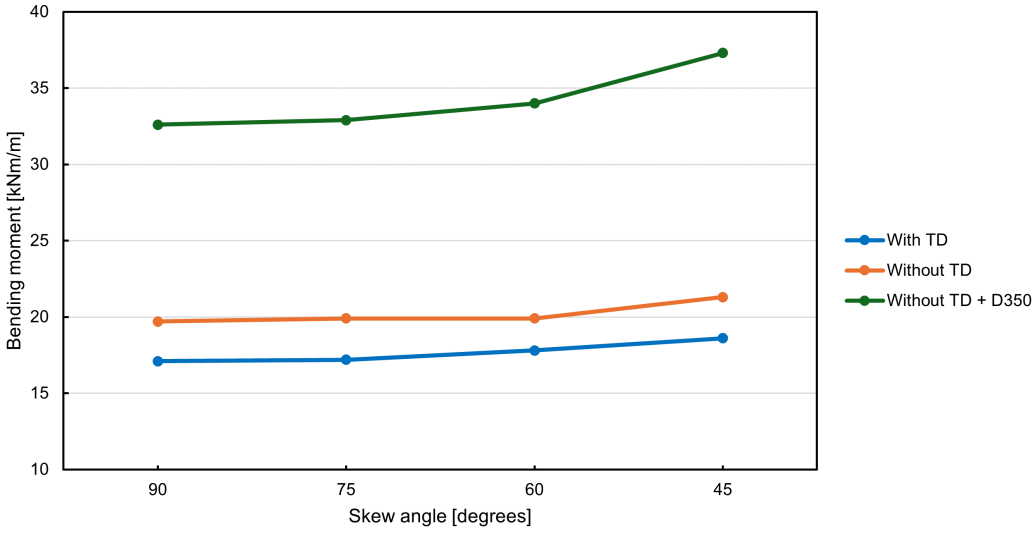

Figure 7.6: Maximum transverse bending moment in the deck slab per system for different skew angles

7.3.3. Effect of skewness for the maximum shear force

The maximum shear forces in the composite girders for each system at various skew angles are displayed in Figure 7.7. As the skew angle decreases, the maximum shear forces in the girders also decrease. The maximum values for the systems with and without end transverse diaphragms occur in the fourth composite girder, while in the thick deck slab system, the maximum value shifts to the third composite girder.

At a skew angle of 45 degrees, the base system shows a maximum reduction of 8.4%. The system without end transverse diaphragms experiences a reduction of 8.2% and the thick deck slab system exhibits a reduction of 9.6%. Unlike other design parameters, the maximum values for the systems with and without end transverse diaphragms differ significantly between skew angles of 90 and 75 degrees.

Additionally, the mutual differences between the systems remain almost consistent across all skew angles. The difference between systems with and without end transverse diaphragms varies between a 3.7% and 3.9% decrease in shear forces per skew angle. The thick deck slab system shows a difference ranging from 9.1% to 10.3% per skew angle relative to the base system.

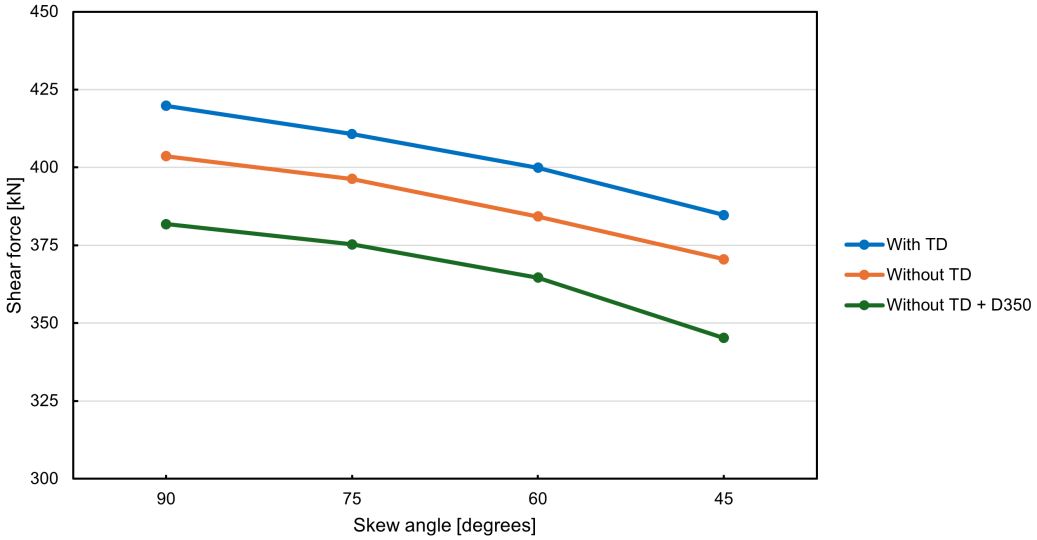

Figure 7.7: Maximum shear forces in the composite girder per system for different skew angles

7.3.4. Effect of skewness for the maximum torsion moment

To assess the effect of the skew angle on the torsion moments in the system, both the twisting moments in the deck slab and the torsion moments in the composite girders are considered, as they are interrelated. Figure 7.8 presents the maximum torsion moments in the composite girder per system for various skew angles, while Figure 7.9 shows the maximum twisting moments in the deck slab for the same skew angles. The overall trend, illustrated in the figures, indicates that as the skew angle decreases, torsion moments in the girders decrease, while the twisting moments increase.

For the base system, the maximum torsion moments in the composite girders decrease by 12.3% as the skew angle reduces to 45 degrees. In contrast, the system without end transverse diaphragms exhibits a maximum reduction of 9.7%, while the system with an increased deck slab thickness shows a 14.6% increase when the skew angle is reduced to 45 degrees. The mutual difference between the systems with and without end transverse diaphragms varies from 26.2% for 60-degree skewed systems to 20.3% for 45-degree skewed systems. For the system with an increased deck slab thickness, the mutual differences relative to the base system decrease from 36.9% for the orthogonal systems to 17.6% for high-skewed systems, indicating a reduced impact as the skew angle decreases.

Compared to the maximum values of other design parameters, a clear shift is observed in the position of the maximum values. For the base system, the maximum torsion moments stay around composite girder 4 and 5 for each skew angle, while for the systems without end transverse diaphragms, the maximum value shifts towards the second composite girder, concentrating around the obtuse corner as the skew angle decreases. The concentration of torsion moments appears higher for the system with an increased deck slab thickness, resulting in an overall increase in maximum torsion moments as the skew angle decreases.

Additionally, the twisting moments in the deck slab show a maximum total increase of 23.8% for the base system and 29.0% for the system without end transverse diaphragms as the skew angle decreases. The mutual differences between these systems increase from 27.4% for orthogonal systems to 32.7% for 45-degree skewed systems. The system with an increased deck slab thickness shows significant discrepancies from the base system, with a minimum increase of 278.6%, rising to a maximum of 387.5% as the skew angle decreases. These substantial differences can be attributed to the fact that the thickness of the deck slab influences the plate moments to the power of three.

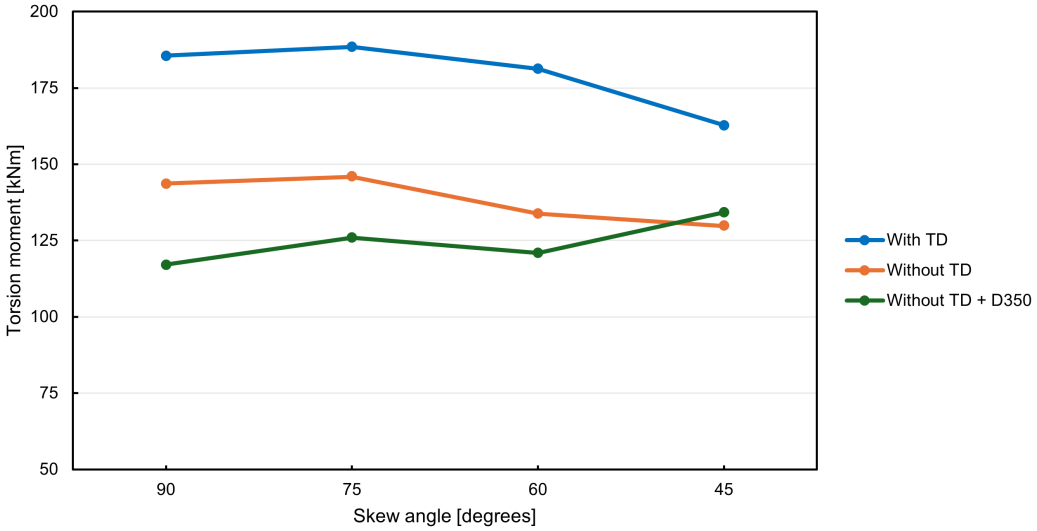

Figure 7.8: Maximum torsion moments in the composite girder per system for different skew angles

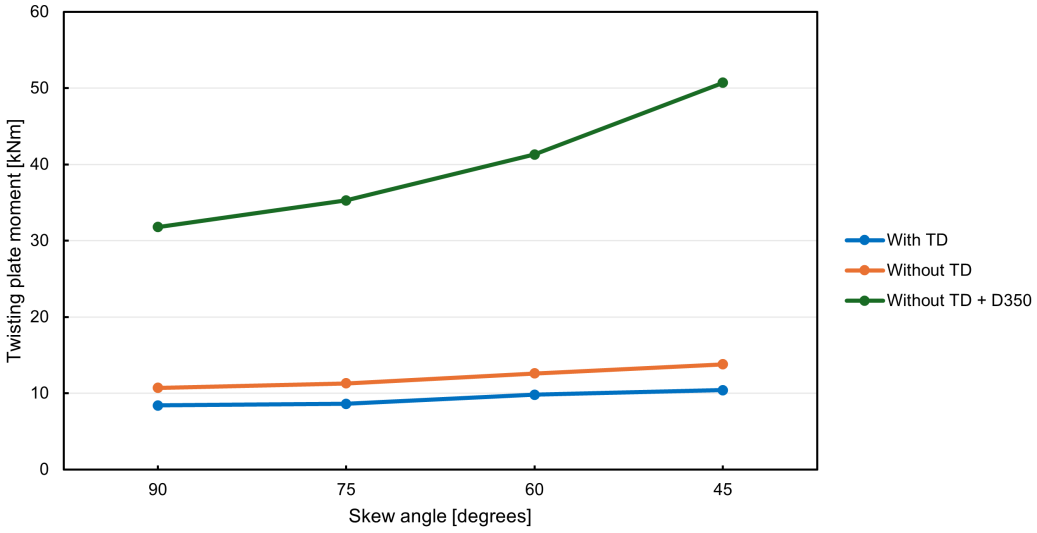

Figure 7.9: Maximum twisting moments in the deck slab per system for different skew angles

7.3.5. Validity of critical load cases

Reducing the skew angle can significantly impact load transfer mechanisms and system behaviour. Large changes in skew angle create different structural configurations due to the altered positioning of supports. Consequently, the critical scenarios for structures with extreme skew angles may differ from those assumed in this study. To ensure that the most critical load configurations are considered, alternative load arrangements have been examined for high-skewed systems.

The validity of the assumed critical load cases was verified by comparing different load arrangements for the 45-degree skewed system. This process involved varying the positioning of the TS loads, either by not adjusting them according to the skew angle or by counteracting this angle. For all design parameters, no other critical load cases were identified. While this finding does not entirely rule out the possibility of other critical load cases for specific skew angles, it suggests that the values used for comparison are likely near the maximum.

Additionally, it is important to note that the ratio between the width and length of the structure also influences load transfer mechanisms. Specifically, for highly skewed systems, the critical load cases could differ as the width/length ratio increases. A structure with more equal dimensions and a width/length ratio closer to one could have different load transfer mechanisms, as the supports of the skewed system are closer to the applied loads. The critical load cases employed in this study and their results are only valid for this specific width/length ratio. In the case of a lower ratio, it is likely that the same critical load cases will remain governing.

7.4. Conclusion

The effects of various skew angles in a simply supported single-span inverted T-girder system were examined using a numerical model. This numerical model performed a linear analysis on shell element-based prefabricated inverted T-girders with a cast in-situ deck slab. Three different skew angles were considered and tested, keeping the system geometry and characteristics unchanged. To clearly understand the effects of skew angles on the modified inverted T-girder systems, the maximum longitudinal bending moment, transverse bending moment, shear force, torsion moment, and twisting moment were compared with those of the reference orthogonal system. This additional comparison helps assess the applicability of the findings from the orthogonal system to skewed systems.

In general, the findings indicate that as the skew angle decreases, the maximum values within the deck slab increase, while the maximum values in the composite girders decrease. The only exception is the maximum torsion moment in the composite girders of the thick deck slab system which increases with the reduction of the skew angle. However, the overall findings indicate that in skewed systems, the deck slab should absorb relatively more forces and moments than the composite girders.

Additionally, the location of the maximum values per system remains generally unchanged across different skew angles. Only the location of the maximum torsion moments within the composite girders of the systems without end transverse diaphragms shifts towards the obtuse corner. While the maximum values in the base system stay at the same location for different skewed systems, the maximum values of the modified systems vary as the skew angle decreases. Eliminating the end transverse diaphragms leads to the concentration of torsion moments towards the girders near the obtuse corner as the skew angle decreases. This effect is enhanced by the thick deck slab system, in which these maximum values even increase when reducing the skew angles.

Furthermore, the maximum values in the composite girders of the base system decrease slightly faster with a reduction in the skew angle compared to the system without end transverse diaphragms. Conversely, the maximum values in the deck slab of the base system increase less with a decreasing skew angle than those in the system without end transverse diaphragms. Despite these differences, the mutual differences between the systems with and without end transverse diaphragms per skew angle do not show clear patterns. For the longitudinal bending moment and twisting moment, the mutual differences between the maximum values of these two systems increase slightly as the skew angle decreases. Meanwhile, the mutual differences in transverse bending moments, shear forces, and torsion moments become smaller with decreasing skew angle. The maximum impact of the skew angle on these mutual differences ranges up to 2.6%, with an exception of 5.6% for the torsion moments at the skew angle of 60 degrees and 5.3% for twisting moments at the skew angle of 45 degrees. Considering these two exceptions, it can be stated that the mutual differences between the systems with and without the end transverse diaphragms remain nearly consistent across various skew angles. Therefore, the results obtained by comparing these two systems are applicable to different skew angle systems with the same order of magnitude.

For the system with an increased deck slab thickness, the maximum values generally follow the same trend as the system without end transverse diaphragms, with the exception of the torsion moments in the composite girders. However, the differences compared to the base system are more pronounced than those observed when only the end transverse diaphragms are removed. In this system, the maximum values in the girders are smaller, while those in the deck slab are greater. Furthermore, the mutual differences with the base system increase as the skew angle decreases, except for the max-

imum torsion moments, where the differences decrease with a reduced skew angle. Especially, the maximum values within the deck slab increase significantly as the skew angle decreases, highlighting that the impact of reducing the skew angle is more significant for systems with an increased deck slab thickness. The substantial increase in moments in the deck slab and the varying developments across different skew angles underscore that this design adjustment is not a suitable option for improving overall structural performance.

8

Discussion

This chapter discusses the numerical model and the analysis considerations adopted in this study. It then presents and compares the results obtained from design adjustments and the effects of various skew angles, contrasting these findings with those of previous studies.

8.1. Discussion on numerical model

To observe the effects of various design adjustments and the system's skew angle, a numerical model based on an inverted T-girder system was employed. This numerical model has been derived and simplified from the case study and transformed into a linear elastic model using multiple assumptions. The case study was reduced to an orthogonal configuration with symmetrical characteristics to balance the dead loads on both sides. Additionally, the linear elastic model focuses solely on the behaviour of prefabricated and cast in-situ concrete elements, excluding reinforcement and prestressing steel. As a result, the model provides valuable insights into the differences in structural behaviour among the modified systems but does not capture the actual behaviour of the system. However, the model's simplicity makes it easy to apply to various systems with different dimensions and characteristics.

Given that this model only examines the effect of various design adjustments on structural behaviour, a linear analysis is appropriate. However, the linear analysis does not account for material and geometric nonlinearity, such as concrete cracking, plasticity, and large deformations. Since concrete exhibits nonlinear behaviour, significant information may be lost, such as the potential extra capacity due to compressive membrane action (CMA). Accounting for concrete cracking in a linear analysis can be challenging because the linear elastic behaviour does not capture the nonlinear cracking. Therefore, the most commonly used method is to reduce the modulus of elasticity to account for the reduced stiffness due to cracking. This method relies on simplified assumptions that may not capture the actual effects of concrete cracking.

Furthermore, the numerical model contains several simplifications that could be questioned. For instance, the supporting conditions of the numerical model in which the bearing pads are transformed to idealised support conditions as a one-node discrete connection to its surroundings. While the support conditions represent the actual constraints, defined as spring stiffnesses in all directions, they can introduce singularities and unrealistic stress concentrations. Additionally, the model was performed using shell elements to ensure time efficiency. While this simplifies the analysis and reduces computational effort, it may not capture all aspects of the structural behaviour, particularly those related to three-dimensional stress states and localised effects. The limitations of this analysis highlight the need for further studies to understand the true behaviour using nonlinear analysis. A more complex model that incorporates all elements with nonlinearity would provide a more realistic representation of the system's behaviour.

When evaluating the applied loads on the system, only the vertical loads from dead loads and traffic loads were considered, as these represent the most significant variable loads. Horizontal loads result-

ing from traffic actions, such as braking, acceleration and potential impact, as well as those from wind, seismic activity, and thermal gradients affecting the entire structure, were not included due to their relatively minor influence on critical load scenarios. However, it is important to recognise that these horizontal loads can significantly influence the transverse bending moments, particularly in the deck slab. Additionally, it is assumed that the system's capacity to resist these horizontal loads does not differ significantly among the various system configurations. To simplify the comparison between the modified systems and focus on their differences in structural response to critical live loads, self-weight was excluded from the analysis. Although the removal of the end transverse diaphragms significantly reduces the total self-weight of the structure, this reduction is considered to have a minimal effect on the differences between systems under critical load conditions, as the diaphragms are located above the supports. Therefore, while incorporating self-weight would increase the absolute values of all design parameters, the relative differences between the systems are expected to remain largely consistent.

The critical load configurations were selected to generate the maximum longitudinal bending moments, transverse bending moments, shear forces, and torsion moments. These load arrangements were derived from previous studies and refined through a process of trial and error. It is important to note that the maximum torsion moments in the composite girders are influenced by the transverse stiffness of the deck slab, which is reduced to account for concrete cracking. Changes in the transverse stiffness of the deck slab stiffness could therefore affect the critical load case for torsion moments. For the skewed systems, the same load configurations were considered critical, with adjustments made to account for the shift in critical locations due to the skew angle. Although various load arrangements were compared to verify the critical load cases for the 45-degree skewed system, other load configurations might produce even more critical internal stresses. Nevertheless, the load cases are consistent across all scenarios, and the values are expected to be near the maximum.

8.2. Discussion on results

This section reviews the results obtained from analysing several test cases with design adjustments and the effects of various skew angles on the modified systems. It involves a critical comparison of these results with the findings of other studies.

8.2.1. Effect of design adjustments

The results that the removal of end transverse diaphragms from the inverted T-girder system has minimal impact on longitudinal bending moments but a more substantial impact on the transverse bending moments in the deck slab align with the findings of Minalu (2010) [45]. However, differences are observed regarding the effect on torsion moments. While Minalu reported an increase in torsion moments when the end transverse diaphragms were removed, this research indicates a decrease. This discrepancy arises because Minalu considers the torsion moments in the first girder, whereas this study evaluates the largest torsion moments across all composite girders. When focusing solely on the first girder, this study also shows an increase in torsion moments. However, the maximum torsion moments at the fourth and fifth composite girders clearly show a reduction. Despite the differences in finite element models, the similarities in findings support the reliability of this research.

This study suggests that the removal of end transverse diaphragms can be effectively compensated by primarily strengthening the deck slab's bending and twisting moment capacity by approximately 16%. This increase in capacity is assumed to be achieved solely by increasing the amount of reinforcement. In some cases, this additional capacity could be achieved without any modifications, as the existing reinforcement may not always be fully utilised. Additionally, the substructure can remain largely unchanged, with the possibility of localised strengthening to accommodate increased maximum support forces. Furthermore, the findings indicate that the maximum stresses in the composite girders will not increase, enabling the use of the same girders in the redesigned system without end transverse diaphragms. This revised system, potentially featuring additional reinforcement and localised substructure strengthening, is expected to have a significantly lower environmental impact than the system incorporating the cast-in-situ concrete end transverse diaphragms with reinforcement.

Coupling these results with the suggestions by Vergoossen (2021) [72] that all functionalities of end transverse diaphragms can be substituted by other structural and non-structural elements enhances the potential for reusing the inverted T-girders in future projects. The primary additional complexity involves jacking the superstructure for maintenance of the supports, which would require each girder to have its own jacks. Furthermore, eliminating end transverse diaphragms significantly reduces the overall robustness of the structure, making it more susceptible to horizontal impacts. Although this reduction in robustness has not been extensively investigated, Vergoossen's work suggests that the compression layer provides sufficient shear action. If necessary, it could be possible to locally increase the deck slab above the supports to enhance the structure's robustness at the edges. This modification offers some practical benefits, such as facilitating the installation of joints, transitioning from abutment to deck, and compensating for the upward deflection of prestressed girders. However, it will not have a substantial impact on load distribution since the additional weight is primarily transferred directly to the supports. While this approach offers practical advantages, further exploration of the impact of eliminating end transverse diaphragms on horizontal forces in more detail could provide valuable insights.

To examine the impact of the end transverse diaphragms, the modified systems are subjected to the most critical load cases, which generate the largest bending moments, shear forces, and torsion moments in single-span systems. Although these critical load cases produce the maximum values, they do not capture the largest impact of the end transverse diaphragms. The maximum effect of the end transverse diaphragms in the inverted T-girder system is likely to occur under different scenarios. For instance, when applied loads are closer to the edges, the effect of incorporating the end transverse diaphragms becomes more pronounced. While these other load cases may not produce the most critical forces or moments overall, they could highlight the maximum impact of the end transverse diaphragms. Additionally, adjusting these load cases could provide valuable insights into the influence of the end transverse diaphragms on local elements rather than the global system.

8.2.2. Effect of skewness

Comparing the results obtained in this study with those of relevant studies addressing the effect of skew angles on design parameters, as described in Section 7.1, reveals several similarities. Despite some differences in study setups, all studies indicate that the maximum longitudinal bending moments in the girders decrease with decreasing skew angle. Moreover, studies addressing transverse bending moments in the deck slab consistently show an increase as the skew angle decreases. However, differences are observed in the impact of skew angles on shear forces and torsion moments in the composite girders. This study demonstrates that a reduction in the skew angle leads to decreased maximum shear forces and torsion moments in almost all situations. In contrast, reference studies by Nagashekhar et al. (2016) [51] and Harba (2011) [32] present varying results, where the impact of skew angles in shear forces and torsion moments differs depending on the location of the girders within the system and the applied load configurations.

Additionally, the impact of skew angles on torsion moments obtained in this study differs from the results by Minalu (2010) [45]. While Minalu reports an increase in torsion moments in the first girder as the skew angle decreases, this study shows a decrease in the system's maximum torsion moments. This discrepancy can be explained by the shift of the maximum value towards the second girder in the obtuse corner of the system as the skew angle decreases. This effect primarily arises when eliminating end transverse diaphragms, leading to a less pronounced decrease as the skew angle decreases. The maximum value in one of the girders may decrease while the overall maximum value of the system increases due to load concentrations or other factors. A more detailed analysis of the critical load cases for each girder could provide conclusive insights into the impact of the skew angle on individual girders.

Furthermore, another difference in the findings of various studies is that the variation in skew angle does not significantly affect the design parameters when it varies less than 20 degrees. Both Menassa et al. (2007) [44] and Nagashekhar et al. (2016) [51] conclude that skewed systems with angles up to 70 degrees can be considered as straight systems. However, Harba (2011) [32] challenges this assertion, noting that shear forces either decrease or increase as the skew angle decreases up to 70 degrees. According to the results of this study, clear discrepancies are observed in shear forces between skew angles of 90 and 75 degrees, while no significant differences are found for other de-

sign parameters. This indicates that, although there may be no distinction for other design parameters between skew angles of 90 and 75 degrees, the differences in shear forces must be considered. Consequently, this result underscores the uncertainty of the recommendation to treat 70-degree skewed systems as straight systems. Therefore, considering small skewed systems as straight systems should be accompanied by additional consideration of the shear forces.

As described in Section 7.3.5, the ratio between the width and length of the structure plays a significant role in the system's operation. Structures with a smaller span and greater width transfer loads differently due to altered support positions. Consequently, the critical load cases used in this study might differ for systems with varying width/length ratios. Therefore, the study's findings are only valid for systems with a similar or smaller width/length ratio, as these systems likely exhibit similar load transfer mechanisms. For systems with a greater width/length ratio, different load cases are expected to be governing, potentially leading to different results. A more detailed analysis of the impact of the width/length ratio on the findings could be valuable for applying these results to other types of systems.

9

Conclusions and Recommendations

The conclusions from this study are presented by answering the sub-questions, after which the main research question is addressed. Subsequently, recommendations for future work are provided.

9.1. Conclusions

Moving towards a more circular construction industry is essential for achieving the objective of operating climate-neutral and fully circular by 2030. Maximising the reuse potential of prefabricated inverted T-girders could significantly contribute to this goal. However, the conventional design of the inverted T-girder system does not accommodate reuse, potentially leading to additional costs associated with disassembly. Therefore, this study investigates various design modifications to enhance the reusability of these girders. The objective is to fully exploit the reuse potential of inverted T-girders by modifying the design of girder systems.

1. What are the main challenges in efficiently disassembling prefabricated inverted T-girders?

A literature review provided a comprehensive overview of the design details and arrangement of structural components within the inverted T-girder system. Additionally, a theoretical approach elucidates the system's operation and the contributions of various structural components, highlighting potential deficiencies and weaknesses, especially in the transverse direction. Examination of current disassembly methods for the girders indicates that the main challenges primarily arise from the end transverse diaphragms and deck slab, which ensure connection in the transverse direction. Given the commonly used deck slab thickness of 200 millimeters and the average dimensions of the end transverse diaphragms exceeding 800 millimeters in height and width, detaching the girders from the end transverse diaphragms is particularly challenging. Few studies have addressed the necessity of incorporating the end transverse diaphragms, raising questions about their effectiveness. This creates an opportunity to eliminate these robust, material- and labour-intensive structural elements, thereby simplifying the disassembly process and enhancing the reusability of the girders

2. How is the stress distributed within the current design of prefabricated inverted T-girder systems and what roles do different structural components play in maintaining overall stability and load-bearing capacity?

A comprehensive assessment of the prefabricated inverted T-girder system demonstrates that longitudinal bending moments are supported by the composite girders, whereas transverse bending moments are carried exclusively by the deck slab. The significant difference in stiffness between these components results in much larger longitudinal bending moments compared to transverse bending moments, causing the longitudinal direction to predominate over the transverse direction. Furthermore, shear forces are transferred to the supports by both the deck slab and girders, leading to uniformly distributed stresses over the girder's web. Torsion moments arise due to the restraint of the imposed rotation of

the girders and are symmetrical when centrally applied loads are present. The shear stresses caused by torsion moments flow through the cross-section of the composite girder, reaching their maximum in the web of the girders.

3. How do different structural design adjustments aimed at improving the disassembly and reassembly efficiency of inverted T-girders affect the overall structural performance of the system?

After identifying the main challenges associated with disassembling the prefabricated girders from the system, the study focuses on the possibility of eliminating the end transverse diaphragms. The findings indicate that excluding the end transverse diaphragms has minimal impact on the distribution of longitudinal bending moments and shear forces. However, the deck slab, as the only transverse connection, bears a greater load. To accommodate this increase, an additional 16% capacity of the deck slab is required, which can be achieved by increasing the amount of reinforcement. Although the support forces show a local 17% increase, the substructure is considered capable of withstanding this because its capacity is generally not fully utilised. Based on this study's findings and suggestions from other studies, the consequences of eliminating end transverse diaphragms can be compensated for by other existing structural elements, with only an increase in deck slab reinforcement. This demonstrates the feasibility of removing the end transverse diaphragms to enhance the disassembly of the girders without significantly affecting overall structural performance. Additionally, attempts to compensate for the reduced transverse stiffness by increasing the deck slab thickness were found to be effective only in reducing the torsion moments in the girders. Given the potential weight increase, it was concluded that a thicker deck slab is neither feasible nor beneficial for improving the overall structural performance of the system without end transverse diaphragms. Additionally, the greater material consumption required for a thicker deck slab would have a negative environmental impact.

4. To what extent is the assessment of an orthogonal system representative of other systems with a certain skew angle?

In skewed systems, a greater proportion of forces and moments are absorbed by the deck slab compared to the composite girders, highlighting a more crucial role for the deck slab. The mutual differences across various skew angles between the systems with and without end transverse diaphragms vary up to 2.6%, except for the 5.6% difference in torsion moments at a 60-degree skewed system and the 5.3% difference in twisting moments at a 45-degree skewed system. Additionally, the location of the maximum torsion moments in the composite girders shifts only in systems without end transverse diaphragms. Decreasing the skew angle in these systems causes the maximum torsion moments to shift towards the obtuse corner. With only two significant differences across various skew angles, the impact of eliminating end transverse diaphragms from the inverted T-girder system remains relatively consistent. Therefore, the assessment for the orthogonal system can be applied with a similar order of magnitude to skewed systems. However, for the system with increased deck slab thickness, the results do not apply to other skewed systems, as this system shows magnifying influences as the skew angle decreases. Moreover, this system has already been deemed unsuitable for improving the structural performance of the inverted T-girder system due to its substantial moment increases in the deck slab.

By obtaining answers to these sub-questions, the main research question can be answered. This allows the study to achieve its objective of making optimal use of the reuse potential of prefabricated inverted T-girders.

> "How can the inverted T-girder system be adapted to improve the circularity during the disassembly and reassembly process in the future?"

To enhance the circularity of the prefabricated inverted T-girders during the disassembly and reassembly, a comprehensive analysis is conducted on these systems. The primary challenges associated with these processes were identified, focusing on the removal of the end transverse diaphragms. To assess their feasibility, two modified systems, both excluding the end transverse diaphragms, were evaluated and compared to the base system.

The study revealed that eliminating the end transverse diaphragms from the inverted T-girder system primarily results in higher stresses in the deck slab. This increase in stress can be effectively managed by adding more reinforcement to the deck slab. Therefore, the findings suggest that implementing a girder system without end transverse diaphragms is a feasible design option, as it does not significantly affect the system's overall structural performance. Moreover, these findings are relevant for skewed systems with skew angles of up to 45 degrees. By eliminating the end transverse diaphragms, the design approach optimises the use of structural elements and facilitates the reuse of the girders, contributing to sustainable construction practices.

Conversely, the study demonstrates that increasing the transverse stiffness of the deck slab by increasing its height does not yield overall positive effects. While this modified system shows similar maximum values in the girders, the maximum values in the deck slab increase substantially. Despite the increased capacity of the deck slab due to its greater thickness, these high values are disadvantageous. Therefore, increasing the deck slab thickness does not contribute to the overall structural performance and is not deemed feasible. Moreover, the impact of skew angles becomes more pronounced as the skew angle decreases, highlighting varying structural responses for different skew angles.

9.2. Recommendations for future research

Based on the findings presented in this study, several recommendations are proposed to improve future studies.

The objective of this study was to examine the impact of various design adjustments, facilitating the disassembly of girders, on the structural performance of the inverted T-girder system. After identifying the main challenges associated with the disassembly and reassembly of the girders, two specific design modifications were evaluated. However, there are probably several other adjustments possible that somehow enhance the disassembly of the girders. It is recommended to initially test these modifications using the linear model developed in this study to obtain a preliminary assessment of their feasibility.

Considering the findings from this linear static analysis, initial insight into the feasibility of eliminating end transverse diaphragms has been provided. However, since the numerical model does not incorporate all aspects, it does not fully capture the actual behaviour of the system. To accurately simulate the system's behaviour, it is crucial to include self-weight, reinforcement and prestressing steel, as well as nonlinear effects such as material and geometric nonlinearity, which includes concrete cracking, plasticity and large deformations. An improved numerical model that includes these factors could offer a more realistic representation of the system. It could account for the potential loss of compressive membrane action due to the elimination of the end transverse diaphragms, which is of significant interest. Additionally, increasing the degree of accuracy by utilising solid elements is possible, though this approach would involve increased modelling and computational time.

Although the findings of this study suggest that eliminating end transverse diaphragms from the system is feasible when considering only vertical forces, and Vergoossen's work indicates that the deck slab should provide sufficient shear action to bear horizontal forces based on experiences from valued constructors, the lack of robustness within the system when eliminating the end transverse diaphragms could be a significant disadvantage in implementing this adjustment in real structures. Therefore, it is recommended to further investigate the impact of not having end transverse diaphragms in girder systems under horizontal loads in particular.

Furthermore, the effect of end transverse diaphragms was investigated in this study by analysing the system's maximum values under four critical load cases. However, these critical load cases do not necessarily represent the scenarios where the importance of end transverse diaphragms is greatest. The impact of the end transverse diaphragms is likely most significant when live loads are applied closer to their location. Additionally, the transverse diaphragms may play a crucial role in local effects. Therefore, it is interesting to explore the most critical scenarios where the end transverse diaphragms have the greatest impact to fully understand their significance.

The current study on the impact of the skew angle on the system considers only the maximum values of the complete system. However, the influence of the skew angle may vary for different girders due to changes in the system's load transfer mechanisms. To investigate the impact of the skew angle at a more localised level, it is recommended to analyse the load distribution of individual girders within the system under various skew angles.

Considering a broader perspective, it would be valuable to assess the environmental impact and feasibility of reusing these inverted T-girders, taking into account factors such as construction, transport, storage, and their suitability for other projects. This assessment should include a life cycle analysis to determine the overall sustainability benefits of reusing prefabricated girders compared to manufacturing new ones. Furthermore, it could be of interest to investigate the environmental impact of reinforcing the deck slab by increasing the amount of reinforcement compared to eliminating end transverse diaphragms. This investigation should consider the potential benefits of excluding end transverse diaphragms, as well as any trade-offs in terms of construction complexity and long-term maintenance. By comparing these factors, a better understanding of the most effective strategies for improving the sustainability of girder bridges can be achieved.

Bibliography

[1] S. Amir, C. Veen, J. Walraven, and A. Boer. “Punching shear capacity of bridge decks regarding compressive membrane action”. In: 60 (Jan. 2015), pp. 235–256.

[2] M. Aria and R. Akbari. “Inspection, condition evaluation and replacement of elastomeric bearings in road bridges”. In: *Structure and Infrastructure Engineering* 9.9 (2013), pp. 918–934. DOI: 10.1080/15732479.2011.638171.

[3] M. Barsottelli and O. Avci. “Fundamentals of Highway Bridge Demolition”. In: May 2013, pp. 680–688. DOI: 10.1061/9780784412848.060.

[4] B. Bezabih. *Bridge and Culvert Hydraulics Lecture Notes UG*. Nov. 2020. DOI: 10.13140/RG.2.2.28101.68325.

[5] J. de Boon. *Quick Scan methode voor T-liggers*. 2018.

[6] G. H. Brundtland. “Our Common Future World Commission On Environment And Developement”. In: (1987).

[7] M. P. Burke Jr. *Integral and semi-integral bridges*. John Wiley & Sons, 2009.

[8] T. Busscher, F. Niekerk, and J. Arts. “Van niets doen naar iets doen: een toekomst voor een programmatische benadering van infrastructuurplanning?” In: Bijdrage aan het Colloquium Verkeersplanologisch Speurwerk. 2009.

[9] Consolis Spanbeton. *Box girder solution SKK*.

[10] Consolis Spanbeton. *Inverted T-beam solution ZIPXL*.

[11] Consolis Spanbeton. *Solid composite constructions SJP Flex*.

[12] H. Cross. “Analysis of Continuous Frames By Distributing Fixed-End Moments”. In: *Transactions of the American Society of Civil Engineers* 96.1 (1932), pp. 1–10. DOI: 10.1061/TACEAT.0004333. URL: https://ascelibrary.org/doi/abs/10.1061/TACEAT.0004333.

[13] P. Crowther. “Design for Disassembly to Extend Service Life and Increase Sustainability”. In: *Durability of Building Materials and Components 8: Service Life and Asset Management*. 1999, pp. 1983–1992. URL: https://eprints.qut.edu.au/2471/.

[14] S. De Boer. “Brugsystemen en viaducten”. In: *BFBN - Bouwen in Prefab Beton* 13 (2002).

[15] R. De Meijer and R. Vergoossen. “Beoordeling voorgespannen constructies. De praktijk van verfijnd herberekenen van voorgespannen constructies”. In: *Cement* 4 (2012), pp. 52–55. URL: https://www.cementonline.nl/artikel/beoordeling-voorgespannen-constructies.

[16] A. Dhar, M. Chowdhury, M. Mazumder, and S. Karmakar. “Effect of skew angle on longitudinal girder (support shear, moment, torsion) and deck slab of an IRC skew bridge”. In: *The Indian Concrete Journal* Vol.87 (Dec. 2013), pp. 46–52.

[17] DIANA FEA BV. *Theory Manual*. 2023. URL: https://manuals.dianafea.com/d107/en/1181807-1181807-theory-107.html.

[18] R. Dornslife. *”Expansion Joints”*. Boca Raton: CRC Press, 2000.

[19] S. El-Gamal, E. El-Salakawy, and B. Benmokrane. “Influence of Reinforcement on the Behavior of Concrete Bridge Deck Slabs Reinforced with FRP Bars”. In: *Journal of Composites for Construction - J COMPOS CONSTR* 11 (Oct. 2007). DOI: 10.1061/(ASCE)1090-0268(2007)11:5(449).

[20] S. Ensink, C. Van der Veen, D. Hordijk, E. Lantsoght, H. Van der Ham, and A. De Boer. “Full-size field test of prestressed concrete T-beam bridge”. In: *Structural Faults & Repair 2018 and European Bridge Conference 2018* (May 2018).

[21] S. Ensink. “System behaviour in prestressed concrete T-beam bridges”. In: (2024). URL: https://doi.org/10.4233/uuid:15f5628b-9175-4ef3-8f39-41a97cb7749a.

[22] *EN 1992-1-1 Eurocode 2: Design of concrete structures - Part 1-1: General rules and rules for buildings*. EN. Brussels: CEN, 2005.

[23] *NEN-EN 1991-2 Eurocode 1: Actions on structures - Part 2: Traffic loads on bridges*. EN. Brussels: CEN, 2021.

[24] E. Ezi, P. Onuamah, D. Ugwuanyi, and I. Agbo. “Advances in the Analysis of Simply Supported Concrete Bridge Deck”. In: *Global Scientific Journal* 6.8 (Aug. 2018), pp. 352–367.

[25] Finecut. *Concrete slab sawing cuts concrete to an even, flat plane*. July 2019. URL: https://www.finecutusa.com/concrete-slab-sawing-blog/.

[26] B. C. Gerwick Jr. *Construction of prestressed concrete structures*. John Wiley & Sons, 1997.

[27] R. I. Gilbert. “Time-dependent Stiffness of Cracked Reinforced and Composite Concrete Slabs”. In: *Procedia Engineering* 57 (2013). Modern Building Materials, Structures and Techniques, pp. 19–34. ISSN: 1877-7058. DOI: https://doi.org/10.1016/j.proeng.2013.04.006. URL: https://www.sciencedirect.com/science/article/pii/S1877705813007364.

[28] M. B. Gutti. “A PRESENTATION ON STATICALLY INDETERMINATE STRUCTURES”. In: (2019).

[29] Haggar. *Installing the correct groundworks foundations - Haggar construction*. Dec. 2021. URL: https://haggarconstruction.co.uk/blog/installing-the-correct-groundworks-foundations/.

[30] Haitsma Beton. *Documentatie HKO*.

[31] Haitsma Beton. *Documentatie HRP & HIP*.

[32] I. Harba. “Effect of skew angle on behavior of simply supported R. C. T-beam bridge decks”. In: *Journal of Engineering and Applied Sciences* 6 (Aug. 2011), pp. 1–14.

[33] C. Hendy and D. Iles. “Guidance Notes on Best Practice in Steel Bridg Construction”. In: *Steel Bridge Group* 6 (2015).

[34] Z. Hosseini, B. Laratte, and P. Blanchet. *Implementing circular economy in the construction sector: Evaluating CE strategies by developing a framework*. hal-04124246. HAL, 2023. DOI: 10.15376/biores.18.3.4699. URL: https://ideas.repec.org/p/hal/journl/hal-04124246.html.

[35] H. A. Hussein and Z. Razzaq. “Strengthening Prestressed Concrete Bridge Girders and Building Beams with Carbon Fiber Reinforced Polymer Sheets”. In: *European Journal of Engineering and Technology Research* 6.1 (2021), pp. 55–57. DOI: 10.24018/ejeng.2021.6.1.2323. URL: https://ej-eng.org/index.php/ejeng/article/view/2323.

[36] Inc. NAHB Research Center. “A Guide To Deconstruction”. In: (2000).

[37] J. kan Kent Hsiao and Y. Jiang. *FOOTING FIXITY EFFECT ON PIER DEFLECTION*. 2014. URL: https://api.semanticscholar.org/CorpusID:55546339.

[38] J. Kirchherr, D. Reike, and M. Hekkert. “Conceptualizing the circular economy: An analysis of 114 definitions”. In: *Resources, Conservation and Recycling* 127 (2017), pp. 221–232. ISSN: 0921-3449. DOI: https://doi.org/10.1016/j.resconrec.2017.09.005. URL: https://www.sciencedirect.com/science/article/pii/S0921344917302835.

[39] J. Korhonen, A. Honkasalo, and J. Seppälä. “Circular Economy: The Concept and its Limitations”. In: *Ecological Economics* 143 (2018), pp. 37–46. ISSN: 0921-8009. DOI: https://doi.org/10.1016/j.ecolecon.2017.06.041. URL: https://www.sciencedirect.com/science/article/pii/S0921800916300325.

[40] E. Lantsoght, C. Veen, and J. Walraven. “Shear capacity of slabs and slab strips loaded close to the support”. In: *ACI SP-287, Recent Development in Reinforced Concrete Slab Analysis, Design and Serviceability* (Jan. 2012), pp. 5.1–5.18.

[41] D. Lee. *Bearings and expansion joints for bridges*. 1982.

[42] W. Macek and N. Mucha. “Evaluation of Fatigue Life Calculation Algorithm of the Multiaxial Stress-Based Concept Applied to S355 Steel under Bending and Torsion”. In: *Mechanics and Mechanical Engineering* (Jan. 2017), pp. 935–951.

[43] R. E. Melchers and I. A. Chaves. “2 - Service life estimation of concrete infrastructures”. In: *Eco-Efficient Repair and Rehabilitation of Concrete Infrastructures*. Ed. by F. Pacheco-Torgal, R. E. Melchers, X. Shi, N. D. Belie, K. V. Tittelboom, and A. Sáez. Woodhead Publishing Series in Civil and Structural Engineering. Woodhead Publishing, 2018, pp. 15–41. ISBN: 978-0-08-102181-1. DOI: https://doi.org/10.1016/B978-0-08-102181-1.00002-2. URL: https://www.sciencedirect.com/science/article/pii/B9780081021811000022.

[44] C. Menassa, M. Mabsout, K. Tarhini, and G. Frederick. “Influence of Skew Angle on Reinforced Concrete Slab Bridges”. In: *Journal of Bridge Engineering - J BRIDGE ENG* 12 (Mar. 2007). DOI: 10.1061/(ASCE)1084-0702(2007)12:2(205).

[45] K. Minalu. *Finite element modelling of skew slab-girder bridges*. 2010.

[46] Ministerie van Infrastructuur en Waterstaat. “Duurzaamheidsverslag 2017 in transitie”. In: *Duurzaamheidsverslag 2017* (2018).

[47] P. Morseletto. “Targets for a circular economy”. In: *Resources, Conservation and Recycling* 153 (2020), p. 104553. ISSN: 0921-3449. DOI: https://doi.org/10.1016/j.resconrec.2019.104553. URL: https://www.sciencedirect.com/science/article/pii/S0921344919304598.

[48] R. N. Mothe. “Partial continuity in prestressed concrete girder bridges with jointless decks”. In: 2006. URL: https://api.semanticscholar.org/CorpusID:115276045.

[49] C. D. Murray, M. Diaz Arancibia, P. Okumus, and R. W. Floyd. “Destructive testing and computer modeling of a scale prestressed concrete I-girder bridge”. In: *Engineering Structures* 183 (2019), pp. 195–205. ISSN: 0141-0296. DOI: https://doi.org/10.1016/j.engstruct.2019.01.018. URL: https://www.sciencedirect.com/science/article/pii/S0141029618321795.

[50] C. Murray and R. Floyd. “Shear and anchorage failure of scale prestressed concrete I-girders and scale bridge section”. In: *Euro-bridge* (2018).

[51] J. P. Nagashekhar, R. Manoli, M. M. Achar, and K. Shiva Kumar. “Effect of skew on the behaviour of RC girder bridges”. In: *International Research Journal of Engineering and Technology (IRJET)* 3.7 (July 2016).

[52] *Nederland circulair in 2050*. Het ministerie van Infrastructuur en Milieu en het ministerie van Economische Zaken, 2016.

[53] A. Niemierko. “Modern Bridge Bearings and Expansion Joints for Road Bridges”. In: *Transportation Research Procedia* 14 (Dec. 2016), pp. 4040–4049. DOI: 10.1016/j.trpro.2016.05.501.

[54] A. Noukari. *Optimizing the assessment of fatigue in inverted T-girder brdiges. A parametric study to the factors influencing the fatigue analysis of concrete under compression*. 2023.

[55] D. Nuijens and K. Quartel. “Hergebruik liggers A9”. In: *Cement* 8 (2022), pp. 24–30.

[56] B. Pritchard. “6 ADVANTAGES OF BRIDGE DECK CONTINUITY”. In: *Continuous and Integral Bridges* (1994), p. 55.

[57] C. Quartel. “Spanbeton historisch overzicht”. In: *Bruggen* 19.1 (2011), pp. 5–9. URL: https://bruggenstichting.nl/104-bruggen/bruggen-2011/bruggen-maart-2011/127-spanbeton-historisch-overzicht.

[58] G. Ramos. *Behavior of Prestressed Concrete Bridges with Closure Pour Connections and Diaphragms*. 2019. URL: https://api.semanticscholar.org/CorpusID:208838942.

[59] K. Rashid, M. Ahmad, T. Ueda, J. Deng, K. Aslam, I. Nazir, and M. Azam Sarwar. “Experimental investigation of the bond strength between new to old concrete using different adhesive layers”. In: *Construction and Building Materials* 249 (2020), p. 118798. ISSN: 0950-0618. DOI: https://doi.org/10.1016/j.conbuildmat.2020.118798. URL: https://www.sciencedirect.com/science/article/pii/S0950061820308035.

[60] I. L. K. Reid, P. A. Thayre, D. E. Jenkins, R. A. Broom, and D. J. Grout. “Bridge accessories”. In: *ICE Manual of Bridge Engineering*, pp. 553–565. DOI: 10.1680/mobe.34525.0553. URL: https://www.icevirtuallibrary.com/doi/abs/10.1680/mobe.34525.0553.

[61] A. Saber and W. Alaywan. “Full Scale Test of Continuity Diaphragms in Skewed Concrete Bridge Girders”. In: *Journal of Bridge Engineering - J BRIDGE ENG* 16 (Jan. 2010). DOI: 10.1061/(ASCE)BE.1943-5592.0000126.

[62] A. Saber, F. Roberts, W. Alaywan, and J. Toups. “Effectiveness of Continuity Diaphragm for Skewed Continuous Prestressed Concrete Girder Bridges”. In: *PCI Journal* 52 (Mar. 2007). DOI: 10.15554/pcij.03012007.109.114.

[63] SBIR Circulaire Viaducten. *Eindrapport fase 1-Haalbaarheidsonderzoek Hergebruik Prefabliggers (HPL)*. Tech. rep. AT/2020/03/V2. Mar. 2021.

[64] I. Stimac-Grandic, D. Grandić, and A. Bjelanović. “Evaluation of torsional stiffness in beam and slab bridge decks based on load testing”. In: *International Journal of Civil Engineering* 13 (Sept. 2014), pp. 255–266.

[65] R. Tomek. “Advantages of Precast Concrete in Highway Infrastructure Construction”. In: *Procedia Engineering* 196 (2017). Creative Construction Conference 2017, CCC 2017, 19-22 June 2017, Primosten, Croatia, pp. 176–180. ISSN: 1877-7058. DOI: https://doi.org/10.1016/j.proeng.2017.07.188. URL: https://www.sciencedirect.com/science/article/pii/S1877705817330473.

[66] E. Ulku, U. Attanayake, and H. Aktan. “Jointless Bridge Deck with Link Slabs: Design for Durability”. In: *Transportation Research Record* 2131.1 (2009), pp. 68–78. DOI: 10.3141/2131-07. URL: https://doi.org/10.3141/2131-07.

[67] N. Van Buren, M. Demmers, R. Van der Heijden, and F. Witlox. “Towards a Circular Economy: The Role of Dutch Logistics Industries and Governments”. In: *Sustainability* 8.7 (2016). ISSN: 2071-1050. DOI: 10.3390/su8070647. URL: https://www.mdpi.com/2071-1050/8/7/647.

[68] E. Van Vliet. *Torsion in ZIP bridge system*. 2012.

[69] H. M. in ’t Veld. *De groei van het Nederlandse personenautopark*. Dec. 2019. URL: https://www.cbs.nl/nl-nl/longread/statistische-trends/2019/de-groei-van-het-nederlandse-personenautopark?onepage=true#c-Referenties.

[70] R. Vergoossen, G.-J. Van Eck, and D. Jilissen. “Hergebruik prefab T-liggers (1)”. In: *Cement* 6 (2022), pp. 18–26.

[71] R. Vergoossen, G.-J. Van Eck, and D. Jilissen. “Hergebruik prefab T-liggers (2)”. In: *Cement* 8 (2022), pp. 40–49.

[72] R. Vergoossen. “SBIR HPL Einddwarsdragers”. In: (Jan. 2021).

[73] A. B. Vesic. “Bearing capacity of deep foundations in sand”. In: *Highway research record* 39 (1963).

[74] C. Wang, Y. Shen, Y. Zou, Y. Zhuang, and T. Li. “Analysis of mechanical characteristics of steel-concrete composite flat link slab on simply-supported beam bridge”. In: *KSCE Journal of Civil Engineering* 23 (2019), pp. 3571–3580.

[75] K. Westenberg and H. Bloksma. “Civiele kunstwerken in Nederland”. In: *Bouwagenda* (May 2021).

[76] Wisconsin Department of Transportation. “Chapter 12 - Abutments”. In: *WisDOT Bridge Manual* (2022).

[77] M. Xu and A. Bloodworth. “The earth pressure behind full-height integral abutments”. In: *IABSE Symposium Report* 90 (Jan. 2005). DOI: 10.2749/222137805796271008.

[78] Y. Yang. *Lecture 3: Introductions of precast bridges*. 2023.

[79] Y. Yang. *Lecture 6: Detailing of precast girder bridges*. 2023.

[80] Y. Yang. *Lecture 6: Guyon Massonnet*. 2019.

[81] Z. Yousif and R. Hindi. “AASHTO-LRFD live load distribution for beam-and-slab bridges: Limitations and applicability”. In: *Journal of Bridge Engineering* 12 (Nov. 2007), pp. 765–773. DOI: 10.1061/(ASCE)1084-0702(2007)12:6(765).

[82] M. Zaumanis, D. Loetscher, S. Mazor, F. Stöckli, and L. Poulikakos. “Impact of milling machine parameters on the properties of reclaimed asphalt pavement”. In: *Construction and Building Materials* 307 (2021), p. 125114. ISSN: 0950-0618. DOI: https://doi.org/10.1016/j.conbuildmat.2021.125114. URL: https://www.sciencedirect.com/science/article/pii/S0950061821028592.

[83] H. Zhu, Y. Yang, and W. Fan. “External Prestressing Bridge Reinforcement Technology Review”. In: *MATEC Web of Conferences* 22 (Jan. 2015), p. 04028. DOI: 10.1051/matecconf/20152204028.

A

Prefabricated girder systems in the Netherlands

This appendix provides an overview of the various types of prefabricated girder systems currently used in the Netherlands.

A.1. Prefabricated girder systems in the Netherlands

An analysis of different prefabricated girder systems in the Netherlands is conducted to make the design of prefabricated girder systems more future-proof. This section presents an overview of different bridge and viaduct designs used in the Netherlands. At first, the beginning of concrete structures with prefab girders is described. Following this, the characteristics of different girder types are explained.

A.1.1. Origin of prefabricated girder systems in the Netherlands

Since the 1960s, the use of cars has become a common phenomenon, experiencing exponential growth [69]. A corresponding expansion of the road network was necessary, leading to the introduction of the 'Rijkswegenplan' in 1968 [8]. This initiative facilitated the construction of numerous bridges and viaducts while focusing on cost-effective and fast construction. This shift in the construction industry paved the way for prefabricated concrete structures. According to Tomek (2017) [65] and Yang (2023) [78], the advantages of using precast concrete in infrastructure construction compared to cast-in-situ concrete are:

- Shorter construction time resulting in less traffic hindrance
- Higher quality due to ideal working environment
- Benefits of pre- and post-tensioning
- Long-term durability due to higher quality
- Higher economic effectiveness due to mass production and optimised cross-section

The use of prefabricated concrete elements started with solid girders, but the evolution soon led to the creation of T-shaped girders for efficient material usage. Subsequent developments resulted in various types of prefabricated concrete structures, leading to the majority of infrastructural concrete structures being constructed using prefabricated girders [75].

In the Netherlands, the predominant types of prefabricated girders can be divided into four main types: T-girder, inverted T-girder, infilled girder, and box girder. While the design of these girders may vary over the years and among different producers, the structural principle is the same. The characteristics and applicability of these main girder types are provided in the next section. The information is based on the girder designs of the two leading producers in recent years in the Netherlands: Spanbeton BV and Haitsma.

A.1.2. T-girder

A prefabricated girder system with T-shaped girders is mainly used for spans ranging from 20 to 40 meters. After placement side by side, a compression layer is poured on-site to create a deck construction [14]. These girders are often prestressed and find application in bridges with a low traffic class and a requisite construction height [14]. The T-girder features a distinctive T-shape with a notably larger upper flange, varying in width from 900 to 1500 millimeters, while the web is around 200 millimeters. Often, a thickening is present at the bottom of the web and the profile height of the girders varies between 1100 and 3600 millimeters. A cast-in-situ deck with a thickness of 150 to 250 millimeters is poured to connect the girders.

During the construction phase, it is crucial to consider the stability of the girders. The relatively small web at the bottom side of the girder makes the structure susceptible to tilting. To enhance transverse stability, girders are commonly connected by cast-in-situ transverse diaphragms at the supports, increasing the stiffness of the entire system.

It is important to note that the T-shaped girder system is not suitable for absorbing collision loads. The absence of a connection between the bottom flanges ensures that the load is transferred to the upper part of the structure through a single girder. The collision load can be substantial and is therefore almost impossible to incorporate into the design requirements. However, the standards and guidelines require compliance with this type of load for structures that cross other roads. This girder type could therefore only be used in structures without any risk of collision. The T-girder became deprecated after 1984 due to its incompatibility with newer and more stringent standards [5].

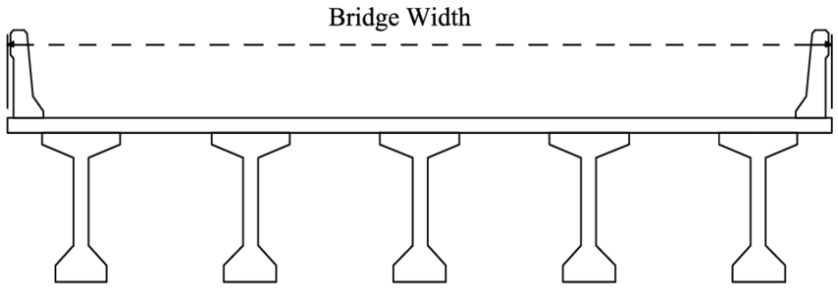

Figure A.1: Cross-section of a T-girder system

A.1.3. Inverted T-girder

The inverted T-shaped girders are used similarly to the T-shaped girder, featuring a cast-in-situ concrete compression layer. This system, distinguished by its inverted girders, offers more stability and is employed to span 15 to 35 meters. It requires a sufficient construction height which ranges significantly from 500 to 2400 millimeters for various girder types [10]. The bottom is nearly universal and varies between 1000 and 1200 millimeters. Some girders incorporate a top flange and are so-called I-girders. These girders are also covered by the inverted T-shaped girders, referred to as rail girders because their shape looks like a rail track.

The inverted T-girder system shares similarities to the T-shaped girder system but is designed to handle larger loads. The inverted T-girders are connected at the bottom flange using mortar, and a lost formwork is applied between the girder's web to facilitate the construction of the in-situ concrete compression layer. The thickness of this deck varies between 200 and 260 millimeters [10]. Extended stirrups connect the compression layer to the girder's web, ensuring the capacity to withstand shear forces. With the compression layer, transverse diaphragms at the supports enhance the transverse stiffness. The reinforcement of the end transverse diaphragm is constructed through holes in the inverted T-girders, followed by in-situ casting to secure connection. For larger spans, additional intermediate transverse diaphragms can be applied if necessary.

In comparison to the T-shaped girder system, the inverted T-girder system can effectively absorb collision loads. The mortar connection between the bottom flanges creates a plate covering the entire

structure, allowing the transfer of collision loads through all supports [14]. It is crucial to consider the difference in concrete between the girders and deck, as it may lead to internal stresses due to shrinkage and relaxation.

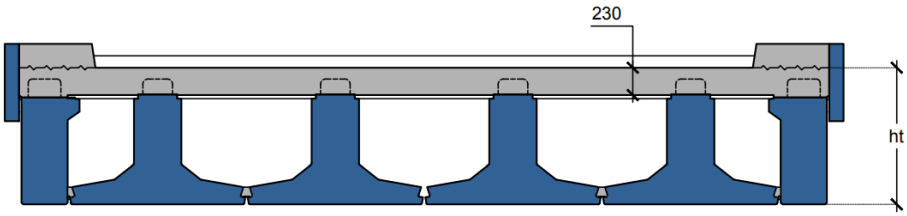

Figure A.2: Cross-section of an inverted T-girder system [30]

A.1.4. Infilled girder

The infilled girder, which is called 'Volstortligger' in the Netherlands, is a variation on the inverted T-girder. Due to fast construction time, this system is the most economical solution to span 7 to 20 meters [30]. The bottom flange's width varies between 1000 and 1200 millimeters [30]. Together with great applicability, this system is most used in Dutch road and water constructions [30]. Because of the minimum amount of prefabricated concrete and the maximum amount of in-situ concrete fast construction can be achieved. However, the great amount of cast-in-situ concrete means that this system is unsuitable for reuse.

The infilled girder system consists of multiple inverted T-girders next to each other with holes at the bottom of the web to enable transverse reinforcement. After this, the total spaces between the girders are filled with in-situ concrete to create a monolith construction [14]. However, the characteristics differ in the longitudinal and transverse directions. This system combines the benefits of prefabricated concrete with the construction speed of in-situ concrete.

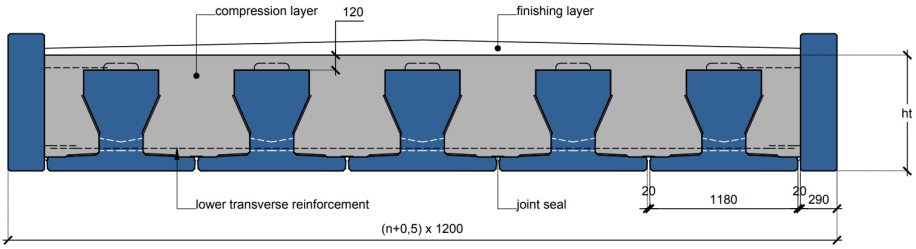

Figure A.3: Cross-section of an infilled girder system [11]

A.1.5. Box girder

The box girder system is preferred for large spans up to 68 meters. Its development has progressed significantly since the 1980s, because of high expectations for its future dominance. As a result, the box girder has a great variety of shapes and cross-sections. The prefabricated girders collectively form a complete deck of prefabricated concrete, eliminating the need for a compression layer [14]. In this way, the full capacity of the girders can be used to bear only variable loads, contributing to a relatively small construction height, ranging from 700 to 1900 millimeters [9].

The box girder system comprises multiple prefabricated girders with a rectangular profile side by side. To minimise weight, the inside of the box girder is left empty. The rectangular shape imparts high torsional stiffness and eliminates the need for special edge girders. Two methods are available for connecting the girders into a unified system. The first method involves a reinforced joint, where each girder is provided with transverse reinforcement extending from the upper flange. When the girders are

placed next to each other, the joint with reinforcement is filled. The second option involves a transverse connection using prestressed steel through holes in the deck of the girders. Subsequently, the joint is filled with low-shrinkage mortar [14]. Figure A.4 shows the cross-section with transverse prestressing at the upper flange between the girders. The box girder system facilitates faster building without the need for reinforcement and a cast-in-situ concrete compression layer. However, transverse post-tensioning will increase costs.

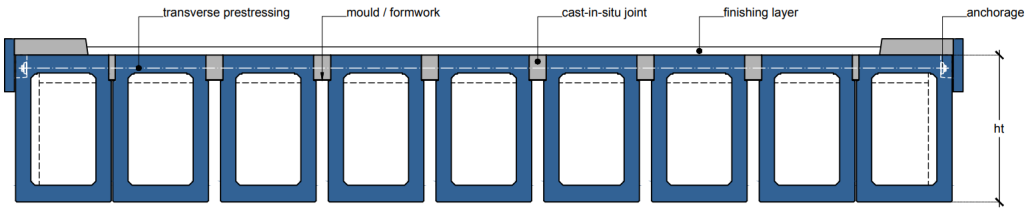

Figure A.4: Cross-section of a box girder system [9]

B

Derivation of the Guyon-Massonnet method

This appendix details the derivation of the Guyon-Massonnet method.

B.1. Derivation of the Guyon-Massonnet method

The distribution of forces and moments in concrete girder bridges can be analysed using the Guyon-Massonnet method. This analytical method describes the deflection of slabs in longitudinal and transverse directions using a fourth-order differential equation in combination with empirical factors based on experimental data. Due to a linear elastic system, the deformation of the slab is proportional to the force. This derivation of the Guyon-Massonnet method is based on Ezi et al (2018) [24] and Yang (2019) [80] and uses the orientation presented in Figure B.1.

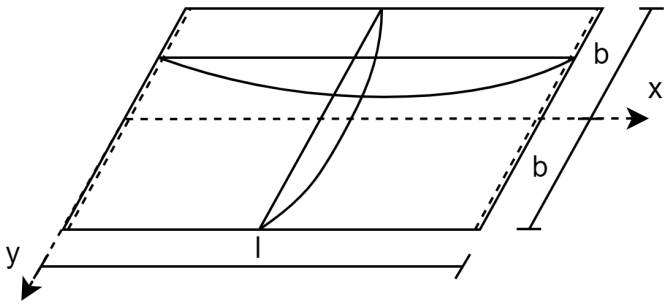

Figure B.1: Orientation of a simply supported slab used in the Guyon-Massonnet method

The Guyon-Massonnet method describes the orthotropic slab behaviour with the following fourth-order differential equation:

$$\rho_x \frac{d^4w}{dx^4} + 2H \frac{d^4w}{dx^2 dy^2} + \rho_y \frac{d^4w}{dy^4} = p(x,y) \tag{B.1}$$

In this equation, the terms ρ_x and ρ_y represent the flexural rigidity per unit width of the slab in both directions. The twisting effect is incorporated in both directions by the term H including the torsional rigidity per unit width, denoted by γ, and the flexural rigidity with the Poisson ratio. The outcome ($p(x,y)$) is the deflection of the slab, which can also be used for the load distribution.

$$\begin{aligned} \rho_x &= \frac{E_x I_x}{l_x} \\ \rho_y &= \frac{E_y I_y}{l_y} \\ H &= \gamma_x + \gamma_y + v\rho_x + v\rho_y \end{aligned} \tag{B.2}$$

Introducing a ratio between the torsional stiffnesses, given by α, the differential equation (B.1) can be written as:

$$\rho_x \frac{d^4w}{dx^4} + 2\alpha\sqrt{\rho_x \rho_y}\frac{d^4w}{dx^2 dy^2} + \rho_y \frac{d^4w}{dy^4} = p(x,y) \tag{B.3}$$

Where

$$\alpha = \frac{\gamma_x + \gamma_y + v\rho_x + v\rho_y}{2\sqrt{\rho_x \rho_y}} \tag{B.4}$$

To solve this fourth-order differential equation, Guyon introduced a summation of sines and cosines to construct the displacement field in the following form:

$$\begin{aligned} p(x,y) &= \sum \frac{p_m}{2b} sin\left(\frac{m\pi x}{l}\right)\left(1 + \sum cos\left(\frac{n\pi}{2b}\right)(y-e)\right) \\ p(x,y) &= f(x) + f(x)f(y) \end{aligned} \tag{B.5}$$

Subsequently, Guyon considered a slab with zero torsional stiffness ($\alpha = 0$), resulting in a displacement field of the form:

$$p(x,y) = \sum \frac{p_m}{2b} sin\left(\frac{m\pi x}{l}\right) \tag{B.6}$$

In this case, equation B.1 can be written in a more simplified equation:

$$\frac{d^4w}{dy^4} + \left(\frac{\theta l}{b}\right)^4 \frac{d^4w}{dx^4} = \frac{P_m}{\rho_y} sin\left(\frac{m\pi x}{l}\right) \tag{B.7}$$

In which θ describes the ratio between flexural stiffnesses, given by:

$$\theta = \frac{b}{l}\sqrt[4]{\frac{\rho_x}{\rho_y}} \tag{B.8}$$

The general solution of this equation is in the form:

$$\begin{aligned} w_m &= Y_m sin\left(\frac{m\pi x}{l}\right) \\ Y_m &= \frac{l^4 p_m}{m^4 \pi^4 \rho_x} \end{aligned} \tag{B.9}$$

When applying a sinusoidal line-load in the x-direction of the form:

$$p(x) = p_1 sin\left(\frac{\pi x}{l}\right) \tag{B.10}$$

the slab deflects to a surface, given by:

$$w(x,y) = W(y) sin\left(\frac{\pi x}{l}\right) \tag{B.11}$$

This equation shows that the deflection distribution can be decoupled in x- and y-direction, with W(y) indicating the deflection of the slab at a certain y-coordinate.

When applying a distributed load over the whole width ($x = 2b$), the load becomes uniform in the y-direction, described by:

$$p(x) = \frac{p_1}{2b} sin\left(\frac{m\pi x}{l}\right) \tag{B.12}$$

In response to this load, the slab deflects to a cylindrical surface defined by

$$w_0(x) = W_0 sin\left(\frac{\pi x}{l}\right) \tag{B.13}$$

These two deflections, caused by a line-load (equation (B.10)) and a distributed load (equation (B.12)), are used to determine the ratio denoted by the term K, also called "the principal coefficient of lateral distribution":

$$K(\alpha)_v = \frac{w(x,y)}{w_0(x)} = \frac{W(y)}{W_0} \tag{B.14}$$

Additionally, this method is extended by considering torsion. To avoid recalculating the coefficient K for every particular value of the torsional parameter α, Massonnet deduced the interpolation formula based on numerical investigations as follows:

$$K_\alpha = K_0 + (K_1 - K_0)\sqrt{\alpha} \tag{B.15}$$

Where

$$\begin{aligned} K_0 &= K(0)_v \\ K_1 &= K(1)_v \end{aligned} \tag{B.16}$$

The number of K values helps to determine the proportion to calculate support forces of girders in the transverse direction. The actual moment due to P is equal to K times the mean moment:

$$\frac{P_w}{2b} = K\frac{P_w}{2b} \tag{B.17}$$

C

Element types

There are several approaches to modelling a structure in a three-dimensional finite element model, each utilising different element types. To ensure a high level of accuracy in the results, this study only considers shell and solid elements. This appendix offers a detailed overview of the characteristics and capabilities of various element types available in the DIANA FEA software, as referenced from the DIANA User's Manual [17].

C.1. Plate and shell elements

Plate or shell elements can be used to model various types of structures, particularly thin-walled structures where one dimension is significantly smaller than the other two dimensions. These elements are characterised by a small out-of-plane thickness relative to their in-plane dimensions. The element shape could be triangular or quadrilateral and linear, quadratic, or cubic interpolation is possible. The DIANA FEA software includes three types of plate or shell elements, involving the plate bending element, the flat shell element, and the curved shell element.

C.1.1. Plate elements

The plate bending elements must meet specific shape and loading criteria, as shown in Figure C.1. The elements should follow a plane configuration, with the coordinates of the element nodes lying in the xy-plane. Additionally, the element's thickness should be small relative to its in-plane dimensions. The force loading (F) must act perpendicular to the element plane, while the moment loading (M) should act around an axis within the plane.

These elements have a zero direct stress component perpendicular to the plane, fulfilling the plane stress condition. After deformation, the normals of the element plane remain straight, and the displacement perpendicular to the plane stays constant across its thickness.

The DIANA FEA software provides two types of plate bending elements based on the Discrete Kirchhoff and Mindlin-Reissner theories. Both types employ numerical integration to ensure adequate precision while maintaining computational efficiency. These plate bending elements are typically applied in floors and other two-dimensional structures that are primarily subjected to out-of-plane forces.

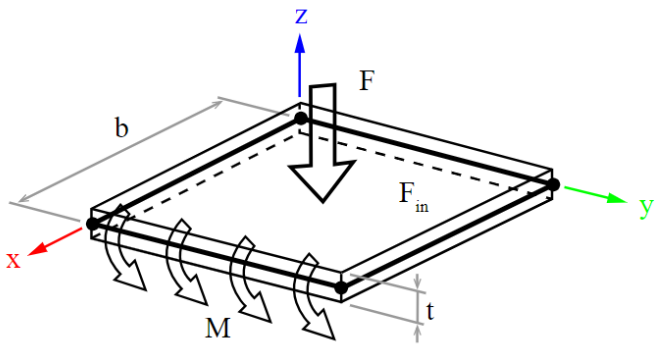

Figure C.1: Characteristics of the plate bending element [17]

C.1.2. Flat shell elements

The flat shell elements combine the characteristics of both plane stress elements and plate bending elements, as shown in Figure C.2. To qualify as a flat shell element, the coordinates of the element nodes must lie in one plane. This shell element also requires a small thickness relative to its in-plane dimensions. Forces can act perpendicular to the plane as well as within the plane of the element, while moment loads must act within the plane.

After deformation, the normals of the element plane remain straight, and the perpendicular deformation remains consistent along its thickness. The membrane behaviour corresponds to that of a plane stress element, however, primary stresses are defined in terms of forces and moments rather than Cauchy stresses. The bending behaviour is primarily based on the Mindlin-Reissner theory and uses numerical integration on the reference surface.

The DIANA FEA software provides three types of flat shell elements: regular elements, elements with drilling rotation, and spline elements. Regular elements offer three translations and two in-plane rotations degrees of freedom at each node. Elements with the drilling rotation provide an additional degree of freedom, allowing for rotation perpendicular to the plane at each node. Spline elements are specifically used for post-buckling analyses of slim-line prismatic structures, which do not apply to this study.

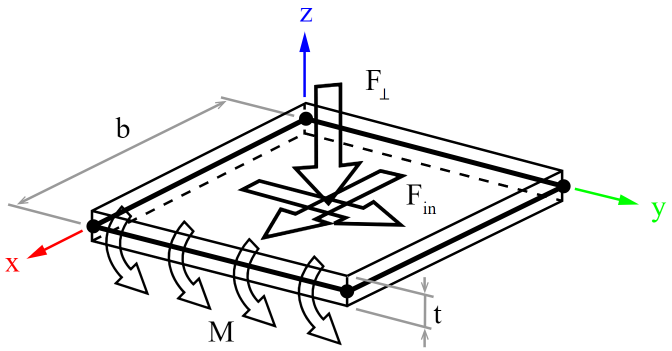

Figure C.2: Characteristics of the flat shell element [17]

C.1.3. Curved shell elements

The curved shell elements in DIANA FEA are characterised by an isoparametric degenerated-solid approach that incorporates two shell hypotheses: the straight-normals hypothesis and the zero-normal stress hypothesis. The straight-normal hypothesis assumes that the normals to the shell surface are

straight, not necessarily perpendicular to the reference surface. Additionally, it includes transverse shear deformation based on the Mindlin-Reissner theory. On the other hand, the zero-normal stress hypothesis imposes a zero-normal stress component in the normal direction of a lamina basis.

The in-plane strains in curved shell elements are characterised by linear variation over their thickness, whereas the transverse shear strains are forced to be constant in the thickness direction. Similar to flat shell elements, the force loads can act in any direction both in and out of the shell plane, while moments act around the in-plane axis of the element, as shown by Figure C.3. Each node of the curved shell elements has five degrees of freedom, including three translations and two rotations. The degrees of freedom can be increased to include rotation perpendicular to the plane by using the curved shell elements with drilling rotation.

When comparing flat shell elements and curved shell elements, flat shell elements are more economical for flat models, especially when the focus is on forces and moments rather than Cauchy stresses. On the other hand, curved shell elements, which are typically used for curved structures, offer additional functionalities in DIANA FEA. These include the capability for eccentric connections and a broader range of nonlinearity options, making them widely used in various applications.

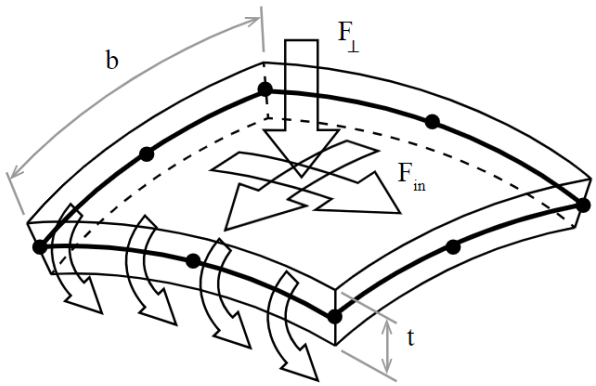

Figure C.3: Characteristics of the curved shell element [17]

The thickness of flat or curved shell elements can be defined as uniform or nonuniform, as shown in Figure C.4. Varying thickness over a single element can be achieved using spatial functions depending on a multiplication factor and gradient between multiple points.

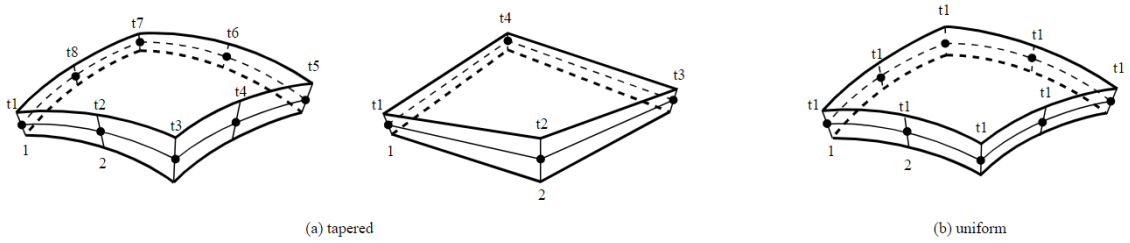

Figure C.4: Thickness of flat or curved shell elements a) uniform and b) tapered [17]

C.2. Solid elements

Solid elements are multi-functional and can be used to model various geometries and are typically employed when other elements are unsuitable. These elements do not require engineering consider-

ations or simplification of actual geometries. Characterised by their three-dimensional properties such as stress distribution, dimensions, and arbitrary loading, these elements provide comprehensive representation, as illustrated by Figure C.5. The disadvantages of solid elements include the need for a fine mesh to produce accurate results and to accurately follow complex geometries. Additionally, these elements require detailed definitions of boundary conditions. These requirements significantly increase the complexity and computational time compared to other element types, such as shell or beam elements.

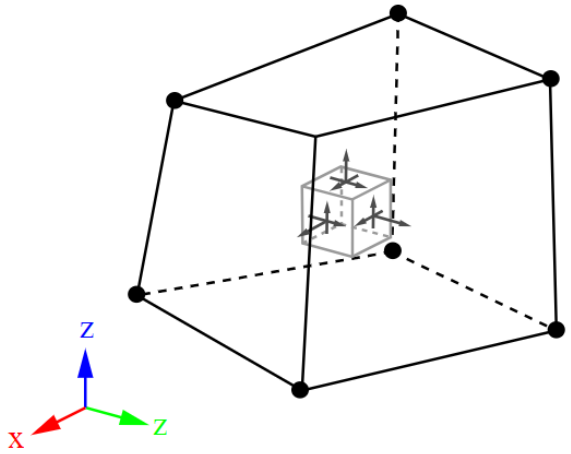

Figure C.5: Characteristics of the solid element [17]

D

Model validation

This appendix presents the validation of the numerical model used in the main study. It includes the test case, various design approaches, and analytical calculations of key variables. Additionally, the load input is validated by comparing the support forces with the applied loads and verifying the total maximum bending moments of all girders.

D.1. Results validation

The accuracy and reliability of the numerical model are validated by using a test case subjected to a straightforward load scenario, allowing for comparison with analytical calculations. Various design approaches are tested and their outputs are compared with analytically derived values.

D.1.1. Test case

The test case comprises a single precast inverted T-girder with part of the cast-in-situ compression layer on top subjected to a distributed load. The two-dimensional representation is presented in Figure D.1. The girder is simply supported using regular supports at both ends, restraining only vertical displacement. Ensuring stability, the transverse displacement is restrained at the top of the girder.

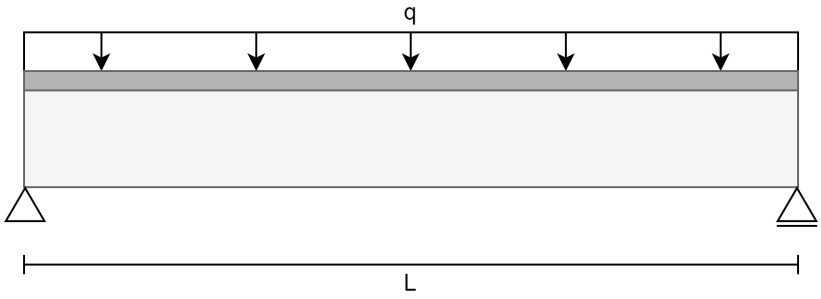

Figure D.1: Overview test case

The total span of the structure corresponds to the length of the girder, with supports provided at both ends. The width of the beam, denoted by parameter B, determines the surface area over which the load is distributed, resulting in a distributed load denoted by q. The elastic modulus of concrete differs for the prefabricated girder (E_{pc}) and the cast-in-situ deck (E_c). The ratio between these different elastic moduli (n) is used to calculate the moment of inertia of the composite girder. Details regarding the geometry of the test case, the applied load, and material properties are outlined in Table D.1.

Table D.1: Details of the geometry, applied load, and material properties of the test case

Parameter	Value
L [m]	32.00
B [m]	1.22
q [kN/m]	-24.34
E_{pc} [N/mm^2]	39100
E_c [N/mm^2]	34077
n [-]	1.15

D.1.2. Design approaches

Modelling the girders with a deck slab on top involves the integration of several structural components, each requiring shell elements oriented in distinct planes. The deck slab is modelled using horizontal shell elements, situated at the centroid of the deck slab, while vertical shell elements represent the girders' geometry with varying thicknesses. Considering both horizontal and vertical shell elements presents a challenge in connectivity. Multiple design approaches are employed to accurately capture the geometries and connections of both the girder and deck, as illustrated by Figure D.2. Subsequently, the chosen modelling approach can be extended to the transverse diaphragms within the main numerical model.

The first design approach utilises vertical shell elements with varying thicknesses throughout the girder's height and horizontal shell elements with uniform thickness for the deck slab. Connectivity between the vertical and horizontal shell elements is achieved by extending the upper shell elements of the girder to the deck slab's centroid. Although this approach establishes a correct connection, it leads to a geometry error due to material overlap.

In the second design iteration, a similar approach is adopted, but the geometry mismatch is avoided by introducing an interface connection between the girder and deck slab elements. This interface connection establishes a special relation between shapes and ensures matching the geometry of the girder and deck. The material properties of these interface elements, specifically regarding normal and shear stiffness moduli, can be adjusted to achieve the correct rigidity. For this design, the optimal values have been used for comparison.

The third design iteration maintains the geometry approach of the previous designs but employs an eccentric connection between the girder and deck elements. This design approach matches the geometry of the girder and deck while incorporating an eccentric connection without additional input properties.

Similarly, the fourth design approach utilises an eccentric connection between the girder and deck complemented by horizontal shell elements to model the girder's bottom flange. This adjustment leads to a less accurate representation of the geometry of the bottom flange but may enhance connectivity between the bottom flange and other components. In the complete model, this adjustment enables the transverse diaphragms to be connected to the bottom flange, providing a better representation of their interaction.

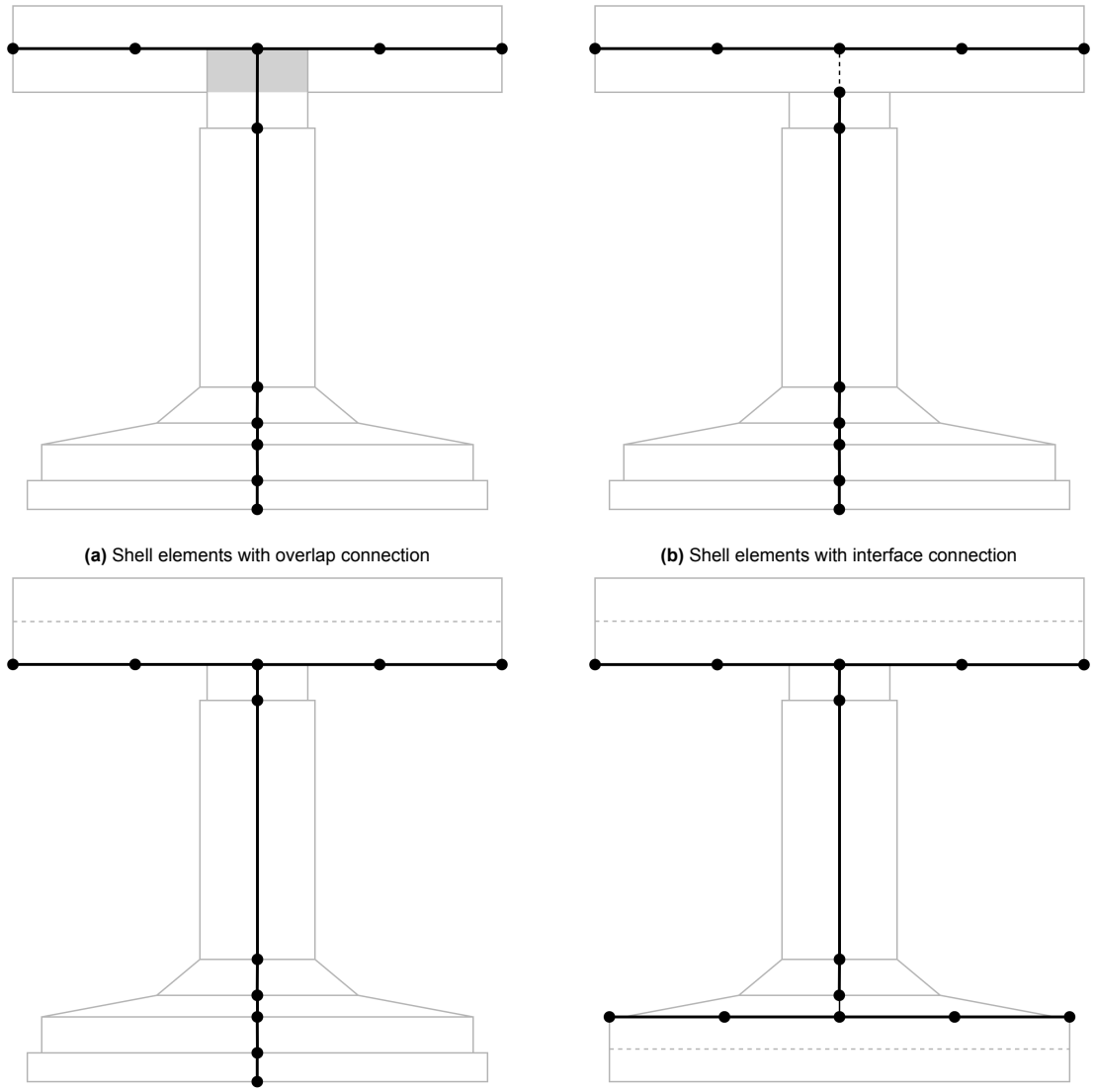

(a) Shell elements with overlap connection

(b) Shell elements with interface connection

(c) Shell elements with eccentric connection

(d) Shell elements with eccentric connection between bottom flange and deck

Figure D.2: Diverse design approaches for modelling the geometry and connection of the inverted T-girder and deck slab with shell elements

D.1.3. Analytical calculation

The accuracy and reliability of the numerical model are evaluated by comparing its results with those obtained from analytical calculations for diverse design approaches. This comparison involves assessing key variables for a simply supported beam, such as the maximum shear force, maximum bending moment, mid-span deflection, and the stresses in the outer top and bottom fibers.

The equations used to determine the maximum shear force and bending moment analytically are based on the static equilibrium of the beam, ensuring that the external forces balance the applied loads. For a simply supported beam, the maximum shear force is equal to the vertical force at one of the supports and is given by:

$$V_{max} = F_z = \frac{1}{2}qL = \frac{1}{2} * -24.34 * 32 = -389.44\text{kN} \tag{D.1}$$

The maximum bending moment arises at midspan and can be determined by analysing the internal forces at a section cut. For simply supported beams, the maximum bending moment is:

$$M_{max} = \frac{1}{8}qL^2 = \frac{1}{8} * -24.34 * 32^2 = -3115.52\text{kNm} \tag{D.2}$$

To determine the mid-span deflection and the maximum stresses in the outer fibers, the moment of inertia of the composite cross-section is required. This property measures the ability of the beam to resist bending and depends on the cross-section geometry. For complex cross-sections like an inverted T-girder with a compression layer, the cross-section is divided into smaller segments. The moment of inertia of the composite beam is calculated using the parallel axes theorem, which incorporates the moment of inertia of each segment about its own neutral axis (Ii), the area of each segment(Ai), and the vertical distance from the segment's centroid to the neutral axis of the composite cross-section (di):

$$I_{tot} = \sum (I_i + A_i d_i^2) \tag{D.3}$$

The cross-section segments can be either rectangular or trapezoidal. For each rectangular segment, the moment of inertia about its own neutral axis, the area, and the centroid distance from the bottom base are calculated as follows:

$$\begin{aligned} I_y &= \frac{1}{12}bh^3 \\ A &= bh \\ y_i &= \frac{1}{2}h \end{aligned} \tag{D.4}$$

For the trapezoidal segments, the calculations are more complex, considering the widths of the top (a) and bottom (b) parts of each segment:

$$\begin{aligned} I_y &= \frac{h^3}{12}(3a + b) \\ A &= \frac{1}{2}h(a + b) \\ y_i &= \frac{h}{3}\frac{2a + b}{a + b} \end{aligned} \tag{D.5}$$

The vertical distance from the centroid of each segment to the neutral axis of the complete cross-section is determined by first finding the centroid of the entire composite cross-section. This is achieved by calculating the areas and centroid distances of each segment from the base of the cross-section. The location of the neutral axis of the composite cross-section is determined relative to the bottom of the girders using the following equation:

$$\bar{y} = \frac{\sum y_i A_i}{\sum A_i} \tag{D.6}$$

Additionally, the cross-section consists of two different materials with varying elastic moduli. When calculating the moment of inertia, this difference in stiffness is addressed by scaling the width of the parts made from the other material. This method only works with a positive scaling factor. Therefore, the material with the lower elastic modulus is used as the base material to ensure a modular ratio greater than one. The adjustment for stiffness is applied only to the width of the segments, thereby preserving the position of the neutral axis of the composite cross-section.

Table D.2 presents the results for all equations for each segment, showing the moment of inertia of the composite cross-section.
After calculating the moment of inertia of the composite beam, the mid-span deflection and the maximum stresses in the outer top and bottom fibers can be determined using standard beam equations. The mid-span deflection of a simply supported beam is given by:

$$w = \frac{5}{384}\frac{qL^4}{EI} = \frac{5}{384}\frac{-24.34 * 32^4}{3.4077E7 * 0.19267} = -0.050615\text{m} = -50.615\text{mm} \tag{D.7}$$

The maximum stresses in the outer top and bottom fibers are determined using the maximum bending moment, the distance to the outer fiber, and the moment of inertia. To accurately calculate the stress

Table D.2: Calculation of the moment of inertia of the test case

Part	b [mm]	b_s [mm]	h [mm]	A [mm^2]	I [mm^4]	y [mm]	Ay [mm^3]	d [mm]	I_y [mm^4]
1	1180	1353.9	60	81236	2.437E7	30	2.437E6	629.0	3.216E10
2	1142	1310.3	103	134964	1.193E8	111.5	1.505E7	547.5	4.057E10
3	456	523.2	47	43088	7.445E6	183.1	7.891E6	475.9	9.764E9
4	300	344.2	82	35565	1.965E7	248.2	8.826E6	410.8	6.022E9
5	300	344.2	778	267804	1.351E10	681	1.824E8	22.0	1.364E10
6	250	286.9	80	22948	1.224E7	1110	2.547E7	451.0	4.680E9
7	1217	1217	200	243400	8.113E8	1250	3.043E8	591.0	8.583E10
Total			**1350**	**829005**			**5.463E8**		**1.927E11**
$\bar{y}$	**658.98**								

in the bottom fiber of the scaled part of the cross-section, the modular ratio (n) should be used for compensation.

For the top fiber:

$$S_{top} = \frac{M_{max} y_{top}}{I} = \frac{-3115.5 * (1.35 - \bar{y})}{0.19267} = \frac{-3115.5 * (1.35 - 0.659)}{0.19267} \\ = -11173.86 \text{kN/m}^2 = -11.17 \text{N/mm}^2 \tag{D.8}$$

For the bottom fiber, incorporating the modular ratio (n):

$$S_{bot} = n\frac{M_{max} y_{bot}}{I} = 1.147\frac{-3115.5 * (0 - \bar{y})}{0.19267} = 1.147\frac{-3115.5 * (0 - 0.659)}{0.19267} \\ = 12226.54 \text{kN/m}^2 = 12.23 \text{N/mm}^2 \tag{D.9}$$

D.1.4. Comparison

After determining the maximum shear force, bending moment, mid-span deflection and maximum stresses using analytically derived equations, a comparison between different numerical design approaches can be made. Table D.3 presents the results of the key variables for both analytical and various numerical design approaches. The numerical design approach using solid elements serves as an additional control value, but it is excluded from practical consideration due to its high computational time.

Table D.3: Comparison of Analytical and Numerical Approaches

Modelling approach	M_{max} [kNm]	F_{max} [kN]	w [mm]	Diff [%]	S_{top} [N/mm^2]	Diff [%]	S_{bot} [N/mm^2]	Diff [%]
Analytical	-3115.5	-388.2	-50.6	0.00	-11.17	0.00	12.23	0.00
Solid elements	-3115.5	-388.2	-51.3	1.33	-11.17	-0.04	12.22	-0.03
Shell interface	-3363.0	-388.2	-59.6	15.09	-11.66	4.15	13.64	10.39
Shell overlap	-3115.5	-388.2	-49.2	-2.81	-10.43	-7.15	12.10	-1.04
Shell eccentric	-3115.5	-388.2	-49.5	-2.19	-10.97	-1.83	12.08	-1.20
Shell ecc. bot.	-3115.5	-388.2	-51.1	0.91	-11.15	-0.25	12.13	-0.79

The comparison indicates that the modelling design approaches involving shell elements with eccentric connections perform the best. Considering the connectivity options with other structural components and the minimal difference compared to the analytical approach, the design approach using horizontal shell elements for the bottom flange and deck slab is assumed most suitable for this model.

D.2. Load input validation

In addition to validating the model's accuracy and reliability through a test case, it is important to verify the load input in the full numerical model. To ensure the accuracy of load input in the model, the external forces of the structure must be in equilibrium. Consequently, the vertical forces at all supports should balance the total applied loads.

For this validation, the complete model is considered, incorporating the entire geometry, boundary conditions, and all potential applied loads. Therefore, this model is subjected to load combination 1, which generates the maximum longitudinal bending moments in the system. Since the applied loads are exclusively vertical, only the vertical forces at the supports are examined.

Additionally, the total bending moments of all girders within the full system can serve as a further verification method. The summation of the maximum bending moments of each girder in a system should match the maximum bending moment of a single simply supported beam subjected to the same loads. However, due to the complexities in the full model concerning the location and stiffness of the supports, the sum of the moments will differ. The equations for maximum bending moments of simply supported beams subjected to a point load or distributed load are given by:

$$M_{max} = \frac{1}{4}FL \tag{D.10}$$

$$M_{max} = \frac{1}{8}qL^2 \tag{D.11}$$

The load inputs can be categorised into three load types: dead loads, TS loads, and UDL. For the analytical determination of maximum bending moments, the TS loads were simplified as a point load at the middle of the span. This simplification does not perfectly match the actual input and will therefore overestimate the bending moments caused by the TS loads.

Table D.4 presents a comparison for each load type between the applied loads and the support forces in the model. Additionally, it includes a comparison of the total bending moments generated by the loads and the model outcomes.

Table D.4: Overview of load inputs in the numerical model

Load type	F_z [kN]	q [kN/m]	F_z model [kN]	M_{max} [kNm]	M_{max} model [kNm]
Dead loads	1773	54.6	1773	7198	6855
TS loads	1200	-	1200	9744	9157
UDL	1969	60.6	1969	7993	7620
Total	**4942**		**4942**	**24935**	**23632**

The results presented in Table D.4 indicate that the vertical forces at the supports correspond accurately to the total applied loads. Furthermore, the maximum bending moments of the system generated by each load type are relatively close to the analytically determined values. The differences can be explained by the simplification of modelling the TS loads as point loads and the complexities of the system. Due to the horizontal stiffness of the supports and their position relative to the edges, the maximum bending moments in the girders are smaller. However, with a difference of around 5% in the total bending moments, it can be concluded that the load inputs are accurately modelled.